THE ROLE OF HOMER SCAFFOLDING TO METABOTROPIC GLUTAMATE RECEPTOR 5 IN THE MOUSE MODELS OF NEURODEVELOPMENT DISORDERS

APPROVED BY

_____

Kimberly Huber, Ph.D. (Supervisor)

_____

Ege Kavalali, Ph.D.

_____

Joseph Albanesi, Ph.D.

_____

Luis Parada, Ph.D.

DEDICATION

First, I would like to thank my mentor, Kimberly Huber. She facilitated my growth as a scientist both technically and analytically. I would also like to thank the members of my graduate committee for their helpful guidance and input throughout my training. I especially would like to thank all the members of the Huber Lab, past and present. They provided lots of technical insight, knowledge, hands on training, and were always there to bounce ideas off of. I especially would like to thank Nicole, the lab technician. Her efforts were invaluable to my success. I would especially like to thank those I collaborated with, Jennifer, Weirui and Gemma. Without their contributions, several questions in this study would have been left unanswered. I would also like to thank all the labs that provide reagents, animals, or advice that was critical to the success of this project. Last and most importantly, I would like to thank my wonderful husband, David. Without his never-ending love and support, none of this would have been possible.

THE ROLE OF HOMER SCAFFOLDING TO METABOTROPIC GLUTAMATE RECEPTOR 5 IN THE MOUSE MODELS OF NEURODEVELOPMENT DISORDERS

by

KATIE ANNE COLLINS

DISSERTATION

Presented to the Faculty of the Graduate School of Biomedical Sciences

The University of Texas Southwestern Medical Center at Dallas

In Partial Fulfillment of the Requirements

For the Degree of

DOCTOR OF PHILOSOPHY

The University of Texas Southwestern Medical Center at Dallas

Dallas, Texas

May, 2014

THE ROLE OF HOMER SCAFFOLDING TO METABOTROPIC GLUTAMATE RECEPTOR 5 IN THE MOUSE MODELS OF NEURODEVELOPMENT DISORDERS

Katie Anne Collins, Ph.D.

The University of Texas Southwestern Medical Center at Dallas, 2014

Kimberly Huber, Ph.D.

Autism is a neurological disorder characterized by repetetive behaviors, social anxiety and verbal and non-verbal communication. Fragile X Syndrome (FXS) is the most common genetic cause of autism and inheritable form of intellectual disability. FXS is caused by the transcriptional silencing of the *Fmr1* gene, which encodes for the Fragile X Mental Retardation Protein (FMRP), which is a Ribonucleic acid (RNA) binding protein. FMRP binds to messenger RNA (mRNA) and suppresses their translation. FMRP regulates hundreds of mRNAs, making it a complex disease with several possible dysfunctions causing the many

symptoms, like audiogenic seizures or hypersensitivity. While there are several studies which rescue phenotypes, there is little known about what causes the abnormalities, and if it is possible to replicate the symptoms with a single genetic manipulation. There is also little know about common links between different genetic causes of autism.

In this study, I manipulate the interaction between metabotropic glutamate receptor 5 (mGluR5) and Homer, and report how these interactions are important in causing some of the phenotypes in FXS. By rescuing disrupted mGluR5-Homer interactions with a Homer 1a knock out I can rescue several phenotypes, and by disrupting mGluR5-Homer interactions with an mGluR5 knock-in mouse that is mutated so it cannot bind to Homer, I was able to mimic them. I was able to rescue/mimic increased basal translation, altered mGluR-signaling, increased neocortical excitability, decreased anxiety, and partial rescue/mimic audiogenic seizures seen in Fragile X mice. However, I was unable to rescue/mimic the enhanced mGluR-LTD.

In this study, I also report how the disrupted mGluR5-Homer interactions are caused by Homer being phosphorylation by CaMKIIα. CaMKIIα is an FMRP target and elevated in the *Fmr1* KO mice, causing increased phosphorylation of Homer. Inhibiting CaMKIIα, rescues mGluR5-Homer interactions, basal protein synthesis rates and increased neocortical excitability.

Lastly, I report how in PTEN conditional KO (cKO) mice, another autism model, also have disrupted mGluR5-Homer interactions. The PTEN cKO mice have increased neocortical excitability, which can be rescued by inhibiting mGluR5. This suggests a common mGluR5 dysfunction in multiple autism models, which could lead to a common treatment.

TABLE OF CONTENTS

PRIOR PUBLICATIONS

Barbara Barylko, Lei Wang, Derk D. Binns, Justin A. Ross, Tara C. Tassin, **Katie A. Collins**, David M. Jameson, Joseph P. Albanesi. (2010) The Proline/Arginine-Rich Domain Is a Major Determinant of Dynamin Self-Activation. *Biochemistry*. *49* (50), 10592-10594. 2010.

Jennifer A. Ronesi, **Katie A. Collins**, Seth A. Hays, Nien-Pei Tsai, Weirui Guo, Shari G. Birnbaum, Jia Hua Hu, Paul F. Worley, Jay R. Gibson, and Kimberly M. Huber. (2012) Disrupted Homer scaffolds mediate abnormal mGluR5 function in a mouse model of fragile X syndrome. Nature Neuroscience 15 (30), 431-40.

Vikram Jakkamsetti, Nien-Pei Tsai , Christina Gross, Gemma Molinaro, **Katie A. Collins**, Ferdinando Nicoletti, Kuan H. Wang, Pavel Osten, Gary J. Bassell, Jay R. Gibson, and Kimberly M. Huber. (2013) Experience-induced Arc/Arg3.1 primes CA1 pyramidal neurons for metabotropic glutamate receptor-dependent long-term synaptic depression. Neuron. Oct 2;80(1):72-9.

LIST OF FIGURES

LIST OF TABLES

LIST OF DEFINITIONS

4E-BP – eIF4E-binding protein

AMPA – α-Amino-3-hydroxy-5-methyl-4-isoxazolepropionic acid

Arc – Activity-regulated cytoskeleton-associated protein

ASD – autism spectrum disorder

B – Basal

BK – Ca^{2+}-dependent big K^{+}

Ca^{2+} – calcium

CaMK – Ca^{2+}/calmodulin-dependent protein kinase

CaMKII – Ca^{2+}/calmodulin-dependent protein kinase II

CB1R – cannabinoid receptor type 1

cKO – conditional KO

co-IP – co-immunoprecipitation

CT – tat-mGluR5CT; YGRKKRRQRRR-ALTPPSPFR

D – DHPG

DAG – diacylglycerol

DHPG – (RS)-3,5-Dihydroxyphenylglycine

eEF2 – eukaryotic elongation factor 2

eEF2K – eukaryotic elongation factor 2 kinase

EF1α – Elongation factor 1α

eIF4A – eukaryotic initiation factor 4A

eIF4B – eukaryotic initiation factor 4B

eIF4E – eukaryotic initiation factor 4E

eIF4G – eukaryotic initiation factor 4G

ER – endoplasmic reticulum

ERK1/2 – extracellular signal-regulated protein kinases 1 and 2

EVH1 – Ena/VASP homology 1

F – phenylalanine

FMRP – Fragile X mental retardation protein

FXS – Fragile X syndrome

GABA – gamma-aminobutyric acid

GDP – guanosine diphosphate

GPCR – G-protein coupled receptor

GTP – guanosine triphosphate

H1a – Homer 1a

H1b/c – Homer 1b/c

IEG – immediate early genes

IP_3 – inositol 1,4,5-trisphosphate

IP3R – inositol 1,4,5-trisphosphate receptor

KO – Knock out

LTD – Long term depression

Map1B – Microtubule-associated protein 1B

MAPK – Mitogen-activated protein kinase

mEPSC – miniature excitatory postsynaptic current

mGluR5 – metabotropic glutamate receptor 5

mGluR5$^{R/R}$ – mGluR5F1128R

Mnk1/2 – MAP kinase-interacting kinase 1 and 2

mRNA – messenger RNA

mTOR – mammalian target of rapamycin

MU – tat-mGluR5MU; YGRKKRRQRRR-ALTPLSPRR

NFAT – Nuclear factor of activated T-cells

NMDA – N-methyl-D-aspartate

p70S6K – Ribosomal protein S6 kinase beta-1

p90RSK – Ribosomal protein S6 kinase, 90kDa, polypeptide 1

PI3K – Phosphoinositide 3-kinase

PIKE-L – PI3K enhancer

Pin1 – Peptidyl-prolyl cis-trans isomerase NIMA-interacting 1

PIP2 – phosphatidylinositol (4,5)-bisphosphate

PIP3 – phosphatidylinositol (3,4,5)-trisphosphate

PLC – phospholipase C

PPI – pre-pulse inhibition

PSD – post synaptic density

PTEN – phosphatase and tensin homolog

R – arginine

RNA – ribonucleic acid

rpS6 – 40S ribosomal subunit protein S6

TRP – transient receptor potential

TSC1/2 – tuberous sclerosis complex 1/2

Tyr – tyrosine

WT – wild type

CHAPTER ONE

Introduction

Fragile X Mental Retardation Protein and mGluR5 dysfunction in the Fragile X mouse model

Autism is a prevalent neurological disease

Autism is a neurological disorder that affects tens of millions worldwide and is becoming increasingly more prevalent (Payakachat et al., 2012). Over the last twenty years, autism spectrum disorders (ASD) have increased from four to ten per 10,000 children in the 1980s, up to thirty to fifty per 10,000 children in the early 2000s (Barbaresi et al., 2005; Kim et al., 2011; Wing and Potter, 2002). In the United States, the Autism and Developmental Disabilities Monitoring Network reported an average of one percent of children have ASD (males 1:70; females 1:315) in 2006 (2007). The disorder takes a toll on the families as well as an economic cost on the United States of approximately $35 to $60 billion a year (Ganz, 2007; Jarbrink and Knapp, 2001). Autism is still largely diagnosed based on behavioral criteria. ASD, as defined by the DSM-V, is characterized by exhibition of repetitive behaviors, social anxiety and verbal and non-verbal communication. ASD has a wide range of symptoms from sensory hypersensation, seizures, from individuals with intellectual disability to individuals being savants. Along with this wide range of symptoms are a wide

range of causes and genes making the disease more complicated to treat and understand (Klauck, 2006; Newschaffer et al., 2007). Because of the large diversity of ASD types among autistic patients, there is a need for different treatments. Therefore, finding common links among these many different forms can improve our understanding of the disease and lead to a more uniform treatment.

Fragile X Syndrome, the most common genetic cause of autism

Fragile X Syndrome (FXS) is the most common form of inherited mental retardation affecting approximately 1:4000 males and 1:8000 females (Bassell and Warren, 2008; Garber et al., 2008). FXS accounts for about two to six percent of all autism patients and is the most common genetic form of autism (Abrahams and Geschwind, 2008; Nishimura et al., 2007; Reddy, 2005). With a range in severity of the disease, thirty to fifty percent of FXS patients are diagnosed with autism (Hagerman et al., 1986; Hagerman et al., 2005; Kaufmann et al., 2004). Patients have reduced IQs ranging from forty to seventy (Merenstein et al., 1996). They also experience hypersensitivity to sensory stimulation, especially to tactile and auditory stimulation (Hagerman and Hagerman, 2002; Miller et al., 1999). Along with hypersensory stimulation, fifteen percent of patients also display seizures (Berry-Kravis, 2002; Berry-Kravis et al., 2010). Patients' brains also display increased neuronal spine density in

several brain regions, however, they are long and thin, consistent with immature or underdeveloped spines (Irwin et al., 2000). Along with the neurological defects, FXS patients typically display peripheral tissue dysfunction in the form of elongated faces, macroorchidism, and hyperextensible joints (Hagerman and Hagerman, 2002).

FXS is caused by the transcriptional silencing of the *Fmr1* gene, which is located on the X chromosome, therefore FXS is more common among boys than girls (Pieretti et al., 1991). *Fmr1* encodes for the Fragile X Mental Retardation Protein (FMRP). The transcriptional silencing is caused by CGG repeats in the 5'-untranslated region (O'Donnell and Warren, 2002). Normal individuals have between six and sixty CGG repeats. Fragile X carriers have between sixty and two hundred repeats, but FMRP expression is unaltered. The trinucleotide repeat region is unstable during meosis, causing carriers to possibly pass expanded repeat region copies on to their offspring. FXS manifests when the CGG repeats exceed two hundred (O'Donnell and Warren, 2002). At that point, *Fmr1* undergoes hypermethylation in the 5'-untranslated region, resulting in reduced transcription and thereby reduced or complete loss of FMRP (Sutcliffe et al., 1992). In rare cases, some patients have point mutations within the gene, for example, a substitution of an isoleucine for an asparagine at site 367 (De Boulle et al., 1993).

FXS can be recapitulated in the mouse model, in which, the *Fmr1* gene is knocked out (The Dutch-Belgian Fragile et al., 1994). Because the *Fmr1* knock out (KO) mouse recapitulates FXS, it allows researchers to test drugs and better understand the disease, which cannot be done with patients. Despite several studies which have involved rescuing of phenotypes, little is known about the underlying causes of the abnormalities, or wether it is possible to replicate the symptoms with a single genetic manipulation.

The function and regulation of FMRP

FMRP is a ribonucleic acid (RNA) binding protein, which binds to messenger RNA (mRNA) and suppresses its translation (Brown et al., 2001; Li et al., 2001; Siomi et al., 1994). FMRP interacts with its various mRNAs through RNA binding motifs. FMRP has an RGG domain and two KH domains, known as KH1 and KH2, which bind to RNA. The I304N mutation disrupts the KH2 domain from binding to mRNA and altering protein expression of FMRP targets (Siomi et al., 1994). However, while the RGG domain binds RNA, it is not necessary for some of FMRP's major functions, like regulating synapse number (Pfeiffer and Huber, 2007). FMRP binding to mRNA is also regulated by posttranslational modification. When FMRP is phosphorylated at Serine 499, FMRP binds to its target mRNA and stalls ribosomes from translating. Upon dephosphorylation, FMRP releases the mRNA and ribosomes begin translating

(Ceman et al., 2003). After dephosphorylation, FMRP is ubiquitylated and degraded (Nalavadi et al., 2012). Since FMRP binds to and regulates its own mRNA, new FMRP is synthesized and suppresses its targets again. While FXS is caused by the loss of one protein, FMRP regulates over a thousand mRNAs, making it a complex disease (Brown et al., 2001; Darnell et al., 2011). FMRP's regulation of its targets could indirectly cause several FXS symptoms, like audiogenic seizures or hypersensitivity.

In the brain, FMRP is thought to transport mRNAs down the dendrites and into spines (Dictenberg et al., 2008). Once in the spine, FMRP continues to suppress the transcripts until signals allow for local translation of the FMRP targets (Li et al., 2001). FMRP regulates the local translation of proteins that are associated with long term depression (LTD), like Activity-regulated cytoskeleton-associated protein (Arc) and Microtubule-associated protein 1B (Map1B) (Bassell and Warren, 2008; Benoist et al., 2013; Davidkova and Carroll, 2007; Jakkamsetti et al., 2013; Waung et al., 2008). The local translation of these FMRP targets leads to changes in spine morphology and synapse elimination (Pfeiffer and Huber, 2007). Preventing FMRP's transportation to the synapse results in increased spine number and more immature spines, similar to what is observed in the *Fmr1* KO (Dictenberg et al., 2008). All of this evidence suggests the important role FMRP plays in spine maintenance and changes in spine morphology through regulation of its targets.

Altered regulation of metabotropic glutamate receptor 5 in FXS

There is substantial evidence of altered metabotropic glutamate receptor 5 (mGluR5) functions in FXS. Currently, mGluR5 antagonists are being used in clinical trials on Fragile X patients (Jacquemont et al., 2011). So far the evidence suggests that patients with a complete loss of FMRP see improvements with the drug. Many of the behavioral phenotypes observed in *Fmr1* KO mice can be rescued by the use of an mGluR5 inverse agonist, 2-methyl-6-(phenylethynyl)pyridine (MPEP) (Thomas et al., 2012). Also, mGluR5 heterozygous mice crossed with *Fmr1* KO mice are able to rescue several behavioral phenotypes (Dolen et al., 2007; Thomas et al., 2011a). This evidence suggests there is increased mGluR5 activity in FXS and regulating some of the phenotypes observed in the disease.

mGluR5, a G-protein coupled receptor

mGluR5 is a seven transmembrane G-protein coupled receptor. mGluR5 is one of two receptors belonging to Group 1 mGluRs, the other being mGluR1 (Conn and Pin, 1997). mGluR5 and 1 are able to form heterodimers, but the role of this heterodimerization is or whether the receptors can affect one another in this form is unknown (Beqollari and Kammermeier, 2010). mGluR5 expression is wide spread throughout the brain with its highest expression in olfactory bulb, cortex, hippocampus, dorsal striatum, and lateral septum (Romano et al., 1995).

mGluR5 and mGluR1 have a complimentary expression pattern with areas of low mGluR1 expression having high mGluR5 expression and vice a versa. From ten to fifty percent of mGluR5 is located on the cell surface (Hubert et al., 2001; Lopez-Bendito et al., 2002), and mGluR5 must be dimeric in order to be trafficked to the surface. The internal pool of mGluR5 is primarily located on the rough endoplasmic reticulum (ER), but a portion is also located on the nuclear membrane (Hubert et al., 2001; O'Malley et al., 2003). Internal mGluR5 receptors are activated by glutamate transported into the cell through excitatory amino acid transporter 3 (Gonzalez et al., 2007; Jong et al., 2009; O'Malley et al., 2003). mGluR5 is primarily located in the dendrites and external mGluR5 can be found in the PSD, concentrated in perisynaptic sites (Baude et al., 1993; Lujan et al., 1996; Romano et al., 1995; Shigemoto et al., 1993). mGluRs are only activated with high frequency presynaptic activity, which is likely due their perisynaptic location (Batchelor et al., 1994). The theory is that closely timed synaptic releases causes glutamate to spillover, and therefore activates mGluRs (Kotecha et al., 2003).

As mentioned above, mGluR5 is a G-protein coupled receptor (GPCR). G-proteins are heterotrimers consisting of alpha, beta, and gamma subunits (McCudden et al., 2005; Oldham and Hamm, 2008). There are 5 beta, 13 gamma, and 20 alpha subunits, which can be expressed in various combinations. In the

inactive state, G-protein heterotrimers are tightly associated. Ligand binding drives the GPCR interaction with its associated G-protein, and its accompanied by exchange of GDP for GTP on the alpha subunit and subsequent dissociation of GTP-alpha from the high affinity dimer of beta and gamma (Katritch et al., 2013; McCudden et al., 2005; Oldham and Hamm, 2008). In the case of mGluR5, the ligand is glutamate, and the coupled G_α is G_q, which activates a phospholipase C (PLC) signaling pathway (Abe et al., 1992; Atkinson et al., 2006; Hermans and Challiss, 2001).

Activation of the PLC pathway results in an increase in inositol 1,4,5-trisphosphate (IP_3) and stimulation of the IP_3 receptor, releasing calcium (Ca^{2+}) from the ER stores (Abe et al., 1992). Ca^{2+} release from the ER activates Ca^{2+}/calmodulin-dependent protein kinase (CaMK), as well as the mitogen-activated protein kinase (MAPK) pathway (Jong et al., 2009). Another product of the PLC reaction is diacylglycerol (DAG), an endocannabinoid precursor (Igal et al., 2001; Johansen et al., 1994). DAG lipase generates 2-arachidonoyl glycerol (2-AG), which is an endocannabinoid and an endogenous agonist of the cannabinoid receptor type 1 (CB1R) (Gao et al., 2010; Tanimura et al., 2010). The endocannabinoid is a retrograde neurotransmitter and is released into the synapse, affecting the presynapse. The endocannabinoids bind to the CB1R, inhibiting presynaptic release of vesicles and thereby inducing LTD of both

excitatory and inhibitory synaptic transmission (Kano et al., 2009; Lafourcade, 2009; Peterfi et al., 2012; Turu and Hunyady, 2010).

Altered endocannabinoid signaling in FXS

In *Fmr1* KO mice, endocannabinoid signaling is altered from mainly inhibiting excitation to over inhibiting inhibitory synapses. Electron microscopy of gold stained DAG lipase shows altered location of DAG lipase in the spine of *Fmr1* KO mice (Jung et al., 2012). In wild type mice, DAG lipase is located around the post synaptic density (PSD), where excitatory synapses form. However, in *Fmr1* KO mice, DAG lipase is located near the shaft of the spine, where inhibitory synapses form. This altered location in the spine is consistent with the change in endocannabinoid signaling seen in *Fmr1* KO mice. While basal DAG lipase activity is increased in the *Fmr1* KO mouse, mGluR stimulation of DAG lipase is absent in the *Fmr1* KO mice (Jung et al., 2012; Maccarrone et al., 2010). The study also shows there is not altered subcellular localization of mGluR5 in the *Fmr1* KO, suggesting mGluR5 is uncoupled from DAG lipase signaling. mGluR1/5 and CB1R activation mGluR5 induces LTD of GABAergic inhibition, called iLTD, this then results in E-S potentiation (Chevaleyre and Castillo, 2003), which is altered in the *Fmr1* KO mouse. 10 μM (RS)-3,5-Dihydroxyphenylglycine (DHPG), a group 1 mGluR agonist, induced strong E–S

coupling potentiation in *Fmr1* KO, but not in the wild type (Zhang and Alger, 2010).

mGluR-LTD

LTD is a form of synaptic plasticity driven by synaptic activity that leads to a decrease in synaptic strength. mGluR-LTD is driven by the activation of group 1 mGluRs, mGluR1 and mGluR5 (Huber et al., 2001; Volk et al., 2006). This form of LTD is not dependent on N-methyl-D-aspartate (NMDA) receptors, and requires protein synthesis for LTD maintenance, not for the early phase of mGluR-LTD (Huber et al., 2000; Huber et al., 2001). The protein synthesis dependence of mGluR-LTD is an age dependent phenomenon and is only present after postnatal day 21 (Nosyreva and Huber, 2005). mGluR-LTD is caused the by the internalization of α-Amino-3-hydroxy-5-methyl-4-isoxazolepropionic acid (AMPA) receptors, which cannot be observed in neonates (Nosyreva and Huber, 2005). The internalization of AMPA receptors is dependent on protein synthesis and requires newly synthesized Arc (Jakkamsetti et al., 2013; Nosyreva and Huber, 2005; Waung et al., 2008). There is some controversy over whether or not mGluR-LTD requires activation of the mTOR pathway. Inhibiting PI3K with wortmannin or inhibiting mTOR with rapamycin has been shown to attenuate mGluR-LTD (Hou and Klann, 2004; Sharma et al., 2010), although others have failed to replicate these findings (Auerbach et al., 2011). Similarly, S6K2 KOs

also display attenuated mGluR-LTD compared to wild type littermates (Antion et al., 2008). Potter et al. (2013) observes rapamycin dependent mGluR-LTD in older mice and not young. In contrast to these data, when TSC1 or TSC2 is knocked out or reduced, there is attenuated mGluR LTD (Auerbach et al., 2011; Bateup et al., 2011; Potter et al., 2013). TSC1/2 inhibits mTOR activity, therefore with the loss of TSC1 or TSC2, there is an increase in mTOR phosphorylation and activity (Bateup et al., 2011; Huang et al., 2008b). The evidence suggests that both increases and decreases in the mTOR pathway can attenuate mGluR-LTD. The ERK1/2 pathway also plays a role in regulating mGluR-LTD, as ERK1/2 and PI3K/mTOR pathways converge (Banko et al., 2006). Inhibiting the ERK1/2 pathway attenuates mGluR-LTD similarly to the PI3K/mTOR pathway (Gallagher et al., 2004). Both the ERK1/2 and PI3K/mTOR pathway are necessary for mGluR-LTD.

Enhanced mGluR-LTD in FXS

In *Fmr1* KO mice, there is no change in NMDA dependent LTD and long term potentiation (Godfraind et al., 1996; Paradee et al., 1999); however, there is enhanced mGluR-LTD (Huber et al., 2002). Enhanced mGluR-LTD in the *Fmr1* KO mice is independent of protein synthesis (Iliff et al., 2013; Nosyreva and Huber, 2006). The enhanced mGluR-LTD and its independent of protein synthesis in *Fmr1* KOs are thought to be due to increased levels of FMRP targets. Synaptic

proteins like Arc and Map1b are basally high in the *Fmr1* KO mice compared to wild type littermates (Hou et al., 2006b; Niere et al., 2012). Normally these proteins are synthesized after DHPG stimulation, but this does not occur in *Fmr1* KO mice (Hou et al., 2006b). However, since the synaptic proteins are basally elevated in the *Fmr1* KO, the synaptic proteins are available for use, therefore no longer require protein synthesis, and leading to the enhanced mGluR-LTD.

The major mechanistic theory describing pathogenesis in FXS is the mGluR theory of Fragile X (Bear et al., 2004). mGluR-LTD is known to require the synthesis of new proteins in order to persist (Huber et al., 2000). FMRP binds many synaptic mRNA transcripts, which mGluR stimulation drives protein synthesis of these FMRP targets (Weiler et al., 1997). FMRP is thought to be regulating the synthesis of new proteins downstream of mGluR stimulation at the synapse. The expectation was that changes in FMRP would result in deficits in LTD. However, mGluR dependent LTD in the *Fmr1* KO is enhanced rather than reduced (Huber et al., 2002). This suggests that while mGluRs stimulate synthesis of new proteins, FMRP works to prevent translation of synaptic proteins. Therefore in the case of mGluR-LTD, the loss of FMRP leads to exaggerated mGluR activity. In the simplest case, this could be described by a model in which mGluRs are the gas and FMRP is the brake.

mGluR5 induces synaptic plasticity through regulation of translation

mGluR5 also signals to three other pathways, the PI3K/mTOR pathway, the ERK1/2 pathway, and the eEF2K pathway, which all the pathways affect translational control (Park et al., 2008; Rong et al., 2003; Thandi et al., 2002; Tu et al., 1998). The phosphoinositide 3-kinase (PI3K)/ mammalian target of rapamycin (mTOR) and the ERK1/2 pathway are both activated by the $G_{\beta\gamma}$ subunits of the G-protein (Brock et al., 2003; Dupre et al., 2009). A key downstream signaling pathway triggered by PI3K activation is: PI3K → AKT → TSC1/2 → mTOR →p70S6K. Some of the proteins in the PI3K pathway are encoded by autism linked genes, including the tuberous sclerosis complex 1 and 2 (TSC1/2) and phosphatase and tensin homolog (PTEN), which are a negative regulators of the PI3K pathway (Berg and Geschwind, 2012; Lv et al., 2013). The eIF4E-binding protein (4E-BP) binds to eukaryotic initiation factor 4E (eIF4E) inhibiting eIF4E and cap dependent translation (Lawrence and Abraham, 1997; Pause et al., 1994). When 4E-BP is phosphorylated by mTOR, and ERK1/2, 4E-BP dissociates from eIF4E and allows eIF4E to bind with other cap dependent translational proteins, increasing translation (Brunn et al., 1997; Gingras et al., 1999; Gingras et al., 2001). The PI3K kinase also negatively regulates translation through p70S6K phosphorylating FMRP, increasing FMRP translational suppression of its targets (Narayanan et al., 2008).

An important ERK1/2 pathway is: MEK1/2 → ERK1/2 → Mnk1/2. MAP kinase-interacting kinase 1 and 2 (Mnk1/2) phosphorylates eIF4E, also decreasing the 4E-BP-eIF4E interaction. ERK1/2 also phosphorylates 4E-BP further decreasing the 4EBP-eIF4E interaction. The convergence of the PI3K/mTOR and ERK pathways on the 4E-BP-eIF4E interactions may both be needed for the dissociation of 4E-BP and eIF4E (She et al., 2010). ERK1/2 also regulates translation via phosphorylation of ribosomal protein S6 kinase, 90kDa, polypeptide 1 (p90RSK). Activation of p90RSK phosphorylates eukaryotic initiation factor 4B (eIF4B), which stimulates cap dependent translation (Anjum and Blenis, 2008; Holz et al., 2005; Shahbazian et al., 2006). Activated eIF4B also potentiates the eukaryotic initiation factor 4A (eIF4A) RNA-helicase activity (Rozen et al., 1990). mRNA's secondary structure slows down the ribosomes from translating, and eIF4A helicase activity unwinds the mRNA, allowing for faster translation. p90RSK also phosphorylates 40S ribosomal subunit protein S6 (rpS6) at sites Serine 235 and 236 (Pende et al., 2004; Roux et al., 2007), which correlates with assembly of the translation pre-initiation complex and increased cap-dependent translation (Anjum and Blenis, 2008; Roux et al., 2007).

The third signaling pathway that affects translation is the eukaryotic elongation factor 2 kinase (eEF2K) pathway. The eEF2K pathway is a negative regulator of translation by inhibiting general elongation. eEF2K phosphorylates

eukaryotic elongation factor 2 (eEF2) inhibiting eEF2's activity. eEF2 mediates the translocation step where translational RNA is moved along in the ribosome so the next codon in the sequence is brought into the ribosome for translation (Proud, 1994). eEF2K is negatively regulated by p70S6K and p90RSK, decreasing phosphorylated levels of eEF2 and increasing elongation (Wang et al., 2001). Translation levels are regulated by integrating all these pathways together.

Increased translation in FXS

FMRP binding to mRNA suppresses the translation of FMRP targets. The loss of FMRP causes increased in basal levels of the FMRP targets and possibly cause increased translation rates. In the *Fmr1* KO mouse, there are increased basal translation rates in hippocampal slices and synaptoneurosomes (Gross et al., 2010; Osterweil et al., 2010a). While FMRP's role as translational suppressor could be causing the increased translation rates, inhibiting mGluR5 with MPEP returns the increased basal translation rates to wild type levels (Gross et al., 2010; Osterweil et al., 2010a). Similarly, activating mGluRs with DHPG in a wild type mouse is able to mimic the *Fmr1* KO phenotype (Osterweil et al., 2010a). Inhibition of the ERK pathway is also able to return *Fmr1* KO translation rates back to wild type levels (Gross et al., 2010; Osterweil et al., 2010a). However, there is some dispute regarding whether inhibiting the PI3K pathway can rescue the increased basal protein synthesis rates in the *Fmr1* KO. Gross et al. (2010) is

able to rescue the increased basal protein synthesis rates in synaptoneurosomes, but Osterweil et al. (2010) is unable to in acute hippocampal slices. This may be due to differences in the protocols used. FMRP regulates several of the proteins in the PI3K/mTOR pathway, including the PI3K enhancer (PIKE-L). PIKE-L is a GTPase that enhances PI3K activity fourfold when bound to PI3K (Ye et al., 2000). PIKE-L is elevated in the *Fmr1* KO which leads to increased PI3K activity and increased basal phosphorylation of the PI3K/mTOR pathway (Gross et al., 2010; Sharma et al., 2010). This increased basal phosphorylation level can be detected in synaptoneurosomes or fresh lysates, but is not maintained in acute slices (Osterweil et al., 2010a). The increased basal phosphorylation of PI3K signaling molecules, such as p70S6K, can also be seen in FXS patients (Hoeffer et al., 2012). There is also an increased association of eIF4E and eukaryotic initiation factor 4G (eIF4G) in the *Fmr1* KO mice (Sharma et al., 2010). A transgenic mouse, over-expressing eIF4E, has increased eIF4E-4G association but normal eIF4E-4E-BP interactions (Santini et al., 2013). In these eIF4E over-expressing mice, there are also increased basal translation rates, as seen in the *Fmr1* KO mice (Santini et al., 2013). The increased eIF4E-4G association suggests that increased cap dependent translation may be causing the increased basal translation in the *Fmr1* KO mice.

Altered agonist induced mGluR-signaling in FXS

While there are changes in basal mGluR5 signaling, there is also altered group 1 mGluR signaling in *Fmr1* KO mice. As mentioned above, when stimulation of mGluRs with DHPG you activates the PI3K/mTOR, ERK1/2, and eEF2K pathways and promotes translation of FMRP targets. However, in the *Fmr1* KO, DHPG is no longer able to stimulate phosphorylation of signaling molecules in the PI3K pathway (Ronesi and Huber, 2008a). As mentioned above, eEF2K is inhibited by being phosphorylated by p70S6K and p90RSK (Wang et al., 2001). Since there is no activation of the negative regulator of eEF2K, one would expect to see increased eEF2K activity. When eEF2 phosphorylation is measured after DHPG, there is a large increase in eEF2 phosphorylation in the *Fmr1* KO compared to wild types (Ronesi and Huber, 2008a). There are conflicting results on the status on the ERK1/2 pathway in *Fmr1* KO mice. Hou et al. (2006) shows a basal increase in phospho-ERK1/2 levels and no further increase with DHPG, along with increased phospho-ERK1/2 levels seen in patients (Wang et al., 2012). However, multiple other labs see no change in phospho-ERK1/2 levels and normal DHPG activated phosphorylation of ERK1/2 (Gross et al., 2010; Osterweil et al., 2010a; Ronesi and Huber, 2008a), and a trend, but lacking significance toward increased phosphorylation of ERK1/2 (Hoeffer et al., 2012). Further complicating the debate, there is evidence for decreased ERK1/2 and MEK1/2 activity in *Fmr1* KO in cortical synaptoneurosomes (Kim et al., 2008). Despite all the conflicting evidence

surrounding the ERK1/2 pathway in the *Fmr1* KO mice, there is nevertheless sustained support for the involvement of the ERK1/2 pathway in some of the phenotypes observed in *Fmr1* KO mice. As pointed out above, inhibiting the ERK1/2 pathway rescues basal protein synthesis rates, and the use of an ERK1/2 inhibitor, lovastatin, can rescue increased neuronal excitability seen in *Fmr1* KOs (Osterweil et al., 2013). Lastly, DHPG stimulates translation of FMRP targets and synaptic proteins (Todd et al., 2003; Weiler et al., 1997). One thing many labs can agree on and replicate is that there is no longer DHPG stimulated synthesis of proteins in *Fmr1* KO mice (Hou et al., 2006b; Muddashetty et al., 2007; Ronesi and Huber, 2008a; Todd et al., 2003). This DHPG stimulated translation is necessary for mGluR-LTD (Huber et al., 2000).

Increased excitability in the Fmr1 KO

There are several pieces of evidence for increased excitability in FXS patients. As mentioned before, patients experience hypersensitivity to sensory stimulation, especially to tactile and auditory stimulation, and several have seizures (Berry-Kravis, 2002). Altered EEG patterns are also commonly observed in FXS patients. The irregularities in activity often include focal frontal rhythmic slow waves and most commonly centrotemporal spikes, which are a spike discharge followed by slow waves (Berry-Kravis, 2002). The seizures and

changes in EEG patterns in FXS reflect the hyperexcitable networks that occur with the loss of FMRP.

There is also some evidence that FMRP affects intrinsic neuronal properties. Input resistance is a neuronal property that represents the sum of open channels, or leakiness, of a cell, which when increased is typically predictive of increased excitability. In layer IV, input resistance is increased in *Fmr1* KO spiny stellate cells compared to wild types (Gibson et al., 2008). This change is accompanied by an increase in spiking frequency in *Fmr1* KO neurons. This data suggests an increased excitability in *Fmr1* KO neurons. Similarly in the basolateral amygdale, *Fmr1* KO cells fire more action potentials in response to depolarizing current steps than wild type counterparts (Olmos-Serrano et al., 2010). Alterations in intrinsic neurological properties can affect cognitive function.

Alterations in intrinsic currents could have significant effects on circuit function and behavior in the *Fmr1* KO. One major network change in *Fmr1* KO is disrupted neuronal connectivity. In layer IV of the somatosensory cortex, the connection probability between fast spiking inhibitory neurons and excitatory spiny stellate neurons is reduced in the *Fmr1* KO (Gibson et al., 2008). Along with reduced connectivity within-layers, *Fmr1* KO mice display a deficit in between layer connections. An experiment, using photostimulation of layer III

neurons, have a decreased response in layer IV neurons in the same barrel column (Bureau et al., 2008). At older ages, differences in the connection probability disappear between genotypes (Bureau et al., 2008; Gibson et al., 2008; Testa-Silva et al., 2012). FMRP may a role in circuit development regulating connectivity, however, even without FMRP; the circuit is ultimately able to mature normally.

One way to measure changes in circuit excitability is look at UP states, a circuit phenomenon that underlies slow oscillation. The slow oscillation is prominent during sleep, but can occur spontaneously under anesthesia and *in vitro* brain slices preparations (Sanchez-Vives and McCormick, 2000; Steriade et al., 1993). The slow oscillation is comprised of two major states: UP states and DOWN states. UP states are cyclic periods of depolarization accompanied by a concurrent increase in both excitatory and inhibitory synaptic barrages (Haider et al., 2006; Sanchez-Vives and McCormick, 2000). The depolarizing shift in membrane potential will make it more likely for neurons to fire action potentials. Interspersed between the UP states are DOWN states, which are periods of quiescence (Sanchez-Vives and McCormick, 2000; Steriade et al., 1993). DOWN states are characterized by a return to resting membrane potential and a cessation of most synaptic input. UP state durations varies depending on the subject and the preparation, but typically lasts around one second (Bazhenov et al., 2011).

The frequency of UP states is rhythmic with UP states occurring at a rate between 0.1 and 1 Hz.

The *Fmr1* KO mouse have increased UP state durations and a decrease in frequency *in vivo* and *in vitro* (Hays et al., 2011). Inhibiting mGluR5 does not affect the wild type, but rescues the *Fmr1* KO durations to wild type levels. Similarly, crossing a mouse heterozygous for mGluR5 with the *Fmr1* KO mouse also rescues the prolonged UP state durations (Hays et al., 2011). Inhibiting mGluR1, does not rescue the prolonged UP state durations, however, it does dramatically reduce the UP state durations in wild types and *Fmr1* KO slices, while still maintaining the difference between genotypes (Hays et al., 2011). There is also evidence of mGluR5 dependent enhanced excitability in CA3 hippocampal neurons. Hippocampal slices exhibit spontaneous synchronized bursting activity, or epileptiform activity, in the presence of bicuculline, gamma-aminobutyric acid (GABA) receptor antagonist, which are prolonged with DHPG (Merlin and Wong, 1997). The epileptiform activity in *Fmr1* KO mice is prolonged and is restored to WT levels by inhibiting mGluR5 (Chuang et al., 2005). Because network function is critically important for information processing, one direct consequence of disruption of network activity is behavioral alterations.

Behavioral changes in Fmr1 KO mice

Fmr1 KO mice display several behavioral changes; however, they are not always consistently seen between labs or strains of mice. One phenotype is audiogenic seizures, which occur to *Fmr1* KO mice are subjected to a 120 decibel sound for five minutes. Wild type mice rarely have audiogenic seizures, whereas about sixty percent of *Fmr1* KO mice seize (Chen and Toth, 2001; Yan et al., 2005). Of that sixty percent, half undergo status epilepticus. Reducing mGluR5 levels or inhibiting mGluR5 with MPEP can partially rescue seizures (Thomas et al., 2012; Yan et al., 2005). High concentrations of MPEP can completely rescue seizures. However, high concentrations of MPEP start to block NMDA receptors (O'Leary et al., 2000), and inhibiting NMDA receptors has an anticonvulsant effect (Lea et al., 2005). Therefore, the full rescue at the higher MPEP concentrations likely do not completely have to do with mGluR5, but NMDA receptors.

There are ways to measure changes in auditory response in mice by looking at the startle response and pre-pulse inhibition (PPI). The startle response is measures how much a mouse jumps to increasing decibel sounds, detecting changes in their basal auditory response. PPI is where a weaker prestimulus (prepulse) inhibits a mouse's reaction to a successive strong startling stimulus (pulse). The reduced amplitude of startle reflects the nervous system's ability to adapt to a strong sensory stimulus when a preceding weaker stimulus is provided

to the mouse. *Fmr1* KO mice have a reduced startle response with an increased PPI (Chen and Toth, 2001; Frankland et al., 2004; Nielsen et al., 2002). The altered auditory response can also been seen in patients (Frankland et al., 2004). The altered PPI in the *Fmr1* KO mice can be rescued with the administration of MPEP (de Vrij et al., 2008). The same group is currently using AFQ056, a selective mGluR5 antagonist, in clinical trials with promising results (Jacquemont et al., 2011). AFQ056 was also able to rescue the altered PPI in the *Fmr1* KO mice (Levenga et al., 2011). However, MPEP is unable to rescue the reduced startle response (Thomas et al., 2012). The data suggest that some of the altered auditory responses, including audiogenic seizures, are in part due to increased mGluR5 activity.

Fmr1 KO mice also show repetitive behaviors mimicking those seen in autistic patients. To measure repetitive behaviors, mice can be observed grooming themselves or burying marbles. Mice that spend more time grooming themselves are considered to be displaying a repetitive behavior. Similarly, mice like to bury marbles in bedding, and mice who bury more marbles are thought to show repetitive behavior as well. *Fmr1* KO mice have been shown to have an increased grooming phenotype, suggesting repetitive behaviors in the mice (Pietropaolo et al., 2011). However, the data surrounding marble burying is inconclusive. The *Fmr1* KO mice have been reported to bury more, less, and the

same amount of marbles as wild type mice (Dansie et al., 2013; Henderson et al., 2012; Spencer et al., 2011; Thomas et al., 2012; Westmark et al., 2011). Inconsistency among behavioral studies makes it difficult to interpret data and their underlying meaning. One study suggests that mGluR5 may play a role in marble burying. While there is no difference between *Fmr1* KO mice and wild type mice in this study, MPEP reduces the number of marbles buried by wild type mice (Thomas et al., 2012). However, this result could also be due to the action of MPEP on NMDA receptors (O'Leary et al., 2000). While the marble burying data are inconclusive, the grooming phenotype suggests a repetitive phenotype, and it is unknown whether mGluR5 regulates the phenotype.

FXS patients have problems with social interaction, and *Fmr1* KO mice also display social deficits (Goebel-Goody et al., 2012; Pietropaolo et al., 2011; Spencer et al., 2005). There are multiple ways to measure social interaction in mice. One is the three box social interaction method, which tests social preference and social recognition. The test mouse is put in the center box and is able to explore the two connected boxes. In one box is placed a novel object, and in the other box is a novel mouse. Mice normally want to spend time with the mouse over an object, and mice with social deficits tend to spend equal time with the object and mouse. Next, they replace the object with a novel mouse, and the original novel mouse is now familiar. Mice will spend more time with the novel

mouse versus the mouse they already met. *Fmr1* KO mice display no social preference for a novel mouse over a familiar mouse (Pietropaolo et al., 2011). However, Spencer et al. (2005) showed the *Fmr1* KO mice had no defects in social interest and social recognition. The same study showed the *Fmr1* KO mice display abnormal social responses consistent with social anxiety. *Fmr1* KO mice spend decreased center mirror ratio in the mirrored chamber test, an earlier retreat in the tube test and decreased investigation of an unfamiliar partner in a familiar cage experiment (Spencer et al., 2005). The mirrored chamber test has one side with mirrors in it, tricking the mouse into thinking there are more mice in the chamber. The appearance of multiple animals in the mirrored chamber is thought to create an artificial social stimulus. Decreased center mirror ratio suggests *Fmr1* KO mice have social anxiety (Spencer et al., 2005). The tube test sets two mice down a tube heading toward one another. When they meet in the center, one mouse will push the other mouse out. If two different sets of wild type mice challenge each other, each would win fifty percent of the time in the tube test. The tube test is generally associated with social dominance. *Fmr1* KO mice win fewer times only with unfamiliar and not with cagemates, again suggesting social anxiety in *Fmr1* KO mice (Goebel-Goody et al., 2012; Spencer et al., 2005). Again, *Fmr1* KO mice show decreased investigation of an unfamiliar partner in a familiar cage suggests social anxiety. All the data suggests the *Fmr1* KO have social anxiety towards novel mice, not familiar mice or cage mates.

While the *Fmr1* KO mice show social anxiety, they show decreased general anxiety. One way to measure anxiety is with an open field test. Mice are placed in a large box, which is unfamiliar to them. In this situation, mice usually spend more time around the edges than in the center. Highly anxious mice will almost exclusively spend time along the edges. *Fmr1* KO mice spend more time in the center of the open field arena than wild type littermates (Dansie et al., 2013; Spencer et al., 2011; Yan et al., 2004). Similar results have been seen in the elevated plus maze as well. The elevated plus maze has two open arms and two closed arms. Just like mice do not like to spend time in the center of the open field area, mice do not like being in the open arms. *Fmr1* KO mice spend more time in the open arms compared to wild type littermates (Dansie et al., 2013; Goebel-Goody et al., 2012; Liu and Smith, 2009). The last anxiety experiment performed on the *Fmr1* KO mice, is the light-dark box. There are two boxes, one lit and the other dark. Mice are placed in the dark side and do not like to spend time in the light side. The *Fmr1* KO mouse spends more time in the light side of the box than wild types and enters more often (Goebel-Goody et al., 2012; Peier et al., 2000; Spencer et al., 2011). While the *Fmr1* KO mice have social anxiety, they also clearly have reduced anxiety outside of social situations.

One possible phenotype that could confound the reduced general anxiety observed in *Fmr1* KO mice is their increased locomotion. To measure

locomotion, a mouse is placed in a new cage and their movement is tracked or there are light beams across the cage, which are broken when the mouse moves through them. The more an animal moves around the cage, the more light beams are broken. When *Fmr1* KO mice are placed in a new cage, they cover a larger distance or have more beam breaks than wild type mice (Dolan et al., 2013; Peier et al., 2000; Pietropaolo et al., 2011; Spencer et al., 2011). Since the *Fmr1* KO mice have an increased locomotion phenotype, the increased time *Fmr1* KO mice spend in the open arms, light side, or center of the open field area could just be due to increased movement. However, some studies normalize the distance the mice travel in the center to the total distance the mouse travelled (Peier et al., 2000), and the phenotype can still be seen.

Homer-mGluR5 interactions in *Fmr1* KO mice

In FXS mice, there is altered mGluR5 function and inhibiting mGluR5 can rescue several FXS phenotypes. The molecular basis of some of these altered mGluR5 functions in *Fmr1* KO mice is unclear. However, it is known that mGluR5-Homer interactions are altered in *Fmr1* KO mice. mGluR5 in *Fmr1* KO mice have an increased association with Homer 1a (H1a), the Homer short form, and a decreased association with long forms of Homer (Giuffrida et al., 2005). What this altered interaction means was unknown and is the topic of my thesis.

Homer, an mGluR5 scaffolding protein

Homer is a scaffolding protein comprised of an Ena/VASP homology 1 (EVH1) domain and a coiled-coil domain. The EVH1 domain is the ligand binding domain, which interacts with a proline-rich sequence, the PPXXF motif (Shiraishi-Yamaguchi and Furuichi, 2007). Among the known Homer binding proteins are mGluR5, mGluR1α, PIKE, IP3R, transient receptor potential (TRP) channels, Shank, and dynamin 3 (Brakeman et al., 1997; Gray et al., 2003; Guhan and Lu, 2004; Tu et al., 1999; Tu et al., 1998; Yuan et al., 2003). The coiled-coiled domain is the domain mediates Homer self-association and allows Homer to serve as a scaffold for its binding partners (Sun et al., 1998; Tadokoro et al., 1999). The coiled-coil domain has also been shown to bind to Syntaxin 3 (Minakami et al., 2000). There are 3 Homers found throughout the body. Of these, only Homer 1 contains a P-motif, which binds to the EVH1 domain (Irie et al., 2002). Although the role the P-motif in Homer 1 is unclear, the evidence suggests it does not bind to the EVH1 domain in the same Homer protein (Irie et al., 2002).

Of the three Homer proteins, only Homer 2 is expressed all throughout the brain (Shiraishi et al., 2004). Homer 1 is also widely expressed in the brain, but is not found in the cerebellum. Homer 1 is expressed in the cerebellum early in development, but is lost completely in adulthood (Shiraishi et al., 2004). Homer 3 is the most sparsely distributed Homer in the nervous system. Homer 3 is only

expressed in the cerebellum, hippocampus, and the olfactory bulb early in development (Shiraishi et al., 2004). The same study showed that Homer family proteins are also expressed in most peripheral tissues, except the spleen.

Not much is known about the differences between three types of Homer proteins. The greatest role in the brain is played by Homer 1, which is divided into three isoforms 1a, 1b and 1c. Homer 1b and 1c (H1b/c) are the long, constitutive forms, and H1a is the short, activity-dependent form. H1a does not contain a coiled-coil domain and is unable to bind to other Homers. Its basal expression is very low, but dramatically increases two hours after a seizure, as well as after exploration of a novel environment (Li et al., 2012; Potschka et al., 2002; Vazdarjanova et al., 2002). H1a acts as a dominate-negative, binding to all the same targets as H1b/c, and thereby disrupting complexes scaffolded by H1b/c. H1a has been shown to lead to the ubiquitylation of Shank (Bangash et al., 2011b). Shank and long Homers form a matrix in the PSD that is disrupted by H1a (Hayashi et al., 2009). Mutations in the coiled-coil domain of H1b of isoleucine 332 to arginine and isoleucine 337 to glutamate cause H1b to form only stable dimers and not tetramers (Hayashi et al., 2009). The mutation disrupts the matrix formation and causes a decrease in spine density. This is consistent with data that shows H1a over-expression leads to a decrease in spine number,

and over-expression of H1b/c and Shank leads to more mature spines (Sala et al., 2003; Sala et al., 2001).

Homer binding can also regulates protein trafficking and function. H1b and H2b inhibit the trafficking of mGluR5 from the ER to the cell surface, and cluster mGluR5 molecules, confining their movement (Kammermeier et al., 2000; Roche et al., 1999; Serge et al., 2002). When mGluR5 and H1a are co-expressed, the distribution of mGluR5 is more diffuse. Similar results are observed in the subthalamic nucleus of Homer 2 KOs. With the loss of long Homers, there is an increase in synaptic mGluR5 at symmetric synapses (Kuwajima et al., 2007). Homer has similar regulation of mGluR1 with the long forms of Homer induce clustering of mGluR1 (Kammermeier, 2006).

Along with Homer regulating mGluRs mobility and trafficking, Homer can also regulate mGluR5's activity. mGluR5 is constitutively active, not requiring agonist to induce activity, when not bound to a long Homer or bound to H1a (Ango et al., 2001). Ca^{2+}-dependent big K^{+} (BK) channel are activated when mGluRs are activated by DHPG. When Homer 3 is knocked down or H1a is overexpressed, the BK channels are open more often (Ango et al., 2001). Expression of a point mutant of mGluR5 (phenylalanine (F) 1128 to arginine (R)) that fails to bind Homer also induces increased opening of the BK channels (Ango et al., 2001). In the same study, IP_3 production was also shown to increase with

DHPG and the mGluR5^{F1128R} mutant, both which can be reversed to control levels by MPEP. mGluR5-Homer interactions may regulate neuron excitability through these BK channels, as well as M-type potassium current and N-type calcium current. M-type potassium current is a noninactivating, delayed rectifier-type potassium current, which is thought to play role in regulating cell excitability (Marrion, 1997). Group 1 mGluRs regulate the M-type current by inhibiting it, however, co-expression of the long Homers reduces this inhibition (Kammermeier et al., 2000). The same study also shows the same modulation of the N-type calcium current by group 1 mGluRs and Homer. Group 1 mGluRs and Homer may play an important role in regulating neuronal excitability.

While Homers interaction with its target proteins affects their trafficking and signaling, there are ways to affect Homers ability to bind to its targets. mGluR5 phosphorylated on the c-terminus by ERK1/2 increases mGluR5-Homer interactions (Hu et al., 2012). However, this phosphorylation also increases H1a binding and required for Peptidyl-prolyl cis-trans isomerase NIMA-interacting 1 (Pin1) binding. Pin1 enhances H1a binding to mGluR5 and cannot bind when long Homers are bound to mGluR5 (Park et al., 2013). While H1a acts as a dominant negative, Homer 3 can be phosphorylated by CaMKIIα and ERK1/2 (Mizutani et al., 2008). The study only examined the role CaMKIIα sites affect Homer binding; showing phosphorylation at the CaMKIIα sites reduces Homer's

affinity for its targets. Homer binding in T cells is also reduced when activated and requires protein kinase B (AKT) activation (Huang et al., 2008a). This suggests AKT also can regulate Homer binding. Phosphorylation of Homer has the potential to regulate Homer targets.

Disrupted mGluR5-Homer interactions in FXS

In *Fmr1* KO mice, Giuffrida et al. (2005) showed there is a change in the balance of long Homers bound to mGluR5 to H1a bound mGluR5. One can mimic disrupted mGluR5-Homer interactions in the *Fmr1* KO by using a peptide of the Homer binding domain in c-terminus of mGluR5 (CT). The CT peptide binds to Homer and acts as a sink, disrupting all Homer interactions. Disrupting Homer interactions artficially with the CT peptide is able to recapitulate some of Fragile X phenotypes. DHPG induced PI3K/mTOR signaling is absent in the *Fmr1* KO mouse as well as in wild type slices treated with the CT peptide (Ronesi and Huber, 2008a). Also, DHPG stimulated protein synthesis is absent in the CT peptide treated slices. However, it is unable to mimic the enhanced mGluR-LTD in the *Fmr1* KO. Instead, disrupting Homer interactions attenuates mGluR-LTD (Ronesi and Huber, 2008a). The reasoning behind the differences is FMRP remains in wild type slices treated with the CT peptide, and therefore FMRP targets are not elevated. Without mGluR induced protein synthesis, there are is no increase in synaptic proteins to remove AMPA receptors. If disrupted Homer

interactions are able to mimic some *Fmr1* KO phenotypes, it is possible other phenotypes may also be regulated by disrupted Homer interactions.

The disrupted mGluR5-Homer interactions in *Fmr1* KO mice could be regulated by FMRP targets. CaMKIIα, which phosphorylates Homer, is an FMRP target (Mizutani et al., 2008). CaMKIIα is elevated in the *Fmr1* KO mouse (Hou et al., 2006b; Osterweil et al., 2010a; Zalfa et al., 2003). With elevated CaMKIIα, it is possible for increased phosphorylation of Homer and therefore causing the disrupted mGluR5-Homer interactions. There is also an increase in AKT phosphorylation in the *Fmr1* KO, and has been shown to regulate Homer interactions in T cells (Gross et al., 2010; Huang et al., 2008a; Sharma et al., 2010). Therefore it is possible that the increased AKT phosphorylation may also be regulating the mGluR5-Homer interactions as well.

PTEN deletion, another model of autism

Recently a link between PTEN mutations and children with ASD and macrocephaly has been found (Butler et al., 2005; Herman et al., 2007). About 5% of children diagnosed with ASD and macrocephaly have a mutation in PTEN (McBride et al., 2010). Children with the PTEN mutations have macrocephaly, which is an enlarged head. Mouse models with PTEN deleted, also display macrocephaly as well as enlarged neurons and dendrites (Kwon et al., 2006a; Kwon et al., 2001). PTEN has also been linked to seizures, which can be found in

some ASD patients (Backman et al., 2001; Kwon et al., 2006a; Ogawa et al., 2007). Kwon et al. have also shown PTEN conditional KO (cKO) mice, with deletion in layers III-V of the cortex and the dendate in the hippocampus, display altered social interactions (Kwon et al., 2006b). PTEN cKO mice did not display social preference by spending equal time with an inanimate object and mouse. The PTEN cKO mice could also not recognize the difference between a novel mouse and a familiar mouse (Kwon et al., 2006a). This study also showed the PTEN cKO mice had a problem with learning and memory in the Morris water maze, which is consistant with patients having intellectual disability (McBride et al., 2010; Varga et al., 2009). The Morris water maze test an animal's locational memory. The mouse is placed in a pool with four quadrants, a platform in one of the quadrants, and spacial ques on the wall to learn the location of the platform. The mouse is taught overseveral days where the platform is located. On the probe day, the platform is removed and mouse is tested to see if it remembers where it was. Normal mice spend most of their time in the quadrant where the platform was located. The PTEN cKO mice spend equal time in all the quadrants, suggesting the mice never learned the task (Kwon et al., 2006a). The PTEN mouse model is a good representation of patients.

PTEN and the PI3K pathway

PTEN is a is a tumor suppressor gene, frequently mutated in human cancers, and plays an important role in brain development (Endersby and Baker, 2008; Li et al., 1997). PTEN is important for embryonic development as the complete KO mice are embryonic lethal (Suzuki et al., 1998). PTEN is a phosphatase which catalyzes the dephosphorylation of phosphatidylinositol (3,4,5)-trisphosphate (PIP3) to phosphatidylinositol (4,5)-bisphosphate (PIP2) (Maehama and Dixon, 1998). PTEN contains a C2 domain, which bind phospholipid membranes and enables PTEN to inhibit cell migration (Lee et al., 1999; Raftopoulou et al., 2004). PTEN also contains a short N-terminal PIP2-binding domain and a PDZ domain-interaction motif. While it is not understood what these regions contribute to the function of PTEN, they are likely important due to the many PTEN mutations found in pateints all through out the protein (Song et al., 2012).

PI3K performs the reverse reaction phosphorylating PIP2 into PIP3 (Vanhaesebroeck and Waterfield, 1999). Therefore, PTEN is a negative regulator of PI3K. PTEN's negative regulation of the PI3K/mTOR pathway is important, because the PI3K/mTOR pathway is involved in cell survival, cell proliferation, cell growth, angiogenesis and cellular metabolism (Manning and Cantley, 2007). The vast many cellular functions PTEN regulates through the PI3K/mTOR pathway make it an important gene and easy to understand why it underlies so

many disease, like ASD, intellectual disability, childhood seizures and highly prevelant in cancers (Ali et al., 1999; Backman et al., 2001; Butler et al., 2005; Endersby and Baker, 2008; Rosen and She, 2006).

Fragile X and PTEN

While both Fragile X patients and those with PTEN mutations both show autism and intellectual disability in patients, there are other molecular similarties seen between the two mouse models. Since PTEN is a negative regulator of the PI3K/mTOR pathway, the PTEN cKO mice have increased phosphorylation of downstream proteins (Kwon et al., 2006a; Kwon et al., 2001). As mentioned before, *Fmr1* KO mice have elevated levels of PIKE-L and therefore increased PI3K activity and phosphorylation of downstream proteins (Gross et al., 2010; Sharma et al., 2010). While PTEN cKO mice have a much more dramatic increased in phosphorylation of proteins, like AKT, it still illustrates some of the molecular similarities between the two mouse models.

The two mouse models are not completely identical either. The loss of FMRP causes increases in spine density, as well are more immature filapodia like spines (Comery et al., 1997; Irwin et al., 2000; Nimchinsky et al., 2001). PTEN deletion on the other hand has no change in spine density, but creates more matures spines (Haws et al., 2013). Consistent with the different spine phenotypes, *Fmr1* KO shows enhanced mGluR-LTD, while the PTEN cKO

mouse decreased mGluR-LTD and increased long term potentiation (Huber et al., 2002; Takeuchi et al., 2013).

While there are clear differences between the two mice models, they still produce similar behavior results. It is possible that these similar behavioral phenotypes may have more commonalities than increased PI3K/mTOR signalling. As mentioned above, AKT can regulate Homer interaction in T cells, and inhibiting AKT increases Homer binding to its target (Huang et al., 2008a). AKT phosphorylation is increased in the PTEN cKO mice and possible that mGluR5-Homer interactions are disrupted in the PTEN cKO mice, and mGluR5 may be contributing to some of its phenotypes (Kwon et al., 2006a; Kwon et al., 2001). Inhibiting mGluR5 in other autism mouse models had improved behavioral phenotypes, so there could be a common link between autism models (Silverman et al., 2010).

Motivation for studies

Autism affects tens of millions worldwide and is becoming increasingly more prevalent (Payakachat et al., 2012) with a couple hundred of genes linked to the disease. However, there is very little linking these many genes and other causes of ASD. It is important to start finding underlying mechanisms of ASD. Therefore, finding common links between these many different forms can improve our understanding of the disease and lead to a more uniform treatment.

FXS is the most common genetic form of autism (Abrahams and Geschwind, 2008; Nishimura et al., 2007; Reddy, 2005) providing a good model to start from. Enhanced mGluR5 function is causally associated with the pathophysiology of FXS, but the mechanism behind the mGluR5 dysfunction is largely unknown. Many researchers have reduced mGluR5 levels and used antagonist or reverse agonists to inhibit mGluR5 activity. While these studies have been able to rescue some of the phenotypes seen in the *Fmr1* KO and now patients, it is still unknown what causes the enhanced mGluR5 activity. mGluR5 is less associated with the long Homer isoforms and more associated with *H1a* in *Fmr1* KO mice (Giuffrida et al., 2005). Homer binding has been shown to regulate mGluR5 activity and function. H1a acts to disrupts mGluR5-long Homer complexes, alters mGluR signaling and causes constitutive, agonist-independent activity of mGluR1/5 (Ango et al., 2001). Homer also effects mGluR5s trafficking and motility. Long Homers cluster mGluR5 together and confining its movement (Kammermeier et al., 2000; Roche et al., 1999; Serge et al., 2002), while H1a causes mGluR5's distribution to be more diffuse. With the effects Homer binding has on mGluR5, it is possible that the altered mGluR5-Homer interactions play a role in FXS.

mGluR5 antagonists have also been used on other forms of autism and been able to rescue phenotypes. However, there is no follow up as to why these inhibitors helped other models (Silverman et al., 2010). What is the common

mechanism between FXS and other forms of autism that allows mGluR5 inhibitors to rescue phenotypes in both models? Homer binding can be regulated by phosphorylation. Homer 3 is known to be phosphorylated by CaMKIIα and ERK1/2 (Mizutani et al., 2008), and phosphorylation at the CaMKIIα sites reduces Homer's affinity for its targets. Homer binding in T cells is reduced when activated, requiring AKT activation (Huang et al., 2008a), and suggesting AKT can also regulate Homer binding. AKT phosphorylation is increased in the PTEN cKO mice, another autism model, and possible that mGluR5-Homer interactions are disrupted in the PTEN cKO mice, and mGluR5 may be contributing to some of its phenotypes (Kwon et al., 2006a; Kwon et al., 2001). The *Fmr1* KO mice, PTEN cKO mice and possibly other autism mouse models may share a common mechanism of mGluR5 dysfunction due to altered Homer binding.

CHAPTER TWO
Results

Disrupted mGluR5-Homer scaffolds mediate abnormal mGluR5 signaling, circuit function and behavior in a mouse model of Fragile X Syndrome

This chapter contains data that was collected as a collaborative effort between several colleagues, Jennifer Ronesi, Seth Hays, Nien-pei Tsai, and Weirui Guo. I contributed the real time PCR, a portion of the signaling data, and a portion of the basal protein synthesis data. However, the other data described in this chapter is important in understanding the mechanism of Homer-mGluR scaffold disruption in the *Fmr1* KO. Work published in *Nature Neuroscience*.

Summary

Enhanced mGluR5 function is causally associated with the pathophysiology of Fragile X Syndrome (FXS), a leading inherited cause of intellectual disability and autism. Here we provide evidence that altered mGluR5-Homer scaffolds contribute to mGluR5 dysfunction and phenotypes in the FXS mouse model, *Fmr1* KO. In *Fmr1* KO mice mGluR5 is less associated with long Homer isoforms, but more associated with the short Homer1a. Genetic deletion of Homer1a restores mGluR5- long Homer scaffolds and corrects multiple phenotypes in *Fmr1* KO mice including altered mGluR5 signaling, neocortical circuit dysfunction, and behavior. Acute, peptide-mediated disruption of mGluR5-Homer scaffolds in wildtype mice mimics many *Fmr1* KO phenotypes.

In contrast, Homer1a deletion does not rescue altered mGluR-dependent long-term synaptic depression or translational control of FMRP target mRNAs. Our findings reveal novel functions for mGluR5-Homer interactions in the brain and delineate distinct mechanisms of mGluR5 dysfunction in a mouse model of cognitive dysfunction and autism.

Introduction

Fragile X Syndrome (FXS) is the most common inherited form of intellectual disability and a leading genetic cause of autism (Abrahams and Geschwind, 2008; Bassell and Warren, 2008). FXS is caused by transcriptional silencing of the *FMR1* gene that encodes the Fragile X Mental Retardation protein (FMRP) – an RNA binding protein, that regulates translation of its interacting mRNAs (Bassell and Warren, 2008). Most patients exhibit multiple neurological deficits, including reduced IQ, seizures, sensory hypersensitivity, social anxiety, hyperactivity and other characteristics of autism (Berry-Kravis, 2002; Hagerman, 2002). In the mouse model of FXS, *Fmr1* knockout (KO), group 1 metabotropic receptor (mGluR1 and mGluR5) and protein synthesis- dependent plasticity is enhanced and dysregulated (Luscher and Huber, 2010). These findings motivated the "mGluR theory of FXS" which posits that altered mGluR-dependent plasticity contributes to the pathophysiology of the disease (Bear et al., 2004; Dolen et al., 2010; Dolen et al., 2007). In support of the mGluR theory, many phenotypes in

animal models of FXS are reversed by pharmacological or genetic reduction of mGluR5 or downstream signaling pathways (Dolen et al., 2010; Dolen et al., 2007). Importantly, a recent report indicates that mGluR5 antagonism can be an effective therapeutic strategy in FXS patients (Jacquemont et al., 2011).

Group 1 mGluR activation stimulates *de novo* protein synthesis in neurons and evidence suggests that FMRP suppresses translation of specific mRNA targets downstream of mGluR activation (Bassell and Warren, 2008). In FXS, the loss of an FMRP-mediated "brake" is proposed to lead to excess mGluR5-driven translation of many FMRP target mRNAs which in turn, leads to an excess of mGluR-dependent plasticity (Bear et al., 2004; Dolen et al., 2010). Although mGluR5 antagonism rescues many phenotypes associated with FXS, it is unknown if this is due to excess mGluR5-driven translation.

Other evidence suggests there may be altered mGluR5 function that is upstream of translation in *Fmr1* KO brains. Although total mGluR5 levels are normal in *Fmr1* KO forebrain, there is less mGluR5 in the postsynaptic density (PSD) fraction and an altered balance of mGluR5 association with short and long isoforms of the postsynaptic scaffolding protein Homer (Giuffrida et al., 2005). The N-terminal EVH1 (Ena-VASP homology) domain of Homer proteins, binds the intracellular C-terminal tail of group 1 mGluRs (mGluR5 and mGluR1a) and affects their trafficking, localization and function (Shiraishi-Yamaguchi and

Furuichi, 2007) Long, constitutively expressed forms of Homer (Homer1b, 1c, 2 and 3) multimerize through their C-terminal coiled-coil domain and localize mGluRs to the PSD through interactions with SHANK, as well as scaffold mGluRs to signaling pathways through Homer interactions with the PI3 Kinase enhancer (PIKE), Elongation Factor 2 kinase (EF2K) and the IP3 receptor (Park et al., 2008; Shiraishi-Yamaguchi and Furuichi, 2007). *Homer1a* (*H1a*), a short, activity-inducible, form of Homer lacks the coiled-coiled domain and cannot multimerize with other Homers. Consequently, *H1a* disrupts mGluR5-long Homer complexes, alters mGluR signaling and causes constitutive, agonist-independent activity of mGluR1/5 (Ango et al., 2001).

In *Fmr1* KO mice mGluR5 is less associated with the long Homer isoforms and more associated with *H1a* (Giuffrida et al., 2005). We hypothesized that the altered balance in mGluR5 interactions with Homer isoforms contributed to the mGluR5 dysfunction and pathophysiology of FXS. To test this hypothesis, we crossed *Fmr1* KO mice with *H1a* KO mice and determined if *H1a* deletion restored mGluR5 function and Homer interactions as well as neurophysiological and behavioral phenotypes of *Fmr1* KO mice. In addition, we determined if acute peptide-mediated disruption of mGluR5-Homer scaffolds in wildtype mice mimicked phenotypes of *Fmr1* KO mice. Our results indicate that altered Homer isoform interactions are responsible for much, but not all, of the mGluR5 dysfunction and pathophysiology of FXS. Specifically, *H1a* deletion did not

rescue the protein synthesis independence of mGluR-LTD or altered translational control of FMRP target mRNAs. The latter results support an essential role for FMRP in translational control of its mRNAs and mGluR-LTD. Our results provide new evidence for altered mGluR5-Homer scaffolds in *Fmr1* KO phenotypes and implicate different mechanisms of mGluR5 dysfunction in distinct phenotypes. Modulation and restoration of mGluR5-Homer interactions may represent a novel therapeutic strategy for Fragile X and related cognitive and autistic disorders.

Methods

Animals

Congenic *Fmr1* KO mice (Consortium, 1994) were bred on the C57/BL6J background. Homer1a specific KO mice were generated as described (Hu et al., 2010) and backcrossed at least 5 generations onto the C57/Bl6J mice from the UT Southwestern mouse breeding core facility. All experiments were performed on littermate controls and blind to mouse genotype. Long Evans Hooded rats were obtained from Charles River Laboratories, Wilmington, MA. The animal use protocols used in this manuscript were approved by the UT Southwestern IACUC committee.

Reagents

Drugs were prepared as stocks and stored at -20°C and used within two weeks. Tat-mGluR5ct (YGRKKRRQRRR-ALTPPSPFR) and tat-mGluR5mu (YGRKKRRQRRR-ALTPLSPRR; 5 μM) (Mao et al., 2005) were synthesized at

the UT Southwestern Protein Chemistry Technology Center. The peptide was dissolved in H_20 at a concentration of 5mM, aliquoted and stored at -20°C. Frozen aliquots were used within 10 days. The mixed group I mGluR agonist (RS)-3,5-dihydroxyphenylglycine (DHPG), U0126 and wortmannin were purchased from Tocris Bioscience and prepared as described (Gross et al., 2010; Osterweil et al., 2010b). Cycloheximide was purchased from Sigma, and freshly prepared daily by dissolving directly in ACSF.

Hippocampal slice preparation and LTD recordings

Acute hippocampal brain slices were prepared from 3-6 wk old rats or wildtype (WT), *Fmr1* knockout (*Fmr1* KO), Homer1a knockout (*H1a*-KO), or *Homer1a/Fmr1* double knockout (*H1a/Fmr1* KO) littermates as described previously (Ronesi and Huber, 2008a). LTD recordings were performed and analyzed as described (Ronesi and Huber, 2008a).

mGluR signaling in slices and western blotting

Western blotting on slices was performed as described(Ronesi and Huber, 2008a). Hippocampal slices were preincubated in a static incubation chamber in ACSF containing 5 µM tatmGluR5CT or MU for 4 hours prior to DHPG treatment (Fig. 1) or 30 min in MPEP (10µM; Fig. 3F). Blotting membranes were incubated with the following antibodies according to the manufacturer's instructions: phospho-T56 EF2, total-EF2, phospho- T389 p70S6K, phospho-S2448 mTOR, total mTOR, phospho-T202/Y204 ERK, total-ERK, phospho

S209-eIF4E, phospho S65-4EBP, 4EBP, eIF4G, eIF4E (all from Cell Signaling Technology), Homer (Sc-8921; Santa Cruz), mGluR5 (Millipore), β3 tubulin (Abcam), Arc (Synaptic Systems), Map1b (gift from Dr. Itzhak Fischer, Drexel University), CaMKIIα (Santa Cruz, sc-5391), actin (Millipore, MAB1501). For comparison of phosphoprotein levels across conditions or genotypes immunoreactive phosphoprotein bands were normalized to total protein levels from the same slice homogenates (e.g. P-mTOR/mTOR), each of which was first normalized to loading control (either tubulin, actin or total ERK where indicated).

Coimmunoprecipitation

Hippocampus was lysed in co-immunoprecipitation buffer (50 mM Tris, pH 7.4, 120 mM NaCl, 0.5% NP40), and protein was tumbled overnight at 4°C with 1 µg of antibody (either Homer (Santa Cruz, D-3), Homer1a (Santa Cruz, M-13) or eIF4G (Cell Signaling)). Protein A/G agarose bead slurry (Thermoscientific) was added for one additional hour and the beads were then washed with co-i.p. buffer. Western blotting was performed with the Homer (Santa Cruz, E-18 sc-8921), Homer1a (Hu et al., 2010), mGluR5 (Millipore), eIF4E (Cell Signaling) or eIF4G (Cell Signaling).

Real-time RT-PCR

Hippocampi were homogenized in TRIzol reagent (Invitrogen) followed by RNA extraction according to manufacturer's protocol. 2 µg RNA from each sample was subjected to first-strand cDNA synthesis by SuperScript III First-

Strand synthesis system (Invitrogen) with two independent primers targeting on the 3'UTR of the mRNAs (Homer1a: 5'-GTG GTA AAG CTT TCC TTC AGA G-3' and 5'-GGC ACC TCT GTG GGC CTG TGG-3'; GAPDH: 5'-GGT ATT CAA GAG AGT AGG GAG-3' and 5'-GGG TGC AGC GAA CTT TAT TG-3'). PCR reaction was performed by GoTag Green DNA polymerase (Promega) with specific primers against Homer1a: (5'-TGA TTG CTG AAT TGA ATG TGT ACC-3' and 5'-GAA GTC GCA GGA GAA GAT G-3') (Potschka et al., 2002) and GAPDH: (5'-AGG TCG GTG TGA ACG GAT TTG-3' and 5'-TGT AGA CCA TGT AGT TGA GGT CA-3').

Metabolic labeling of hippocampal slices

Hippocampal slices were prepared as described(Ronesi and Huber, 2008a), (Osterweil et al., 2010b). For these experiments (Fig. 3) the most ventral slices (2 per hippocampus) were used since basal protein synthesis rates differ between dorsal and ventral hippocampal slices (Osterweil et al., 2010b). Slices recovered for 3.5 hours in ACSF at 32°C, and then were incubated in actinomycin D (25 µM) for 30 min. Where indicated, 20 µM U0126, or 100 nM wortmannin was added at this step. For experiments with tatmGluR5 peptides, slices were preincubated in ACSF containing 5 µM tatmGluR5CT or MU for 4 hours prior to actinomycin incubation.

Neocortical Slice preparation and UP state recordings

UP state experiments in neocortical slices were performed and analyzed as described (Hays et al., 2011).To allow time for the tatmGluR5 peptides to permeate slices, the peptide containing ACSF was perfused onto the slices in the interface chamber for 4 hr prior to recording and was supplemented with 10 μM HEPES pH7.4, 0.05% BSA, and 5 μM of the appropriate peptide. The peptide-BSA containing ACSF was not oxygenated directly, but slices were oxygenated in the interface recording chamber.

Audiogenic seizures

In order to evaluate audiogenic seizures, mice were placed in a plastic chamber (30X19X12cm) containing a 120 decibel siren (GE 50246 personal security alarm) and covered with a Styrofoam lid. A 120 dB siren was presented to mice for 5 minutes. Mice were videotaped and scored for behavioral phenotype: 0=no response, 1=wild running, 2=tonic-clonic seizures, 3=status epilepticus/death as described (Dolen et al., 2007).

Behavioral measurements

Open Field Activity: Mice were placed individually into the periphery of a novel open field environment (44 cm x 44 cm, walls 30 cm high) in a dimly lit room and allowed to explore for 5 min. The animals were monitored from above by a video camera connected to a computer running video tracking software (Ethovision 3.0, Noldus) to determine the time, distance moved and number of entries into two areas: the periphery (5 cm from the walls) and the center (all areas excluding the

periphery). The open field arenas were wiped and allowed to dry between mice. Time in the center was used as a measure of anxiety.

Locomotor Activity: Mice were placed individually into a new, plastic mouse cage (18 cm x 28 cm) which was located inside a dark Plexiglas box. Movement was monitored by 5 photobeams in one dimension (Photobeam Activity System, San Diego Instruments) for 2 hours, with the number of beam breaks recorded every 5 min. Data were analyzed with an ANOVA with genotype and time as the dependent variables.

Statistics:

Data plotted in the figures represents the mean ± SEM. Significant differences were determined using independent or paired t-tests (for determining effects of mGluR5CT peptide). For comparisons between WT, *Fmr1* KO, *H1a* KO and *H1a/Fmr1* KO a 2-way ANOVA and Bonferroni posttests were used. Statistics on nominal data, such as seizure severity and incidence (Fig. 6A; Supplementary Table 3), a Chi squared (Fisher's Exact test) was used. Group data is presented in the figures as mean ±SEM. *p< 0.05; **p< 0.01; ***p<0.001.

Results

Disruption of mGluR5-Homer regulates signaling to translation

To investigate if the altered mGluR5-Homer scaffolds contribute to the mGluR5 dysfunction in *Fmr1* KO mice we determined if disruption of mGluR5-

Homer scaffolds with a peptide in wildtype (WT) mice mimicked mGluR5 signaling alterations in the *Fmr1* KO mice. The rationale for this approach is based on data that *H1a*-bound mGluR5, which is increased in *Fmr1* KO, is functionally equivalent to mGluR5 that cannot interact with any Homer isoform (Ango et al., 2001; Tu et al., 1998; Xiao et al., 1998). To disrupt mGluR5-Homer, we incubated acute hippocampal slices from WT mice in a cell permeable (Tat-fused) peptide containing the Proline-rich motif (PPxxF) of the mGluR5 C-terminal tail that binds the EVH1 domain of Homer, mGluR5CT (CT; 5 μM) (Mao et al., 2005; Ronesi and Huber, 2008b; Tu et al., 1998). mGluR5CT reduced mGluR5-Homer interactions to 41±6% of that observed in slices with no peptide treatment (n = 3 mice; p = 0.003) as determined by co-immunoprecipitation of mGluR5 and Homer (Fig. 1A). Importantly, CT peptide treatment roughly mimics the 50% decrease in mGluR5-long Homer interaction observed in *Fmr1* KO hippocampal lysates (Fig. 2A). As a control, slices were incubated in a peptide with a mutated Homer binding motif, mGluR5MU (MU) (Mao et al., 2005; Tu et al., 1998). mGluR5MU peptide had no effect on mGluR-Homer in comparison in slices with no peptide treatment (103±8% of untreated; n = 3; Fig. 1A).

Fmr1 KO mice display a deficit in mGluR1/5 stimulation of protein synthesis which may be a result of altered mGluR5- Homer interactions.

Previously, we reported that CT-peptide mediated disruption of mGluR5-Homer interactions in rat hippocampal slices inhibited group 1 mGluR activation of the PI3K-mTOR pathway and translation initiation, but not ERK (Ronesi and Huber, 2008b). Here we observed similar effects in hippocampal slices from WT mice. mGluR5CT peptide incubation blocked activation of PI3K-mTOR in response to the group 1 mGluR agonist, (RS)-3,5-Dihydroxyphenylglycine (DHPG; 100 μM; 5 min) as measured by phosphorylation of mTOR (S2448) and S6K (Thr389) (P-mTOR: MU: 196±27% of basal, n=8; CT: 94±20% of basal, n=8; $p < 0.01$; P-S6K; MU: 300±80% of basal, n=6; CT: 114±13% of basal, n=6; $p < 0.05$; Fig. 1B,C) and had no effect on ERK activation (Thr202/Tyr204; P-ERK; MU: 495±117% of basal, n=4; CT: 477±162% of basal, n=4; n.s.; Fig. 1D) (Ronesi and Huber, 2008b). The CT peptide did not affect basal levels of P-mTOR, P-S6K or P-ERK (Supplementary Table 1) (Ronesi and Huber, 2008a)

Homer and mGluR5 each directly interact with another translational regulatory factor, Elongation Factor 2 kinase (EF2K) (Park et al., 2008). Although phosphorylation of elongation factor 2 (EF2) by EF2K inhibits translation elongation globally, EF2K is required for translational activation of mRNAs such as such as *Arc* (activity-regulated cytoskeleton associated protein), and *αCaMKII*(Park et al., 2008). A moderate inhibition of elongation globally by EF2K is thought to release translation factors that are then available for translational activation of poorly initiated transcripts. Surprisingly, mGluR5CT-

treated slices displayed a robust increase in phosphorylation of EF2 (T56) in response to DHPG (590±118% of basal; n = 15 slices, Fig. 1E) in comparison to mGluR5MU treated slices (294±63% of basal; n = 15; p< 0.05;.Supplementary Fig. 1). The CT peptide did not affect basal levels of P-EF2 (Supplementary Table 1). Taken together, our data suggest that Homer interactions facilitate mGluR activation of the PI3K-mTOR pathway to translation initiation, but dampen mGluR-induced phosphorylation of P-EF2 and thus restrain inhibition of global elongation rates. Consequently, disruption of mGluR5-Homer would be expected to block mRNA translation by blocking activation of the PI3K-mTOR pathway and translation initiation and enhancing inhibition of elongation to a level that may block elongation of all transcripts, including *Arc*. Consistent with this model, disrupting mGluR5-Homer interactions in hippocampal slices with CT peptide blocks DHPG-induced synthesis of Arc (MU: 122+/-5% of untreated, n=7; CT: 95+/-7% of untreated, n=7; Supplementary Fig. 1) and Elongation factor 1α (EF1α)(Ronesi and Huber, 2008b).

Deletion of Homer1a rescues mGluR signaling in Fmr1 KO

mGluR5-long Homer interactions are reduced in *Fmr1* KO mice and we hypothesize that this contributes to altered mGluR5 function. If so, then mGluR signaling to translation in *Fmr1* KO slices may mimic what is observed with CT peptide treatment of WT slices (as in Fig. 1). In support of our hypothesis, DHPG-induced activation of PI3K, mTOR and p70 ribosomal S6 kinase (S6K) is

deficient in *Fmr1* KO hippocampal slices and ERK activation is unaffected (Fig. 2B; (Osterweil et al., 2010b; Ronesi and Huber, 2008a; Sharma et al., 2010)). Furthermore, DHPG-induced phosphorylation of EF2 is enhanced in *Fmr1* KO slices relative to WT littermates (WT: 787±135% of untreated, n=7 mice; *Fmr1* KO: 1452±176% of untreated, n=6 mice; Fig. 2C). Remarkably, these alterations in mGluR signaling parallel what is observed with CT peptide treatment of WT slices (Fig. 1). Basal levels of Phospho- or total EF2 or S6K are unchanged in *Fmr1* KO slices (Supplementary Table 2) (Ronesi and Huber, 2008a). These results indicate that mGluR5 function is not generally enhanced or decreased in *Fmr1* KO mice, but is changed in a complex way that is mimicked in WT mice by disruption of mGluR5-Homer interactions.

In *Fmr1* KO mice, mGluR5 is more associated with H1a (Giuffrida et al., 2005) (Supplementary Fig. 2a). Because long Homers compete with H1a for interactions with their effectors (Tu et al., 1998; Xiao et al., 1998), we hypothesized that genetic deletion of *H1a* in *Fmr1* KO mice may restore normal mGluR5-long Homer interactions and mGluR5 function. To test this idea, *Fmr1* KO mice were bred with mice with a genetic deletion of *H1a* to create *H1a/Fmr1* double knockouts (Hu et al., 2010). *H1a* KOs have normal levels of the long Homer isoforms 1, 2 and 3 (Hu et al., 2010). In agreement with Giuffrida et al., (2005), co-immunoprecipitation of long Homer isoforms from *Fmr1* KO forebrain revealed a reduced association of mGluR5 in comparison to WT littermates (Fig.

2A), whereas, co-IP of *H1a* revealed an increased association with mGluR5 (Supplementary Fig. 2). Total levels of mGluR5, long Homers and H1a (protein and mRNA) in *Fmr1* KO hippocampi were not different from WT (Fig. 2A; Supplementary Fig. 2). Genetic deletion of *H1a* restored normal mGluR5-Homer interactions in *Fmr1* KO mice (n = 4 mice per genotype; Fig. 2A) but did not affect levels of mGluR5, long Homers or their interactions on a WT background (Fig. 2A; Supplementary Fig. 2)(Hu et al., 2010). To determine if *H1a* deletion restored normal mGluR5 signaling in *Fmr1* KO mice, we examined mGluR signaling to the mTOR and EF2K translational regulatory pathways. The deficit in mGluR5 signaling to mTOR in *Fmr1* KO, as measured by S6K (T389) phosphorylation, (WT: 242±34% of basal, n=21; *Fmr1* KO: 135±15%, n=19; Fig. 2B) was restored in *H1a/Fmr1* KO (220±28% of untreated, n=18). Similarly, enhanced mGluR activation of EF2K was rescued to wildtype levels by H1a deletion (*H1a/Fmr1* KO; 826±192% of basal, n=7; Fig. 2C). *H1a* KOs exhibited normal DHPG-induced phosphorylation of EF2 (796±159% of untreated, n=6) and S6K (227±34% of treated, n=14). There was no effect of *Fmr1* or *H1a* genotype on basal levels of phosphorylated or total EF2 or S6K (Supplementary Table 2). Furthermore, DHPG treatment did not alter levels of total EF2 or S6K in any genotype (Supplementary Table 2) (Ronesi and Huber, 2008b; Sharma et al., 2010)

H1a deletion rescues enhanced translation rates in Fmr1 KO

Although DHPG-induced translation is absent in *Fmr1* KO mice, basal translation rates in brain are elevated (Bassell and Warren, 2008; Dolen et al., 2010; Gross et al., 2010; Osterweil et al., 2010b). Enhanced protein synthesis in hippocampal slices is reversed by pharmacological blockade of mGluR5 or ERK activation, but not by an inhibitor of PI3K or mTOR (Osterweil et al., 2010b) (Fig. 3C; Supplementary Fig. 4). Another consequence of mGluR5-*H1a* interactions is constitutive, or agonist-independent mGluR5 activity (Ango et al., 2001) which may drive translation rates through ERK activation, a pathway that remains intact in *Fmr1* KO mice and with Homer disruption (Fig. 1D) (Osterweil et al., 2010b; Ronesi and Huber, 2008a). In support of this hypothesis, genetic deletion of *H1a* rescues enhanced translation rates as measured by ^{35}S Met incorporation in hippocampal slice proteins (*Fmr1* KO 122±4% of WT, n=14 slices from 7 mice; *H1a* KO 102±4% of WT, n=8 slices from 4 mice; double *H1a/Fmr1* KO 106±6% of WT, n=7 slices from 4 mice; Fig. 3A). Furthermore, CT peptide-mediated disruption of mGluR5-Homer in WT slices is sufficient to mimic enhanced protein synthesis rates to that observed in *Fmr1* KO slices (CT =123 ± 6% of MU treated, n=16 slices per peptide from 10 mice; p = 0.002; Fig. 3B). In contrast, mGluR5CT has no effect on protein synthesis rates in *Fmr1* KO slices (CT =106 ± 8% of MU treated, n=14 (CT) or 15 (MU) slices from 8 mice; p = 0.5; Fig. 3B).

Translation initiation is the rate limiting step in translation (Proud, 2007). To determine if enhanced translation rates in *Fmr1* KO stem from increased initiation, we measured eIF4F translation initiation complexes in hippocampal slices prepared from WT, *Fmr1* KO, *H1a* KO and *H1a/Fmr1* KO mice. The eIF4F complex is composed of the 5' cap binding protein eIF4E, a scaffolding protein eIF4G, and the RNA helicase eIF4A (Proud, 2007). eIF4F complex assembly can be measured by co-immunoprecipitation of eIF4G and eIF4E and is stimulated by DHPG in WT animals (Banko et al., 2006). Therefore, we also measured eIF4F complex in DHPG-stimulated slices from each genotype. Consistent with previous reports, eIF4F complex levels are enhanced basally in *Fmr1* KO slices and no longer stimulated by DHPG (Fig. 3D) (Sharma et al., 2010). Like ^{35}S Met incorporation, eIF4F complex levels in *Fmr1* KO slices are restored to WT levels by *H1a* deletion (Fig. 3D; n = 3 mice per condition). Genetic deletion of *H1a* also rescues the deficit in DHPG-stimulated eIF4F complex assembly in the *Fmr1* KO (Fig. 3D). These results suggest that elevated protein synthesis rates in *Fmr1* KO mice are due to enhanced translation initiation that is driven by *H1a*-bound mGluR5. The deficit in mGluR-stimulated translation initiation in *Fmr1* KO mice may be because eIF4F complex levels are saturated basally. Furthermore, mGluR-activation of mTOR is rescued in *Fmr1* KO mice by *H1a* deletion (see Fig.2) which may also contribute to restoration of DHPG-induced eIF4F complex assembly (Banko et al., 2006).

To determine how increased *H1a*-mGluR5 interactions lead to enhanced signaling to translation downstream of ERK, we examined phosphorylation of initiation factors known to be regulated by ERK in WT and *Fmr1* KO cortical homogenates and the effects of *H1a* deletion. ERK phosphorylates and activates MAPK-interacting kinase (Mnk) which in turn phosphorylates the cap-binding protein eIF4E (S209) (Proud, 2007). ERK also phosphorylates eIF4E binding protein (4EBP) at S65, a distinct site from mTOR regulated sites (T36/45) (Herbert et al., 2002). ERK- dependent phosphorylation of eIF4E and 4EBP (S65) is associated with increased translation rates in neurons and other cell types (Banko et al., 2006; Kelleher et al., 2004). Consistent with a role for ERK in phosphorylation of these initiation factors in hippocampal slices, Phospho-(S209)-eIF4E and (S65)-4EBP, was strongly reduced or abolished by U0126 treatment (Supplementary Fig. 3). P-4EBP and P-eIF4E levels were enhanced in cortical homogenates from *Fmr1* KO mice, an effect that was rescued by *H1a* deletion (Fig. 3E). As reported in hippocampal slices (Fig. 1D) (Osterweil et al., 2010b; Ronesi and Huber, 2008b), P-ERK levels were unchanged in *Fmr1* KO lysates (Fig. 3E). To determine if mGluR5 activity abnormally drives phosphorylation of ERK, eIF4E and 4EBP (S65) in *Fmr1* KO mice, hippocampal slices from both WT and *Fmr1* KO mice were treated with the mGluR5 inverse agonist, MPEP (10 μM). MPEP treatment did not affect P-4EBP or P-eIF4E in WT slices. However, in *Fmr1* KO slices, MPEP reduced P-4EBP and P-eIF4E by ~50% (Fig. 3F).

Surprisingly, MPEP had no effect on P-ERK levels in either WT or *Fmr1* KO slices. These results support our hypothesis that *H1a*-mediated mGluR5 activity drives translation initiation through ERK phosphorylation of initiation factors. Because P-ERK levels are not affected in *Fmr1* KO or with MPEP, this suggests that mGluR5 may regulate accessibility or localization of eIF4E or 4EBP with ERK, as opposed to ERK activity per se.

Altered LTD is not rescued by deletion of Homer1a

In wildtype animals, mGluR-dependent long-term synaptic depression (mGluR-LTD) within the CA1 region of the hippocampus requires dendritic protein synthesis of FMRP-interacting mRNAs such as Arc and MAP1b (Luscher and Huber, 2010; Park et al., 2008; Waung et al., 2008). Although mGluR activation induces robust LTD in *Fmr1* KO mice, mGluR-induced synthesis of Arc and MAP1b is deficient and LTD is independent of new protein synthesis (Luscher and Huber, 2010; Park et al., 2008). From this work it has been suggested that loss of FMRP-mediated translational suppression leads to enhanced steady state levels of "LTD proteins" which allow mGluR-LTD to persist without new protein synthesis (Luscher and Huber, 2010). Consistent with this hypothesis, elevated levels of MAP1b and Arc have been reported in *Fmr1* KO neurons (Luscher and Huber, 2010; Zalfa et al., 2003). Alternatively, *H1a* bound, and constitutively active mGluR5 which drives total protein synthesis rates (Fig. 3) (Osterweil et al., 2010b) could elevate "LTD protein" levels and lead to protein synthesis-

independent LTD. To distinguish between these possibilities, we determined if genetic deletion of *H1a* reversed the protein synthesis independence of mGluR-LTD and enhanced levels of specific FMRP target mRNAs. To test the protein synthesis dependence of mGluR-LTD, slices were preincubated in the translation inhibitor cycloheximide (60 μM). Although mGluR-LTD was reliably induced with DHPG in the double *H1a/Fmr1* KO (81±3% of baseline 60-70 min after DHPG application, n=11 slices), LTD was not sensitive to cycloheximide (78±1% of baseline, n=9), similar to the *Fmr1* KO (control: 74±4% of baseline, n=7; cycloheximide: 79±3% of baseline, n=9; Fig. 4B,C) (Park et al., 2008). LTD was inhibited by cycloheximide treatment in both WT (control: 76±1% of baseline, n=7; cycloheximide 92±4% of baseline, n=8; p = 0.002) and *H1a* KO mice (control: 65±5% of baseline, n=6; cycloheximide: 88±5% of baseline, n=6; p = 0.01; Fig. 4A, D). These results suggest that the altered mGluR5-Homer scaffolds in *Fmr1* KO mice do not mediate the protein synthesis independence of mGluR-LTD.

To determine if H1a deletion in *Fmr1* KO mice rescued elevated steady state levels of LTD-promoting proteins or other FMRP target mRNAs we performed western blots of MAP1b, Arc and αCaMKII in hippocampal homogenates of WT, *Fmr1* KO, *H1a* KO and *H1a/Fmr1* KO mice (Fig. 4E). MAP1b and αCaMKII, were elevated in both *Fmr1* KO mice and *H1a/Fmr1* KO mice in comparison to WT and *H1a* KO mice (Fig. 4E) indicating that *H1a*

deletion does not restore normal levels of Map1b and αCaMKII in *Fmr1* KO mice. Although we did not detect elevated steady state protein levels of Arc in hippocampal homogenates of *Fmr1* KO mice, we observed a deficit in DHPG-induced synthesis of Arc in hippocampal slices from *Fmr1* KO mice in comparison to WT (WT: 140±17% of basal or untreated, n=12; *Fmr1* KO: 98±12% of untreated, n=12; Fig. 4F). However, *H1a* deletion did not restore mGluR-induced synthesis of Arc in *Fmr1* KO mice (Park et al., 2008) (*H1a/Fmr1* KO: 91±12% of untreated, n=11). DHPG induced synthesis of Arc was normal in *H1a* KO mice (139±11% of untreated, n=11). These results reveal that altered mGluR5-Homer scaffolds in the *Fmr1* KO mice do not mediate abnormal mGluR-LTD or altered translational control of specific FMRP target mRNAs. Instead, these results support an essential role for FMRP interactions with its target mRNAs in mGluR-LTD and translational control of these mRNAs (Supplementary Fig. 6B) (Bassell and Warren, 2008; Muddashetty et al., 2011).

mGluR5-Homer and hyperexcitable neocortical circuits

FXS patients and *Fmr1* KO mice exhibit sensory hypersensitivity, epilepsy and/or audiogenic seizures suggestive of an underlying sensory circuit hyperexcitability (Berry-Kravis, 2002; Dolen et al., 2010). We recently discovered synaptic and circuit alterations indicative of hyperexcitability in the somatosensory, barrel neocortex of *Fmr1* KO mice. Neocortical slices of *Fmr1* KO mice have decreased excitatory drive onto layer IV fast-spiking interneurons

and prolonged thalamically-evoked and spontaneously-occurring persistent activity, or UP, states (Gibson et al., 2008; Hays et al., 2011). UP states represent a normal physiological rhythm generated by the recurrent neocortical synaptic connections and is observed in alert and slow-wave sleep states *in vivo* as well as neocortical slice preparations (Haider and McCormick, 2009; Sanchez-Vives and McCormick, 2000). Importantly, genetic or pharmacological reduction of mGluR5 in *Fmr1* KO mice rescues the prolonged UP states in acute slices and *in vivo* (Hays et al., 2011). To determine if altered mGluR5-Homer interactions contribute to altered neocortical circuit function and hyperexcitability in *Fmr1* KO mice we measured spontaneously occurring UP states in acute slices from somatosensory, barrel cortex using extracellular multiunit recordings (Sanchez-Vives and McCormick, 2000). As previously reported (Gibson et al., 2008; Hays et al., 2011), UP states are longer in slices of *Fmr1* KO mice in comparison to WT littermates (WT: 797.4±31.47 ms, n=22 slices; *Fmr1*-KO: 1212±87.9 ms, n=13; Fig. 5A,B). In support for a role for altered Homer interactions, UP state duration was shortened to WT levels by *H1a* deletion (*H1a/Fmr1* KO; 872.2±42.1 ms, n=44; Fig. 5A, B). Loss of *H1a* alone does not affect UP states, ruling out general alterations in excitability (*H1a*-KO: 767.7±35.8 ms, n=18).

We next determined if CT peptide-mediated disruption of mGluR5-Homer was sufficient to prolong UP states in WT slices. Preincubation of WT neocortical slices in CT peptide increased the duration of UP states in comparison

to control peptide (mGluR5MU) treatment (WT+MU: 909.8±103.7 ms, n=13 slices; WT+CT: 1408.8±156.4 ms, n=15; Fig. 5C,D). Therefore, acute disruption of mGluR5-Homer complexes is sufficient to mimic the circuit hyperexcitability in *Fmr1* KO mice. In contrast, mGluR5CT had no effect on the duration of UP states in *Fmr1* KO slices (KO+MU: 2014.9±117.9 ms, n=15; KO+CT: 1819.8±163.8 ms, n=12; Fig. 5C,D), likely because Homer complexes are already disrupted in these mice.

H1a deletion reverses behavioral phenotypes in Fmr1 KO

To determine if *H1a* deletion rescued any *in vivo* or behavioral phenotypes in *Fmr1* KO mice, we measured the incidence of audiogenic seizures and anxiety as measured using the open field activity test across the 4 genotypes. We chose these phenotypes because they are robust in the C57BL6 strain of *Fmr1* KO mice and sensitive to mGluR5 antagonists (Dolen et al., 2010). Consistent with previous reports, *Fmr1* KO display increased seizure incidence and severity following exposure to a loud sound relative to WT and *H1a* KO mice whom exhibited little or no incidence of seizure (Seizure score (0-3; 3 being most severe; see methods); WT = 0.12±0.12; n = 16 mice; *H1a* KO = 0.04±0.04; n = 24; *Fmr1* KO=1.6 ±0.2; n = 39; $p< 0.001$ (*Fmr1* KO vs. WT or *H1a* KO; Fig. 6A; Supplementary Table 3)). *H1a/Fmr1* KO mice responded with a reduced incidence and severity of seizure in comparison to *Fmr1* KO littermates

(*H1a/Fmr1* KO mice = 1.1±0.2; n = 37; $p < 0.05$ (*H1a/Fmr1* KO vs. *Fmr1* KO)). However, *H1a/Fmr1* KO mice displayed an increased level of seizures in comparison to WT or *H1a* KO ($p< 0.001$; Fig. 6A). Such a partial rescue of the audiogenic seizures by *H1a* deletion is similar to what is observed with genetic reduction of mGluR5 in *Fmr1* KO mice (Dolen et al., 2007).

As previously reported, *Fmr1* KO mice spend more time in the center of a lit open field in comparison to WT littermates which has been interpreted as reduced generalized anxiety in the mice(Liu and Smith, 2009) (Fig. 6B; WT = 85±8 sec; n = 18 mice; *Fmr1* KO = 138±12; n = 24; $p< 0.01$). *H1a* KO mice were not different than WT mice in this behavior (*H1a* KO = 75±10 sec; n = 17). Importantly, *H1a/Fmr1* KO behave as WT mice (*H1a/Fmr1* KO = 91±10 sec; n = 17), spending significantly less time than *Fmr1* KO mice ($p< 0.01$) in the center of an open arena. There were no differences in locomotor activity between any genotype (Supplementary Figure 4). Therefore, *H1a* deletion completely rescued the open field activity phenotype and suggests that altered mGluR5- Homer interactions contribute to altered behavior in *Fmr1* KO mice and may be relevant for altered behaviors in FXS patients.

Discussion

Two mechanisms for mGluR dysfunction in Fragile X Syndrome

Here we demonstrate a causative role for reduced Homer scaffolds in mGluR5 dysfunction in a model of human neurological disease. MGluR5 dysfunction in animal models of FXS is well established and genetic or pharmacological reduction of mGluR5 activity reduces or rescues many disease phenotypes in animal models (Dolen et al., 2010) and most recently in patients (Jacquemont et al., 2011). However, the molecular basis for mGluR5 dysfunction in FXS was essentially unknown. It has been suggested that loss of an FMRP mediated translational "brake" downstream of mGluR5 leads to enhanced mGluR5 function (Bear et al., 2004; Dolen et al., 2010), but this mechanism cannot account for the deficits in mGluR5 signaling or translation independent dysfunction of mGluR5 associated with FXS (Hays et al., 2011; Ronesi and Huber, 2008a). Our results reveal two mechanisms for mGluR5 dysfunction in *Fmr1* KO mice. First, an imbalance of mGluR5 interactions from long to short Homer1a isoforms, leads to altered mGluR5 signaling, enhanced basal translation rates, neocortical hyperexcitability, audiogenic seizures and open field activity (Supplementary Fig. 6A). Because *H1a* bound mGluR5 is constitutively active or agonist-independent, our results strongly suggest that the therapeutic action of mGluR5 inverse agonists, such as MPEP (Ango et al., 2001), in FXS phenotypes are due, in part, to inhibition of *H1a*-bound, constitutively active mGluR5. Second, our results reveal that disrupted Homer scaffolds in *Fmr1* KO mice cannot account for altered mGluR-LTD or abnormal translational control of

FMRP target mRNAs (Fig. 4; Supplementary Fig. 6B) and implicate an essential role for FMRP binding to and translational regulation of specific mRNAs in mGluR-LTD. The discovery that altered Homer scaffolds account for much of the complex dysfunction of mGluR5 in FXS will help to develop alternative, targeted therapies for the disease and provide mechanistic links to other genetic causes of autism.

Homer scaffolds coordinate mGluR regulation of translation

Our data demonstrate novel functional roles for Homer scaffolds in coordination of mGluR-stimulated translation by facilitating activation of the PI3K-mTOR pathway and translation initiation (Ronesi and Huber, 2008a), as well as limiting activation of EF2K and subsequent inhibition of elongation (Figs. 1,2). Homer scaffolds with the PI3K enhancer (PIKE), a small GTPase which binds and activates PI3K in response to mGluR activation (Shiraishi-Yamaguchi and Furuichi, 2007). The PI3K pathway stimulates mTOR to phosphorylate eIF4E binding protein (4EBP) which in turn releases eIF4E to interact with eIF4G and form the eIF4F translation initiation complex(Proud, 2007). Furthermore, mTOR phosphorylates p70 S6K to stimulate translation of 5' terminal oligopyrmidine tract (5' TOP) mRNAs that encode ribosomes and translation factors, thus increasing the translational capacity of the cell (Proud, 2007). mGluR activation of PI3K-mTOR-S6K pathway is blocked by mGluR5CT and the deficits in mGluR-activation of mTOR and initiation complex (eIF4F)

formation in *Fmr1* KO mice are restored by *H1a* deletion indicating a key role for Homer scaffolds in mGluR-stimulated translation initiation (Ronesi and Huber, 2008a).

Although somewhat counterintuitive, mGluRs stimulate phosphorylation of EF2 which in turn inhibits elongation rate (Park et al., 2008). EF2K and moderate inhibition of elongation are necessary for mGluR-induced synthesis of Arc, as well as mGluR-LTD (Park et al., 2008). Submaximal inhibition of global elongation may make available rate limiting factors to translate mRNAs that are poorly initiated and cannot compete effectively for these factors (Scheetz et al., 2000). Long Homer interactions limit EF2K activation by mGluRs and thus would be expected to temper mGluR-mediated inhibition of general elongation, and in turn, promote translation of poorly initiated mRNAs (Park et al., 2008). Consequently, disruption of mGluR5-Homer enhances EF2K activity and would be expected to strongly inhibit elongation and block translational activation. Although we do not rescue abnormal mGluR-LTD in *Fmr1* KO neurons by deletion of H1a, in WT slices mGluR5Ct peptide treatment blocks mGluR-induced synthesis of Arc (Supplementary Fig. 1C) and mGluR-LTD (Ronesi and Huber, 2008a). These results indicate that in WT neurons, where mGluR-LTD requires de novo protein synthesis, mGluR5-Homer interactions are necessary to properly stimulate translation and induce LTD.

In *Fmr1* KO mice there is a deficit in mGluR stimulation of PI3K-mTOR and eIF4F initiation complex formation, whereas EF2K activation is dramatically enhanced. These changes would be expected to block mGluR-induced translational initiation and strongly inhibit elongation. mGluR-induced rapid synthesis of many proteins (e.g. PSD-95, EF1a, APP, Arc, CaMKII, MAP1b), is absent in *Fmr1* KO mice (Bassell and Warren, 2008) that may be mediated, in part, by disrupted mGluR-Homer scaffolds and altered signaling to translation machinery. Alternatively or in addition, because FMRP interacts with these mRNAs, it is likely required for mGluR-triggered translational activation of specific target mRNAs (Bassell and Warren, 2008; Muddashetty et al., 2011). The fact that *H1a* deletion rescues mGluR-mediated translation initiation complex formation (Fig. 3D) but not synthesis of Arc (Fig. 4), suggests a requirement for both mGluR5-Homer scaffolds and FMRP in mGluR-triggered Arc translation.

Altered mGluR5-Homer scaffolds increase translation rates

Although there is a deficit in mGluR agonist-stimulated translation in *Fmr1* KO mice, steady state translation rates and levels of specific proteins are elevated (Osterweil et al., 2010b; Sharma et al., 2010), thus reflecting the complexity of translational control. Because one function of FMRP is to suppress translation of its mRNA targets (Bassell and Warren, 2008), an obvious possibility was that the elevated protein synthesis rates and levels directly result from loss of FMRP-mediated suppression of mRNA targets. In support of this

hypothesis, *H1a* deletion does not reverse enhanced protein levels of Map1b and CaMKII (Fig. 4). However, elevated total protein synthesis rates and translation initiation (eIF4F) complexes were rescued by *H1a* deletion and mimicked in WT mice by mGluR5CT peptide treatment (Fig. 3). Thus, increased steady state translation rates in *Fmr1* KO tissue are a result of altered mGluR5-Homer scaffolds that are a secondary consequence of FMRP loss. Elevated protein synthesis rates in *Fmr1* KO hippocampal slices are reversed by the genetic reduction of mGluR5 (*Grm5het*), the mGluR5 inverse agonist MPEP, and inhibitors of ERK (Dolen et al., 2010; Osterweil et al., 2010b) (Fig. 3C). In *Fmr1* KO cortical lysates, we observed enhanced phosphorylation of translation initiation factors that are downstream of ERK (eIF4E and 4EBP) which was reversed by *H1a* deletion (Fig. 3E). Furthermore, blocking mGluR5 activity with MPEP strongly reduced P-eIF4E and P-4EBP in *Fmr1* KO, but not WT, hippocampal slices (Fig. 3F). Together these results suggest that *H1a*-bound and constitutively active mGluR5 in *Fmr1* KO neurons (Ango et al., 2001) drives ERK-dependent phosphorylation of eIF4E and 4EBP which enhances eIF4F initiation complex formation and translation rates. Because we do not observe an effect of *Fmr1* KO or MPEP on Phospho-ERK levels as detected by western blot, this suggests that mGluR5 drives ERK activity that is either not detectable by phosphorylation at T202/Y204 and/or regulates accessibility of eIF4E and 4EBP to ERK.

In contrast to hippocampus, recent results from neocortical synaptoneurosomes of *Fmr1* KO mice demonstrate a role for PI3K activity in enhanced protein synthesis rates (Gross et al., 2010). We observed that the PI3K inhibitor wortmannin equalized translation rates between WT and *Fmr1* KO hippocampal slices, but this was because wortmannin increased translation rates in WT, but not *Fmr1* KO, slices (Supplementary Fig. 4). Furthermore, elevated basal phosphorylation of PI3K, mTOR and 4EBP (at the mTOR sites) was recently reported in fresh hippocampal lysates of *Fmr1* KO mice, perhaps a result of increased PIKE levels (Osterweil et al., 2010b; Sharma et al., 2010). Although we are unable to detect elevated basal activation of PI3K-mTOR pathway in our slice preparation (Ronesi and Huber, 2008a) (Supplementary Table 2), persistent activation of downstream effectors of PI3K and mTOR together with constitutive mGluR5-driven ERK may elevate translation rates in *Fmr1* KO. P-EF2 levels are unchanged in *Fmr1* KO slices (Supplementary Table 2) suggesting that basal or constitutive mGluR5 activity is not sufficient to activate EF2K. The detailed mechanisms by which ERK, PI3K and mTOR, and EF2K contribute to elevated, basal protein synthesis rates in *Fmr1* KO mice requires further study and may differ depending on the brain region, subcellular compartment or preparation.

An essential role for FMRP in proper regulation of LTD

H1a deletion and restoration of mGluR5-Homer scaffolds in *Fmr1* KO mice did not rescue the protein synthesis independence of mGluR-LTD nor elevated steady state protein levels of FMRP target mRNAs, MAP1b and αCaMKII (Fig. 4). This supports the hypothesis that the protein synthesis independence of mGluR-LTD in *Fmr1* KO mice is a result of loss of FMRP-mediated translational suppression of LTD promoting proteins, such as Map1b (Waung and Huber, 2009). Because *H1a* deletion rescued the elevated ^{35}S Met incorporation, but not altered mGluR-LTD and enhanced MAP1b and CaMKII levels, this suggests that altered LTD and elevated Map1b and CaMKII are not a result of elevated total protein synthesis rates. Furthermore, the fact that mGluR-triggered Arc synthesis was not rescued by *H1a* deletion supports an essential role for FMRP in mGluR-triggered translational activation of Arc. Recent work has implicated mGluR-triggered dephosphorylation of FMRP in translational activation of FMRP target mRNAs, such as SAPAP3 and PSD-95 (Bassell and Warren, 2008; Muddashetty et al., 2011).

Altered mGluR5-Homer and neocortical network dysfunction

Altered neocortical circuit function and hyperexcitability have been predicted to contribute to cognitive disorders and autism (Rubenstein and Merzenich, 2003; Uhlhaas and Singer, 2006). The epilepsy and EEG abnormalities observed in FXS patients are indicative of brain hyperexcitability (Berry-Kravis, 2002; Dolen et al., 2010). Furthermore, FXS patients display

hypersensitivity to sensory stimuli, and *Fmr1* KO mice have audiogenic seizures reflecting hyperexcitability of sensory circuits (Berry-Kravis, 2002; Dolen et al., 2010). Although UP states are a normal physiological rhythm and are not epileptiform activity, they provide an effective readout of the state of circuit function and excitability (Sanchez-Vives and McCormick, 2000). Furthermore, UP states underlie the slow oscillations that occur during slow wave sleep and are implicated in memory consolidation as well as sensory processing in waking states (Haider and McCormick, 2009). Therefore, altered neocortical UP states in the *Fmr1* KO (Gibson et al., 2008; Hays et al., 2011) may be relevant to the sensory processing and cognitive abnormalities in FXS patients.

Our findings indicate that the longer UP states in *Fmr1* KO neocortex are mediated by enhanced, likely constitutive, activity of H1a-bound mGluR5(Hays et al., 2011). In support of this conclusion, prolonged UP states in the *Fmr1* KO are reversed by genetic or acute, pharmacological blockade of mGluR5 (Hays et al., 2011) and genetic deletion of *H1a* (Fig. 5A). Peptide-mediated disruption of mGluR5-Homer interactions prolongs UP states in WT, but not *Fmr1* KO, slices (Fig. 5C) which suggests that regulation of Homer scaffolds, by *H1a* or other means, may regulate neocortical slow oscillations in the normal brain. Interestingly, *H1a* is induced in neocortex with sleep deprivation and contributes to the homeostatic increase in slow wave sleep that occurs in response to sleep deprivation (Mackiewicz et al., 2008). Consequently, altered UP states, Homer

interactions and responses to *H1a* may contribute to the reported sleep problems in FXS patients (Hagerman, 2002).

How does mGluR5 activity lead to longer UP states? Prolonged UP states are not due to mGluR5-driven translation because the protein synthesis inhibitor anisomycin does not affect UP state duration in either WT or *Fmr1* KO slices (Hays et al., 2011). Therefore, mGluR5 activity likely leads to prolonged UP states through posttranslational regulation of the intrinsic excitability and/or synaptic function of neocortical neurons.

Altered behavior in Fmr1 KO mice is rescued by H1a deletion

Genetic reduction of mGluR5 (heterozygosity), or *H1a* deletion, completely rescue neocortical hyperexcitability (e.g. long UP states) in *Fmr1* KO mice, but only partially rescue audiogenic seizures (Fig. 6A) (Dolen et al., 2007; Hays et al., 2011). This suggests that hyperexcitability in other brain regions, such as the auditory brain stem, also contribute to audiogenic seizures in *Fmr1* KO mice, through mGluR5 and *H1a* independent mechanisms (Brown et al., 2010). Importantly, mGluR5 antagonism and *H1a* deletion (Fig. 6B) rescue the increased open field activity in *Fmr1* KO mice suggesting that abnormal Homer scaffolds contribute to behavioral symptoms associated with FXS and may represent a new therapeutic target for the disease. In contrast to initial studies(Dolen et al., 2010; Dolen et al., 2007; Osterweil et al., 2010b), recent

reports have failed to rescue some *Fmr1* KO mouse behaviors by reduction of mGluR5 activity(Thomas et al., 2011a; Thomas et al., 2011b), suggesting mGluR5-independent mechanisms in FXS pathology. Interestingly, in these studies inhibition of mGluR1 proved efficacious in reducing some *Fmr1* KO phenotypes (Thomas et al., 2011a; Thomas et al., 2011b). MGluR1a, is a Homer binding protein, and mGluR1a-Homer scaffolds may also be affected in *Fmr1* KO mice. Alternatively, because of the diverse mRNA targets of FMRP (Darnell et al., 2011) other signaling pathways are likely affected in FXS. However, because mGluR5 antagonism has proven effective in some FXS patients (Jacquemont et al., 2011) the understanding mGluR5 function in the normal brain and its dysfunction in FXS may provide additional and more targeted treatments for the disease and provide insight into autism.

For the phenotypes we studied here, *H1a* deletion had no effect on the WT background, but only on the *Fmr1* KO background. This is likely because *H1a* expression is typically low under basal conditions and is strongly induced in response to neuronal activity and experience (Shiraishi-Yamaguchi and Furuichi, 2007). The effects of *H1a* induction in WT mice are expected to be mimicked by the mGluR5CT peptide, where we observe effects on mGluR5 signaling, protein synthesis rates, LTD (Ronesi and Huber, 2008a) and UP state duration (Figs. 1,3,5). In contrast, CT peptide had no effect on these measures in *Fmr1* KO mice (Ronesi and Huber, 2008a) (Figs. 3,5) . Therefore, we would expect that

experience-dependent *H1a* induction would affect mGluR5 function in WT, but not *Fmr1* KO mice. Such insensitivity to experience-induced *H1a* could contribute to deficits in experience-dependent plasticity associated with FXS (Dolen et al., 2007).

Mechanism of disrupted Homer scaffolds in Fmr1 KO

How does loss of FMRP lead to altered mGluR5-Homer scaffolds? Protein levels of long Homers and *H1a* are unchanged in total homogenates of *Fmr1* KO hippocampi (Giuffrida et al., 2005) (Supplementary Fig. 2) and FMRP is not reported to interact with mRNA for any Homer isoforms (Darnell et al., 2011). Previous work reported a decrease in Tyr phosphorylation of long Homer in *Fmr1* KO forebrain (Giuffrida et al., 2005), but it is unknown if or how this affects interactions with mGluR5. Phosphorylation of Homer3 regulates interactions with other Homer effectors (Huang et al., 2008a; Mizutani et al., 2008). Similarly, phosphorylation of mGluR5 at the C-terminal Homer interaction domain reduces the affinity of mGluR5 for Homer (Orlando et al., 2009). Therefore, posttranslational modification of mGluR5 and/or Homer in *Fmr1* KO mice may underlie the decreased interactions.

Disrupted or destabilized synaptic scaffolds that affect Homer and/or mGluR5 may also contribute more generally to cognitive disorders and autism behaviors. Mutations in the Homer binding domain of SHANK3 and the Homer binding protein oligophrenin 1 are implicated in autism and intellectual disability,

respectively (Bangash et al., 2011a; Billuart et al., 1998). Expression of a truncated SHANK3 without the Homer binding domain in mice results in degradation of SHANK3 and autistic behaviors in mice. Importantly, reduction of long Homers or induction of H1a recapitulates the degradation of synaptic SHANK3 (Bangash et al., 2011a). An interesting possibility is that mGluR5 dysfunction, of the kind we describe here, may occur in individuals with mutations in SHANK3 or other genes that destabilize Homer scaffolds.

Figure 2.1: Peptide- mediated disruption of mGluR5-Homer scaffolds in wildtype mice hippocampus bidirectionally regulates group 1 mGluR signaling to translation initiation and elongation.

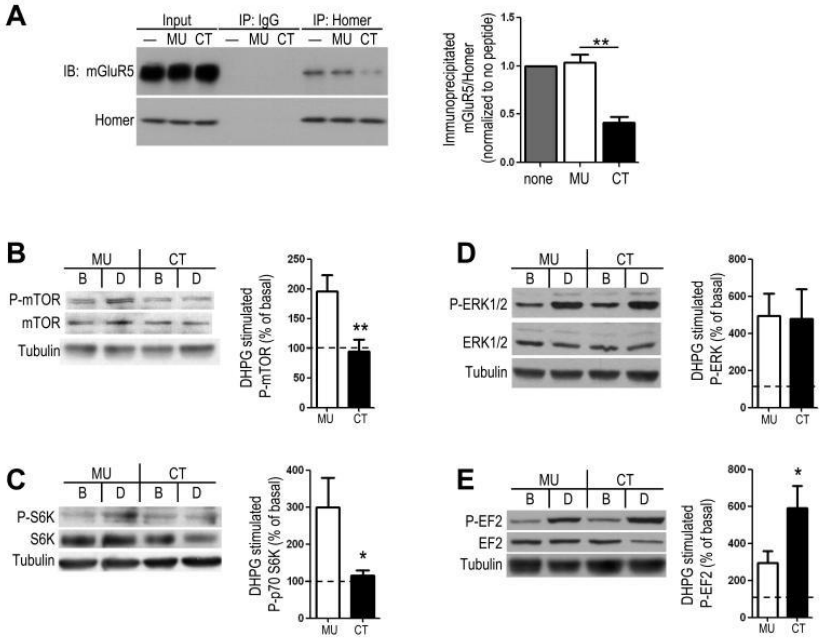

Figure 2.1: Peptide- mediated disruption of mGluR5-Homer scaffolds in wildtype mice hippocampus bidirectionally regulates group 1 mGluR signaling to translation initiation and elongation. A. Pretreatment of acute hippocampal slices from wildtype (WT) mice with a tat-fused peptide containing the Homer binding motif of the mGluR5 (tat-mGluR5CT; CT; YGRKKRRQRRR-ALTPPSPFR; 5 hours; 5 μM) reduces mGluR5-Homer interactions as determined using co-immunoprecipitation (co-IP) with a Pan-Homer antibody and immunoblotting for mGluR5. A control peptide containing point mutations in the Homer binding motif (tat-mGluR5-MU; YGRKKRRQRRR-ALTPLSPRR; 5 hours; 5 μM) has no effect on mGluR5-Homer co-IP in comparison to untreated slices ("-"). One-half of the input for the co-IP was run on separate blots. **B-E.** Disruption of mGluR5-Homer interaction alters signaling to translation. Western blots of (**B**) phosphorylation of mTOR (S2448), (**C**) phosphorylation of S6K (T389), (**D**) phosphorylation of ERK T202/Y204 and (**E**) phosphorylation of EF2 (T56), in the basal (B) condition and DHPG (D) treated hippocampal slices (100 μM; 5 min) from WT mice. Slices were pretreated with the CT or MU peptide as indicated. Left: Representative Western blots of each phosphorylated and total protein as well as β-tubulin in the conditions as indicated. Right: Group data (averages ± SEM) of each protein

monitored (phosphorylated/total) (normalized to basal, or untreated, slices from the same mouse). n = 4-15 slices/per condition from 3-8 mice. *p< 0.05; **p < 0.01. Full length western blots for this figure are shown in Supplementary Fig. 7.

Figure 2.2. mGluR5-Homer scaffolds and Group 1 mGluR signaling are altered in *Fmr1* KO mice and rescued by genetic deletion of *Homer1a*.

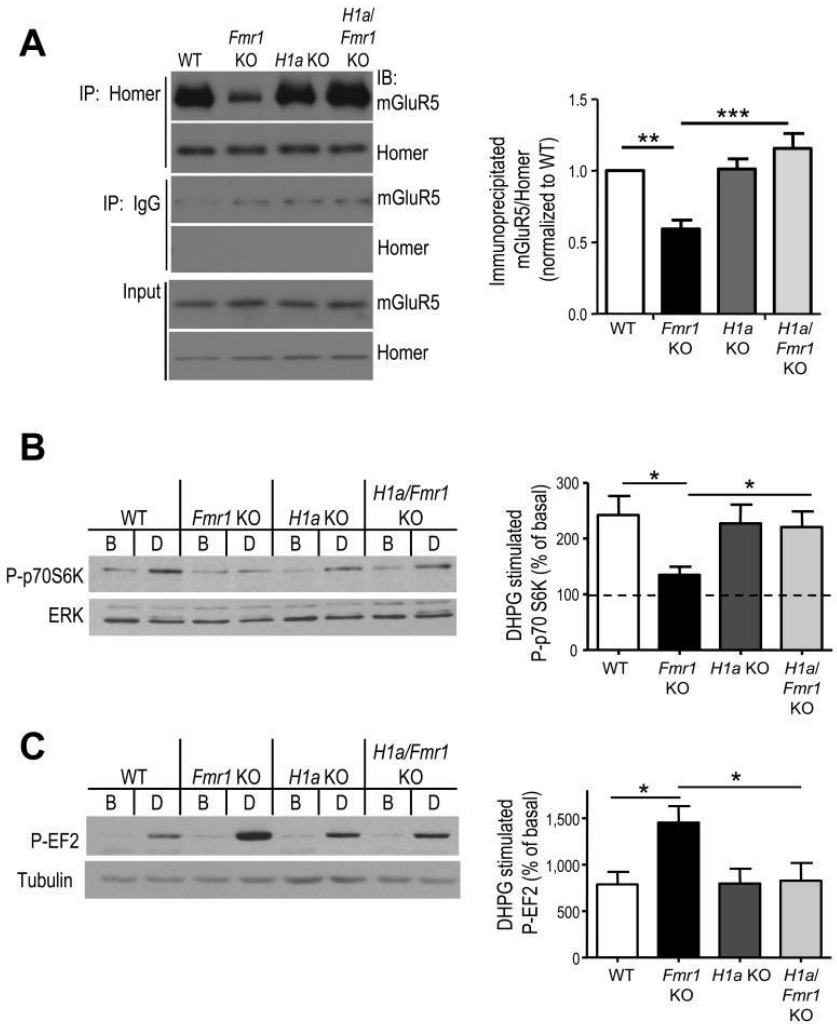

Figure 2.2. mGluR5-Homer scaffolds and Group 1 mGluR signaling are altered in *Fmr1* KO mice and rescued by genetic deletion of *Homer1a*. A. Decreased mGluR5-long Homer interactions in *Fmr1* KO hippocampus are restored to WT levels in the *H1a/Fmr1* double knockout littermates. The level of mGluR5 that coimmunoprecipitated with Homer was quantified and normalized to levels of immunoprecipitated Homer. Left: Representative blots from 1 set of littermates reveals a decrease in Homer/mGluR5 in *Fmr1* KO that is reversed in the *H1a/Fmr1* KO. One-fifth of the input for the immunoprecipitation was run on separate blots and demonstrates normal levels of mGluR5 and Homer across all genotypes. Right: Group data from independent co-IPs in 4 litters reveals a

reliable decrease in mGluR5-Homer co-IP in *Fmr1* KO mice and rescue by *H1a* deletion. **B.** Treatment of acute hippocampal slices from littermates of each of the four genotypes with DHPG (100 μm; 5 min) reveals a deficit in phosphorylation of p70S6K in *Fmr1* KO mice that is restored to wildtype levels in *H1a/Fmr1* KO. Left: Representative Western blots of P-S6K and total ERK (loading control) in the basal (B) condition and DHPG (D) treated slices. Right: Group data of P-S6K/ERK (normalized to basal levels in untreated slices from the same mouse). n = 14-21 slices/per condition from 14-21 mice. **C**. DHPG induced P-EF2 is enhanced in *Fmr1* KO slices, an effect that is reversed in the *H1a/Fmr1* KO. Left: Representative western blot of P-EF2 and β-tubulin in the basal (B), or untreated, condition and DHPG (D) treated slices from each genotype. Right: Group data (averages ± SEM) for P-EF2/tubulin (normalized to basal levels). n = 6-7 slices and mice per genotype). *p< 0.05, **p< 0.01; ***p<0.001. Full length western blots for this figure are shown in Supplementary Fig. 8.

Figure 2.3: Altered mGluR5-Homer scaffolds in *Fmr1* KO mice mediate enhanced basal translation rates and initiation complex formation.

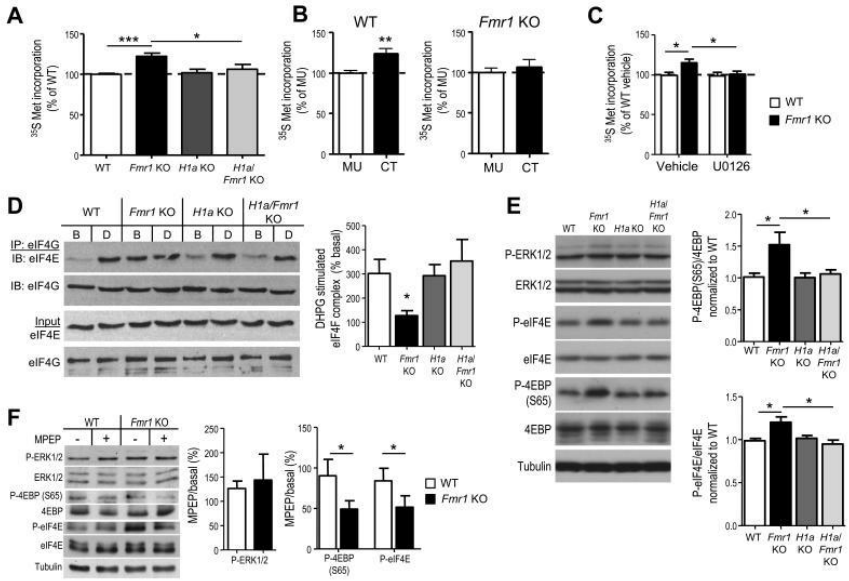

Figure 2.3: Altered mGluR5-Homer scaffolds in *Fmr1* KO mice mediate enhanced basal translation rates and initiation complex formation. **A.** Acute hippocampal slices from *Fmr1* KO mice display elevated protein synthesis rate in comparison to WT littermates as measured by incorporation of ^{35}S Met/Cys into total protein (n = 14 slices from 7 mice/genotype). Elevated protein synthesis rates in *Fmr1* KO slices are reversed by *H1a* deletion (*H1a/Fmr1* KO; n = 7 slices/ 4 mice), whereas *H1a* KO alone (n = 8 slices/4 mice) has no effect. **B.** Pretreatment of WT hippocampal slices with mGluR5CT (CT; 5 µM; 5 hours; n = 16 slices/4 mice) enhanced ^{35}S Met/Cys incorporation in comparison to control (mGluR5MU; MU; n = 16 slices/ 4 mice) peptide. In contrast, pretreatment of *Fmr1* KO hippocampal slices (n = 15 slices/ 4 mice) with CT peptide had no effect. **C.** Preincubation of WT or *Fmr1* KO slices with an inhibitor of the upstream kinase of ERK (MAP/ERK kinase; MEK) U0126 (20 µM; 30 min) prior to ^{35}S Met/Cys incorporation (n = 12 slices/ 6 mice per condition) equalizes protein synthesis rates. **D_1.** Representative Western blots of eIF4E that co-immunoprecipitated with eIF4G from hippocampal slices reveal that DHPG (D) induces an increase in eIF4E association with eIF4G, forming the translation initiation (eIF4F) complex, in WT but not in *Fmr1* KO littermates despite an elevated level of eIF4F complex under basal (B) conditions. *H1a* deletion alone has no effect on eIF4E/4G levels under basal or DHPG stimulated conditions, whereas, *H1a* deletion on the *Fmr1* KO background reverses the enhanced eIF4F complex levels and restores DHPG induced eIF4F complex formation. **D_2.**

Quantified group data of the levels of eIF4E that coimmunoprecipitated with eIF4G (eIF4E/4G) in DHPG treated samples (normalized to the levels of eIF4E/4G in basal, or untreated slices). n = 3 mice per genotype. **E_1**. Representative Western blots of phospho- and total ERK and translation initiation factors that are regulated by ERK, (phospho- and total eIF4E and 4EBP) from cortical homogenates in each of four genotypes. **E_2**. Quantified group data reveals elevated P-4EBP and P-eIF4E in *Fmr1* KO brains as compared to WT, which is rescued by *H1a* deletion. P-ERK levels were not different across any genotype (n = 4-6 mice per genotype). **F_1**. Representative Western blots from acute hippocampal slices prepared from WT and *Fmr1* KO mice treated with MPEP (10 μM) or vehicle (H_2O). **F_2**. Quantified group data of the level of phosphoproteins in MPEP treated slices expressed as a percent of basal (untreated) slices reveals a genotypic difference in P-4EBP (S65) and P-eIF4E, but not P-ERK (n = 2 slices/mouse; 4- 8 mice/condition). *p< 0.05; **p< 0.01; ***p<0.001. Full length western blots for this figure are shown in Supplementary Fig. 9.

Figure 2.4: Genetic deletion of Homer1a does not reverse the protein synthesis-independence of mGluR-induced LTD or altered protein levels of FMRP target mRNAs.

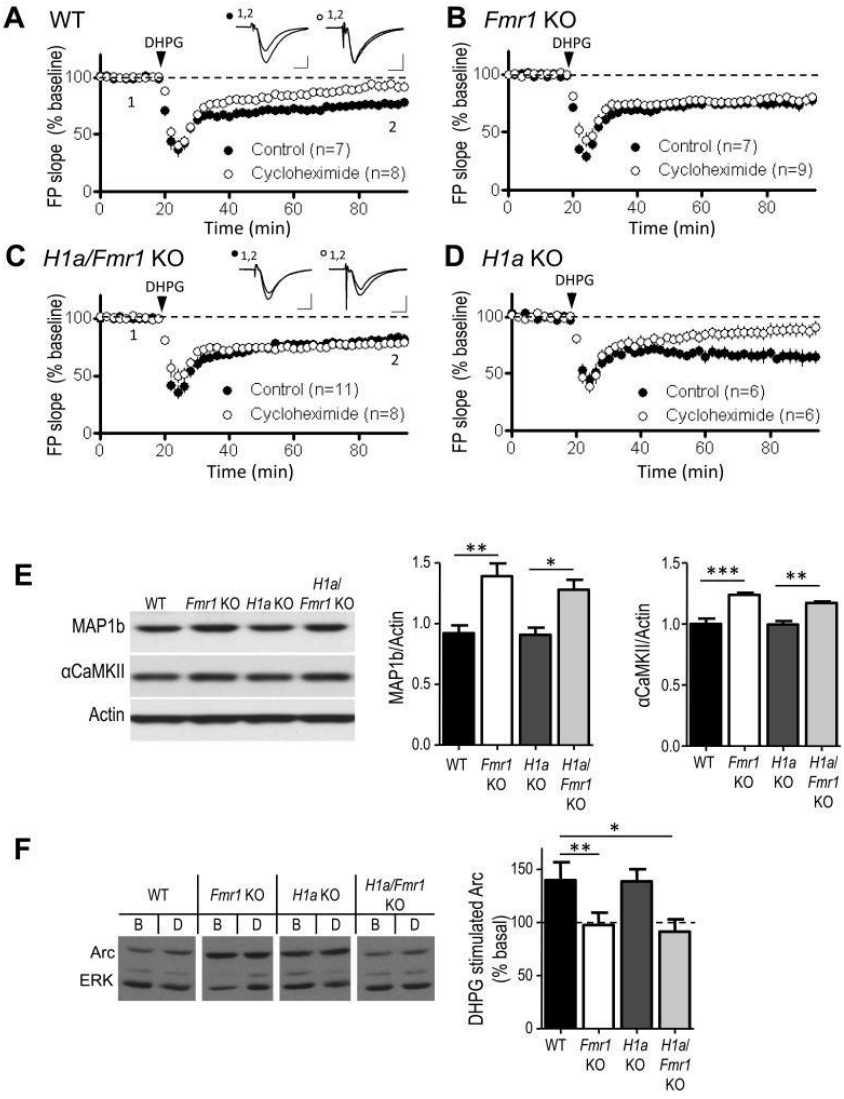

Figure 2.4: Genetic deletion of Homer1a does not reverse the protein synthesis-independence of mGluR-induced LTD or altered protein levels of FMRP target mRNAs. **A.** Brief DHPG (100 μM; 5 min) induces long-term depression (LTD) of synaptic transmission in WT hippocampal slices that is reduced by the protein synthesis inhibitor cycloheximide (60μM; $p<0.01$). Plotted are group averages of field excitatory postsynaptic potential (fEPSPs) slope (average±SEM) normalized to pre-DHPG baseline as a function of time.

Inset, average of 10 fEPSPs taken during the baseline period (1) and 55-60 min after DHPG treatment (2). Calibration = 0.5 mV, 5 ms. **B, C.** In *Fmr1* KO and *H1a/Fmr1* KO mice, DHPG-induced LTD is unaffected by cycloheximide. **D.** In *H1a* KO DHPG-induced LTD is normal and blocked by cycloheximide ($p < 0.05$). n = number of slices. **E.** Map1b and αCaMKII levels are elevated in *Fmr1* KO mice, and are unaffected by *H1a* deletion. Left: Representative western blots of Map1b, αCaMKII and actin (loading control) from hippocampal homogenates of each genotype. Right: Quantified group data of MAP1b/actin and αCaMKII/actin ratios in each genotype. (MAP1b/actin ratio; WT = 0.92±0.06; *Fmr1* KO = 1.4±0.1; *H1a* KO = 0.8±0.06; *H1a/Fmr1* KO = 1.28±0.08; αCaMKII/actin ratio; WT = 1.0±0.04; *Fmr1* KO = 1.23±0.02; *H1a* KO = 1.0±0.03; *H1a/Fmr1* KO = 1.17±0.01; n = 3-4 mice per genotype). **F.** DHPG-induced Arc synthesis is deficient in *Fmr1* KO mice and is not rescued by *H1a* deletion. Left: Representative western blots of basal (B) Arc levels and DHPG (D) induced Arc from hippocampal slices of each genotype. Full length western blots for this figure are shown in Supplementary Fig.10. Group averages reveal a deficit in DHPG-induced Arc synthesis slices taken from *Fmr1* KO (n = 10 mice) and *H1a/Fmr1* KO (n = 11) mice. DHPG induces Arc synthesis in both WT (n = 12) and *H1a* KO (n = 14) littermates. *$p< 0.05$; **$p< 0.01$; ***$p<0.001$.

Figure 2.5. Disruption of mGluR5-Homer interactions mediates prolonged neocortical UP states in *Fmr1* KO mice.

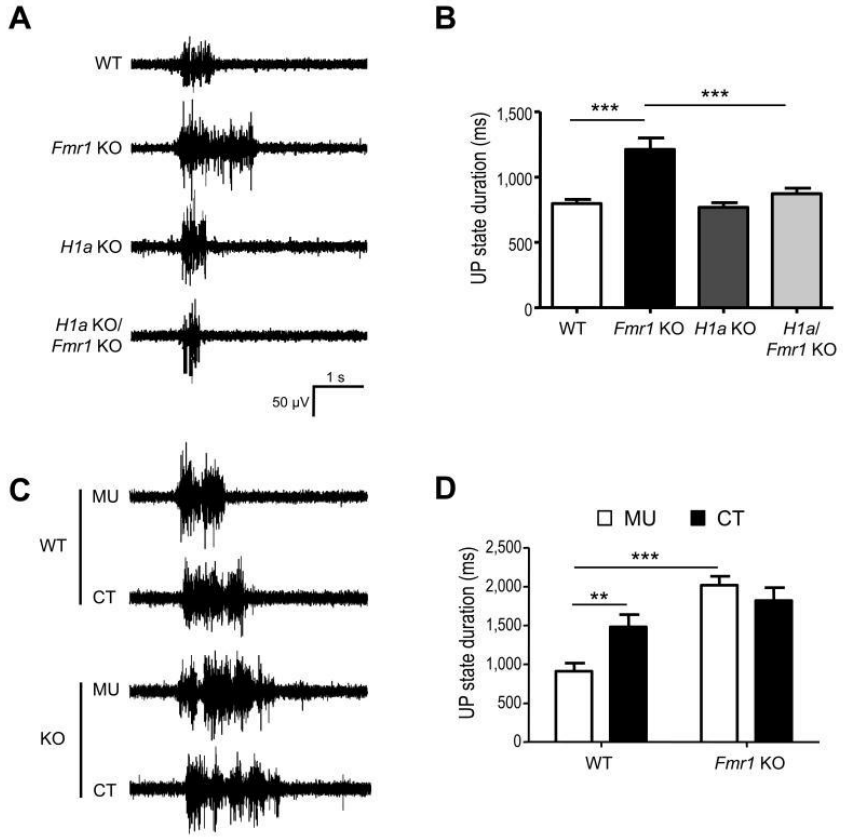

Figure 2.5. Disruption of mGluR5-Homer interactions mediates prolonged neocortical UP states in *Fmr1* KO mice. A,B. Genetic deletion of *H1a* rescues prolonged UP states in the *Fmr1* KO. **A.** Representative extracellular multiunit recordings of spontaneous, persistent activity or UP states from layer 4 of somatosensory, barrel neocortical slices from each genotype. **B.** Group averages reveal that the UP state duration is prolonged in the *Fmr1* KO slices (n = 13) in comparison to WT (n = 22) UP state duration in the *H1a/Fmr1* KO (n = 44 slices) is reduced from the *Fmr1* KO and is not different from WT. There is no difference between WT and *H1a* single KO (n = 18), suggesting that the rescue is dependent on *Fmr1*, and not a general decrease in excitability due to loss of *H1a*. **C.** Representative UP state recordings from WT and *Fmr1* KO slices treated with the appropriate peptide. **D.** Pretreatment of WT neocortical slices with mGluR5CT peptide (CT; 4 hours; 5 μM; n = 15 slices) to acutely disrupt mGluR5-Homer interactions increases UP state duration in comparison to slices pretreated with control (mGluR5MU; MU; 5 μM; n = 13) peptide. In contrast,

treatment of *Fmr1* KO slices (n = 12) with CT peptide had no effect on UP state duration in comparison to MU treated slices (n = 15). **p< 0.01; ***p<0.001.

Figure 2.6. Homer1a deletion reduces audiogenic seizures and corrects open field activity in the *Fmr1* KO.

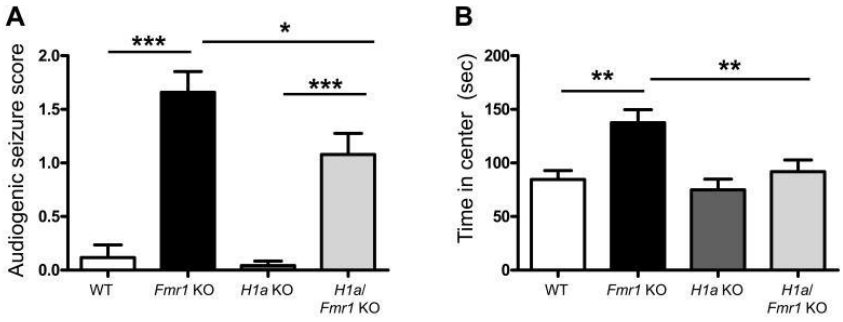

Figure 2.6. Homer1a deletion reduces audiogenic seizures and corrects open field activity in the *Fmr1* KO. A. The incidence and severity of audiogenic seizures was scored as described in methods. *Fmr1* KO mice have an increased seizure score that was reduced in *H1a/Fmr1* KO mice. (N = 16, 39, 24, 37 mice for WT, *Fmr1* KO, *H1a* KO and *H1a/Fmr1* KO, respectively). **B.** Open field activity, measured as time spent in the center of a lit open arena was increased in *Fmr1* KO mice and reversed to WT levels in the *H1a/Fmr1* KO mice. (N = 18, 24, 17, 17 mice for WT, *Fmr1* KO, *H1a* KO and *H1a/Fmr1* KO, respectively) *p< 0.05; **p< 0.01; ***p<0.001.

Supplementary Table 2.1: mGluR5CT peptide treatment does not affect the basal levels of phosphoproteins examined or total levels of EF2 or Arc in comparison to mGluR5MU.

Wildtype mouse slices	MU		CT		
Basal	Mean	SEM	Mean	SEM	n
P-mTOR/mTOR	1.39	0.37	2.08	0.64	15
P-p70S6K/p70S6K	1.07	0.4	0.89	0.16	7
P-EF2/EF2	0.97	1.46	0.7	0.69	14
P-ERK/ERK	0.4	0.11	0.48	0.13	4

Rat slices	MU					
	Basal			DHPG		
Basal (% of MU)	Mean	SEM	n	Mean	SEM	n
P-EF2	100	9	13			
Total EF2	100	11	9	116	18	10
Arc	100	5	11			
Rat slices	CT					
	Basal			DHPG		
Basal (% of MU)	Mean	SEM	n	Mean	SEM	n
P-EF2	121	24	13			
Total EF2	131	16	10	98	8	9
Arc	102	10	14			

Supplementary Table 2.1: mGluR5CT peptide treatment does not affect the basal levels of phosphoproteins examined or total levels of EF2 or Arc in comparison to mGluR5MU. Related to Figure 2.1. ***Upper*:** Quantitative western blotting of acute hippocampal slices from WT mice demonstrates that mGluR5CT peptide (CT) treatment has no effect on basal levels P-mTOR, P-p70S6K, P-EF2 and P-ERK in comparison to mGluR5MU (MU) control peptide treated slices. For this analysis phosphoprotein levels were normalized to total protein levels from the same slice homogenates (e.g. P-mTOR/mTOR), each of which was first normalized to tubulin loading control. ***Lower*:** mGluR5CT peptide treatment of

rat hippocampal slices has no effect on basal levels of Phospho-EF2, total EF2, or Arc in comparison to MU treated slices. Previous work demonstrated no effect of the CT peptide basal Phospho or total S6K (Ronesi and Huber, 2008a). DHPG treatment does not affect total EF2 levels. Data is normalized to within animal, mGluR5MU peptide treated slices and expressed as the mean ± SEM; n = # slices.

Supplementary Figure 2.1. Disruption of mGluR5-Homer scaffolds in rat hippocampal slices bidirectionally regulates mGluR signaling to translation initiation and elongation and blocks synthesis of Arc.

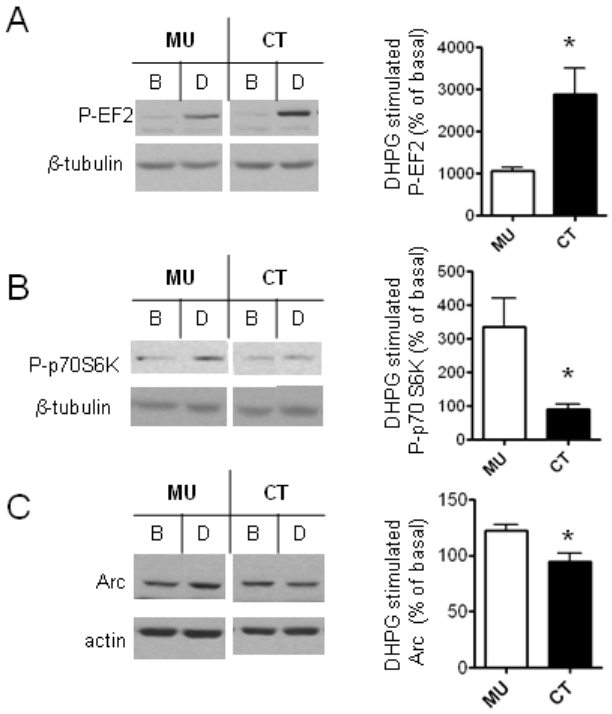

Supplementary Figure 2.1. Disruption of mGluR5-Homer scaffolds in rat hippocampal slices bidirectionally regulates mGluR signaling to translation initiation and elongation and blocks synthesis of Arc. Related to Fig. 2.1 **A.** Pretreatment of rat hippocampal slices with a peptide that disrupts mGluR5-Homer interactions (tat-mGluR5CT; CT; 5 hours; 5 μM) results in enhanced DHPG-induced (100 μM; 5 min) phosphorylation of EF2 in comparison to slices treated with a control peptide that does not disrupt mGluR5-Homer interactions (tat-mGluR5MU; MU) (CT; 2876±633% of basal; n = 7 rats; MU; 1060±87% of basal; n = 6). Left: Representative western blot of Thr56 phosphorylated (P)-EF2 and β-tubulin (loading control) in the basal (B), or untreated, condition and DHPG (D) treated slices. Right: To obtain group data for panels A-C, in each rat, levels of P-EF2 or P-p70S6K or Arc in DHPG treated slices were normalized a loading control (tubulin or actin) and expressed as a percentage of basal levels (as

measured in untreated slices) and averaged across animals. **B.** For a subset of the samples analyzed in panel A, DHPG-induced Thr389 phosphorylation of p70S6K was evaluated. MU pretreated slices exhibited robust DHPG- induced phosphorylation of p70S6K, whereas in CT pretreated slices DHPG induced P-p70S6K was blocked (CT; 91±15% of basal, n=5; MU: 337±83% of basal, n=4). **C.** In a separate set of animals, DHPG-induced increases in total Arc protein is blocked with CT peptide (CT: 95±7% of basal, n=7; MU: 122±5% of basal, n=7). *$p < 0.05$.

Supplementary Table 2.2: *H1a* or *Fmr1* genotype does not affect basal levels of P-p70S6K, P-EF2 or total EF2.

	WT			***Fmr1* KO**		
% of WT	**Mean**	**SEM**	**n**	**Mean**	**SEM**	**n**
P-p70S6K	100	9	12	125	23	13
P-EF2	100	11	9	86	16	9
T-p70S6K	100	5	4	101	5	4
	***H1a* KO**			***H1a/Fmr1* KO**		
% of WT	**Mean**	**SEM**	**n**	**Mean**	**SEM**	**n**
P-p70S6K	90	7	13	123	25	11
P-EF2	89	25	8	106	16	8
T-p70S6K	102	10	4	102	9	4

	WT						*Fmr1* KO					
% of WT basal	Basal			DHPG			Basal			DHPG		
	Mean	SEM	n	Mean	SEM	n	Mean	SEM	n	Mean	SEM	n
T-EF2	100	7	5	130	15	5	94	19	5	109	31	4
	H1a KO						*H1a/Fmr1* KO					
% of WT basal	Basal			DHPG			Basal			DHPG		
	Mean	SEM	n	Mean	SEM	n	Mean	SEM	n	Mean	SEM	n
T-EF2	118	29	4	120	24	5	117	13	4	141	22	4

Supplementary Table 2.2: *H1a* or *Fmr1* genotype does not affect basal levels of P-p70S6K, P-EF2 or total EF2. Upper: Basal levels of phosphorylated or total EF2 or p70S6K are not different in acute hippocampal slices across genotypes (WT, *Fmr1* KO, *H1a* KO, or *H1a/Fmr1* KO). Data is normalized to levels in slices from WT littermates and expressed as the mean ± SEM; n = # slices. Lower: There is no effect of genotype or DHPG treatment on total EF2 levels in acute hippocampal slices. Data is normalized to levels from untreated slices of WT littermates and expressed as the mean ± SEM; n = # slices.

Supplementary Figure 2.2: H1a-mGluR5 interactions are elevated in *Fmr1* KO mice, but total levels of H1a, long Homers or mGluR5 are unchanged.

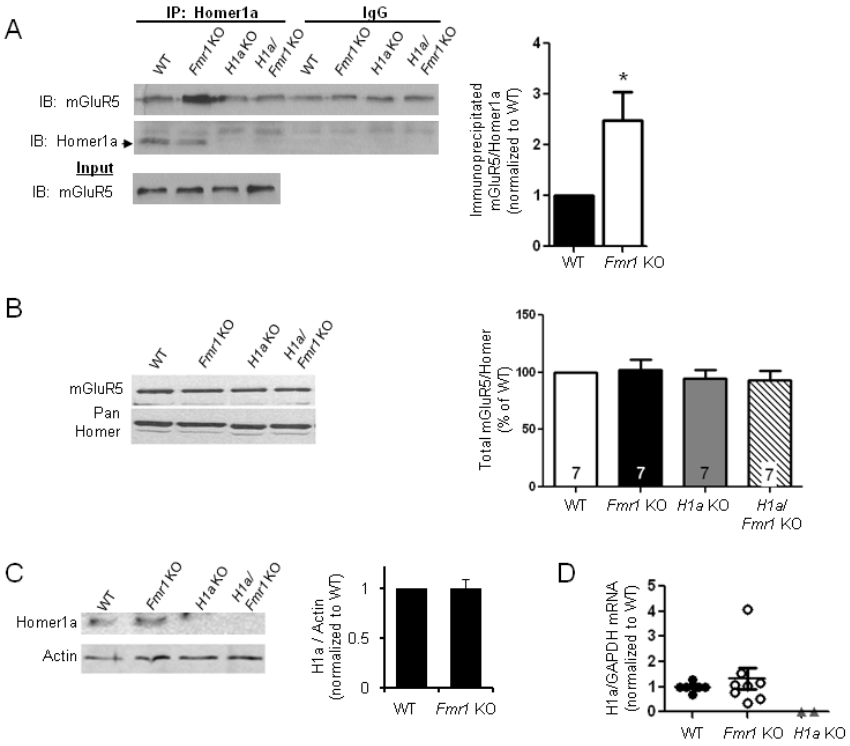

Supplementary Figure 2.2: H1a-mGluR5 interactions are elevated in *Fmr1* KO mice, but total levels of H1a, long Homers or mGluR5 are unchanged. Related to Figure 2.2. **A.** mGluR5-Homer1a interactions are increased in hippocampal homogenates of *Fmr1* KO mice. Homer1a was immunoprecipitated from total mouse hippocampal lysate. The level of mGluR5 that coimmunoprecipitated with Homer1a was quantified and normalized to levels of immunoprecipitated Homer1a. Arrowhead indicates specific H1a band that is absent in the *H1a* KO lysates. There is a low level of mGluR5 that nonspecifically pulls down with goat IgG. Group data from 4 set of littermates reveals an increase in Homer1a/mGluR5 in *Fmr1* KO. *p< 0.05. **B.** Total mGluR5 and long Homer (with pan-Homer antibody) is normal in WT, *Fmr1* KO, *H1a* KO and *H1a/Fmr1* KO. **C.** Homer1a protein levels (normalized to actin) are

unaffected in total lysates of whole hippocampus of *Fmr1* KO mice. **D.** Quantitative RT-PCR hippocampal *H1a* and *GAPDH* mRNA reveal there is no change in H1a mRNA levels in *Fmr1* KO mice. Note: Homogenates prepared from *H1a* KO mice demonstrate the specificity of the *H1a* RT-PCR primers.

Supplemental Figure 2.3: Effects of the PI3K inhibitor, wortmannin, on protein synthesis rates in WT and *Fmr1* KO hippocampal slices.

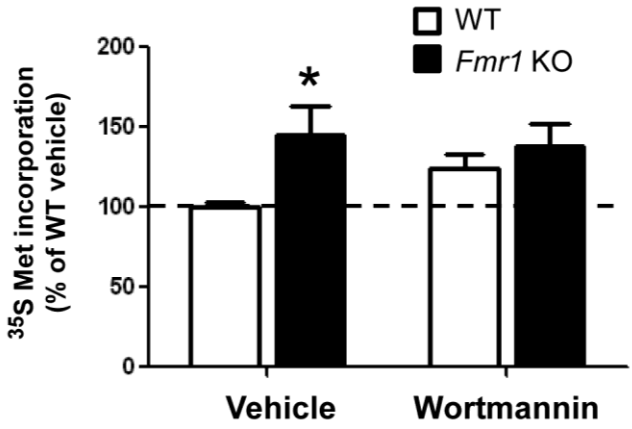

Supplemental Figure 2.3: Effects of the PI3K inhibitor, wortmannin, on protein synthesis rates in WT and *Fmr1* KO hippocampal slices. Related to Figure 2.3C. Acute hippocampal slices from *Fmr1* KO mice display elevated protein synthesis rate in comparison to WT littermates as measured by incorporation of ^{35}S Met/Cys into total protein. Slices from WT or *Fmr1* KO mice were preincubated in the PI3K inhibitor wortmannin (100 nM; 30 min) prior to ^{35}S Met incorporation (n = 12 slices/ 6 mice per condition). Inhibition of PI3K using wortmannin (100 nM) pathway equalizes protein synthesis rates between WT and *Fmr1* KO slices, but this may be due to an increase in protein synthesis rates in WT slices ($p < 0.05$; t-test), as opposed to a decrease of protein synthesis rates in *Fmr1* KO slices**.**

Supplementary Figure. 2.4. Inhibition of ERK activation in hippocampal slices reduces or abolishes phosphospecific antibody detection of P-ERK, P(S209) eIF4E, and P(65) 4EBP

A.

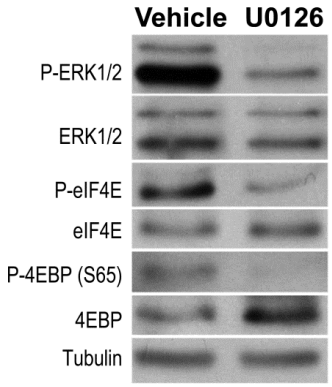

B.

	WT		*Fmr1* KO	
MPEP	% of Basal	SEM	% of Basal	SEM
ERK	81	2	106	14
eIF4E	110	9	133	30
4EBP	109	13	116	11

Supplementary Figure. 2.4. Inhibition of ERK activation in hippocampal slices reduces or abolishes phosphospecific antibody detection of P-ERK, P(S209) eIF4E, and P(65) 4EBP. Related to Fig. 2.3. Acute hippocampal slices from WT mice were preincubated in the MEK inhibitor U0126 (20 µM) or vehicle (0.01% DMSO) for 30 min prior to lysis and western blotting. **B. MPEP treatment of hippocampal slices from WT or *Fmr1* KO mice has no effect on total levels of ERK, eIF4E or 4EBP.** Related to Fig. 2.3F. Acute hippocampal slices were incubated in MPEP (10 µM) or untreated (basal). Total protein levels for ERK, eIF4E, 4EBP were normalized to a loading control (tubulin) on the same blot each for MPEP and untreated slices. Representative blots of this data are shown in Fig. $3F_1$. (n = 2 slices/mouse; 4- 8 mice/condition).

Supplemental Figure 2.5: *Fmr1, H1a,* or *H1a/Fmr1* KO do not affect locomotor activity and therefore do not underlie the rescue of open field activity.

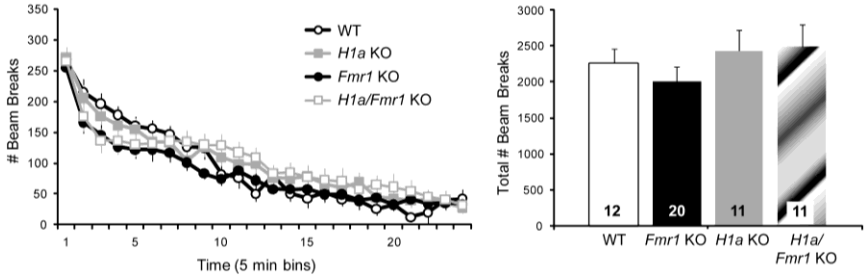

Supplemental Figure 2.5: *Fmr1, H1a,* or *H1a/Fmr1* KO do not affect locomotor activity and therefore do not underlie the rescue of open field activity. Related to Fig. 2.6. Locomotor activity, as measured by number of beam breaks per unit time, is unaffected by *Fmr1* KO, *H1a* KO or *H1a/Fmr1* KO. N = # of mice is indicated on each bar.

Supplementary Table 2.3. Seizure occurrence and severity in WT, *Fmr1* KO, H1a KO and H1a/*Fmr1* KO genotypes.

	Wild running	Seizure (clonic/tonic)	Status Epilepticus	% Incidence
WT	1/17	1/17	0/17	5.8%
***Fmr1* KO**	29/41	25/41	14/41	61.0%
***H1a* KO**	1/24	0/24	0/24	0.0%
***H1a* KO/*Fmr1* KO**	20/38	13/38	8/38	34.2%*

Supplementary Table 2.3. Seizure occurrence and severity in WT, *Fmr1* KO, H1a KO and H1a/*Fmr1* KO genotypes. * $p < 0.05$ Fisher's Exact test. Related to Fig. 2.6.

Supplementary Figure 2.6. Model illustrating two mechanisms for mGluR5 dysfunction in Fragile X Syndrome A. An altered balance of long and short Homer isoforms bound to mGluR5 accounts for many *Fmr1* KO mouse phenotypes.

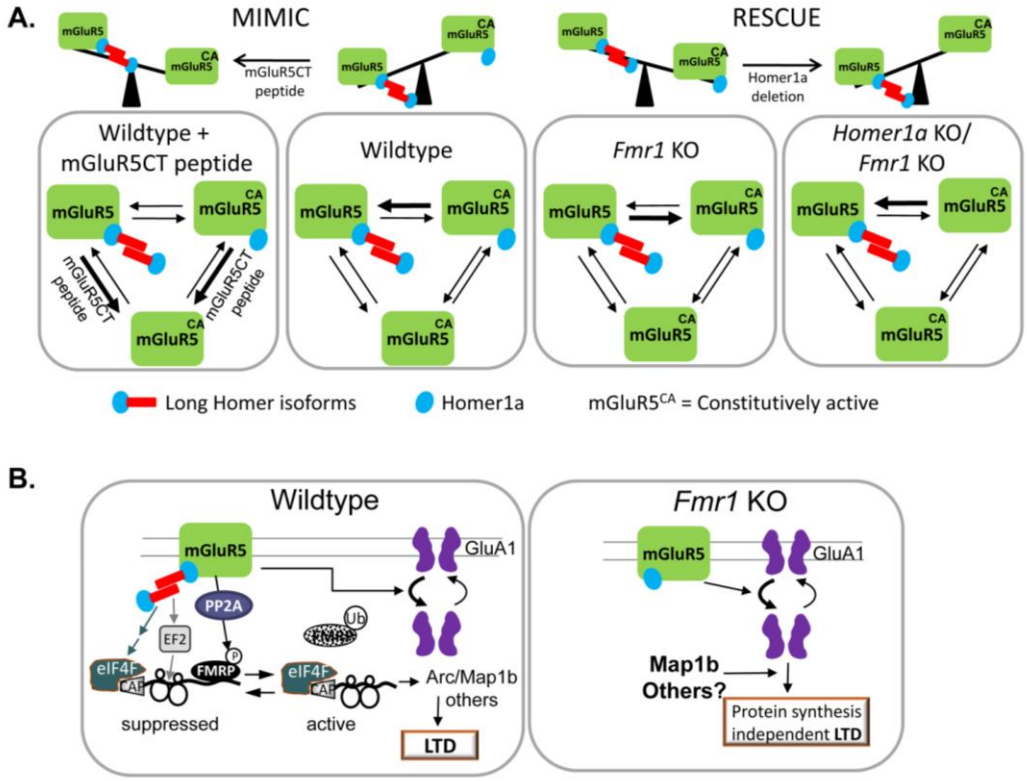

Supplementary Figure 2.6. Model illustrating two mechanisms for mGluR5 dysfunction in Fragile X Syndrome A. An altered balance of long and short Homer isoforms bound to mGluR5 accounts for many *Fmr1* KO mouse phenotypes. There is a competition and equilibrium and between long and short Homer (Homer1a) isoforms bound to mGluR5. When bound to the long Homer isoforms, mGluR5 is scaffolded to its effectors (other Homer interacting proteins) and normally gated by glutamate. Free mGluR5 (no Homer bound) or H1a bound mGluR5 is uncoupled from its effectors and constitutively active ($mGluR5^{CA}$) (Ango et al., 2001) . Therefore, free mGluR5 and H1a bound mGluR5 are functionally equivalent. In WT mice, there is more mGluR5 bound to long Homer isoforms, in comparison to WT mice (Fig. 2.2A). In contrast, in *Fmr1* KO

mice, more mGluR5 is bound to the short Homer isoform, Homer1a (Supplementary Fig. 2.2). The imbalance in long Homer and H1a bound mGluR5 in *Fmr1* KO mice can be reversed by genetic deletion of H1a which reestablishes the normal levels of long Homer bound mGluR5, mGluR5 signaling (Fig. 2.2) and many *Fmr1* KO phenotypes. (Figs. 2.3, 5, 6). In WT mice, a peptide consisting of the C-terminal Homer interacting motif of mGluR5 (mGluR5CT) disrupts both short and long Homer interactions with mGluR5 and shifts the balance from long Homer bound mGluR5 to free mGluR5 which would be expected to mimic H1a bound mGluR5 with respect to decreased scaffolding to effectors and constitutive activity. mGluR5CT peptide mimics the altered mGluR5 signaling, enhanced protein synthesis rates and neocortical hyperexcitability observed in *Fmr1* KO mice (Figs. 2.1, 3, 5). **B. Alterations in mGluR-LTD are hypothesized to be due to loss of FMRP-mediated translational control of dendritic mRNAs such as Arc and Map1b and not altered mGluR5-Homer scaffolds.** In WT mice, brief activation of mGluR5 causes a rapid endocytosis of postsynaptic AMPARs (primarily GluA1) as well translation of Arc and Map1b which are required for LTD and/or the prolonged decrease in surface AMPARs (Davidkova and Carroll, 2007; Waung and Huber, 2009). FMRP interacts with Arc and Map1b mRNA and is thought to suppress steady state translation of these and perhaps other LTD promoting proteins (reviewed in (Waung and Huber, 2009)). mGluRs rapidly stimulate dephosphorylation of FMRP through PP2A as well as ubiquitylation and degradation of FMRP which results in translational activation of FMRP interacting mRNAs (Muddashetty et al., 2011) (reviewed in (Bassell and Warren, 2008)). mGluR5-triggered Arc translation requires both mGluR5-Homer interactions (to trigger translation initiation and regulate EF2; Fig. 2.1; Supp. Fig. 2.1), as well as FMRP (Fig. 2.4) indicating multiple levels of translational control of Arc (Niere and Huber, 2010; Zalfa et al., 2003). In *Fmr1* KO neurons, loss of steady state translational suppression of Map1b and other mRNAs leads to elevated protein expression *Fmr1* KO neurons (Niere and Huber, 2010; Park et al., 2008; Zalfa et al., 2003) which may allow mGluR-LTD to persist in the presence of protein synthesis inhibitors. Restoration of mGluR5-Homer scaffolds in *Fmr1* KO mice by deletion of *H1a* does not rescue elevated MAP1b levels, altered mGluR-LTD or mGluR-stimulated Arc synthesis (Fig. 2.4).

CHAPTER THREE

Results

Specific disruption of mGluR5-Homer is sufficient to mimic some Fragile X phenotypes

This chapter contains data that was collected as a collaborative effort between several colleagues Weirui Guo, Gemma Molinaro, Seth Hays, and Nien-pei Tsai. I contributed the signaling, basal protein synthesis, the UP states, the audiogenic seizure, immunohystochemistry, and surface biotinylation data. However, the other data described in this chapter is important in understanding the contribution of disrupted Homer-mGluR scaffold to the *Fmr1* KO phenotypes.

Summary

Enhanced mGluR5 function is causally associated with the pathophysiology of Fragile X Syndrome (FXS), a leading inherited cause of intellectual disability and autism. Here we provide evidence that altered mGluR5-Homer scaffolds contribute to mGluR5 dysfunction and phenotypes in the FXS mouse model, *Fmr1* KO. In *Fmr1* KO mice mGluR5 is less associated with long Homer isoforms, but more associated with the short Homer1a. Genetically disrupting only mGluR5-Homer interactions with a mutant form of mGluR5, which cannot bind to Homer, mimics multiple phenotypes in *Fmr1* KO mice including altered mGluR5 signaling, translational control of FMRP target mRNAs neocortical circuit dysfunction, and behavior. In contrast, disrupting mGluR5-

Homer interactions does not mimic altered mGluR-dependent long-term synaptic depression. Our findings reveal novel functions for mGluR5-Homer interactions in the brain and delineate distinct mechanisms of mGluR5 dysfunction in a mouse model of cognitive dysfunction and autism.

Introduction

In the mouse model of FXS, *Fmr1* knockout (KO), group 1 metabotropic receptor (mGluR1 and mGluR5) and protein synthesis-dependent plasticity is enhanced and dysregulated (Luscher and Huber, 2010). These findings motivated the "mGluR theory of FXS" which posits that altered mGluR-dependent plasticity contributes to the pathophysiology of the disease (Bear et al., 2004; Dolen et al., 2010; Dolen et al., 2007). In support of the mGluR theory, many phenotypes in animal models of FXS are reversed by pharmacological or genetic reduction of mGluR5 or downstream signaling pathways (Dolen et al., 2010; Dolen et al., 2007). Importantly, a recent report indicates that mGluR5 antagonism can be an effective therapeutic strategy in FXS patients (Jacquemont et al., 2011). Although mGluR5 antagonism rescues many phenotypes associated with FXS, it is unknown if this is due to excess mGluR5-driven translation and/or altered mGluR5 function itself in *Fmr1* KO brains. There is an altered balance of mGluR5 association with short and long isoforms of the postsynaptic scaffolding protein Homer (Giuffrida et al., 2005). Long, constitutively expressed forms of Homer (Homer1b, 1c, 2 and 3) multimerize through their C-terminal coiled-coil

domain forming scaffolds, while Homer1a (H1a), a short, activity-inducible, form lacking the coiled-coiled domain cannot multimerize with other Homers. Consequently, H1a disrupts mGluR5-long Homer complexes, alters mGluR signaling and causes constitutive, agonist-independent activity of mGluR1/5 (Ango et al., 2001). H1a bound mGluR5 is functionally equivalent to mGluR5 unbound to any Homers (Ango et al., 2001). In *Fmr1* KO mice, mGluR5 is less associated with long Homers and more associated with H1a (Giuffrida et al., 2005). By deleting *H1a*, we were able to restore the balance of mGluR5 association with short and long forms of Homer, as well as, several phenotypes in *Fmr1* KO mice are rescued. Deleting *H1a* was able to rescue the decreased anxiety in the open field test, increased basal translation rates, and altered mGluR signaling, as well as, partially rescuing the audiogenic seizures in the *Fmr1* KO mice (Ronesi et al., 2012b). However, the mGluR-LTD in the *Fmr1* KO mice is insensitive to protein synthesis inhibitors and was not rescued by deleting *H1a*. *H1a* deletion was also unable to rescue the inability of mGluRs to stimulate translation in the *Fmr1* KO mice. The *H1a* deletion was able to rescue much of the mGluR dysfunction seen in the *Fmr1* KO mice, but some phenotypes, like mGluR-LTD, are due to other changes caused by the loss of FMRP. Disrupted Homer interactions contribute to Homer interactions, but there could be other altered Homer interactions than just with mGluR5, and deleting *H1a* could rescue those interactions as well.

It is still unknown if disrupting mGluR5-Homer interactions alone is sufficient to cause some of the phenotypes seen in *Fmr1* KO mice. Previous, we have shown disrupting mGluR5-Homer interaction with an mGluR5 C-terminus peptide can mimic some *Fmr1* KO phenotypes, and deleting *H1a* rescues these phenotypes (Ronesi et al., 2012b; Ronesi and Huber, 2008a). However, based on the conserved sequences of the proline rich motif in Homer binding proteins, it may be expected that mGluR5 C-terminus peptide would disrupt many or most interactions with Homer (Ronesi et al., 2012a). Similarly, it is currently unknown if other Homer interactions are disrupted in the *Fmr1* KO mice, and if present, they would be predicted to be rescued by deleting *H1a.* While we were able to rescue phenotypes in the *Fmr1* KO mice by restoring the mGluR5-Homer scaffoldings, can the reverse, disrupting the scaffolds, cause the phenotypes? We hypothesized that the altered balance in mGluR5 interactions with Homer isoforms contributed to the mGluR5 dysfunction and pathophysiology of FXS. Since mGluR5 bound to H1a is functionally equivalent to unbound mGluR5, as measured by Calcium-Activated Potassium channels and phosphatidylinositol hydrolysis (Ango et al., 2001), we can utilize a mutant form of mGluR5 which does not bind to Homer. The Homer binding mutant of mGluR5 has a point mutation in the Homer binding domain from a phenylalanine to an arginine at site 1128 (Ango et al., 2001; Cozzoli et al., 2009; Tu et al., 1998). To test this hypothesis, we utilized the mGluR5F1128R knock-in mice ($mGluR5^{R/R}$) to

determine if disrupting only mGluR5-Homer interactions is sufficient to mimic phenotypes of the *Fmr1* KO mice. Our results indicate that altered Homer isoform interactions are responsible for much, but not all, of the mGluR5 dysfunction and pathophysiology of FXS. Specifically, the mGluR5$^{R/R}$ did not mimic the enhanced mGluR-LTD and partially mimicked the audiogenic seizure rate and severity. Our results confirm our previous results that altered mGluR5-Homer interactions regulate mGluR5 dysfunction in *Fmr1* KO mice (Ronesi et al., 2012a), and specifically disrupting mGluR5-Homer is sufficient to cause mGluR5 dysfunction.

Methods

Animals

Congenic mGluR5F1128R Knock-in mice were generated as described (Cozzoli et al., 2009) and backcrossed at least 5 generations onto the C57/Bl6J mice from the UT Southwestern mouse breeding core facility. Congenic *Fmr1* KO mice (Consortium, 1994) were bred on the C57/BL6J background. All experiments were performed on littermate controls and blind to mouse genotype.

Reagents

Drugs were prepared as stocks and stored at -20°C and used within two weeks. The mixed group I mGluR agonist (RS)-3,5-dihydroxyphenylglycine (DHPG), U0126, MPEP, and Rapamycin were purchased from Tocris Bioscience and prepared as described (Gross et al., 2010; Osterweil et al., 2010b; Ronesi et al., 2012b).

Hippocampal slice preparation and LTD recordings

Acute hippocampal brain slices were prepared from 3-6 wk old mGluR5$^{F/F}$ and mGluR5$^{R/R}$ littermates as described previously (Ronesi and Huber, 2008a). LTD recordings were performed and analyzed as described (Ronesi and Huber, 2008a).

mGluR signaling in slices and western blotting

Western blotting on slices was performed as described (Ronesi et al., 2012b; Ronesi and Huber, 2008a). Blotting membranes were incubated with the following antibodies according to the manufacturer's instructions: phospho-T56 EF2, total-EF2, phospho- T389 p70S6K, phospho-S2448 mTOR, total mTOR, phospho-T202/Y204 ERK, total-ERK, phospho S209-eIF4E, phospho S65-4EBP, 4EBP, eIF4G, eIF4E (all from Cell Signaling Technology), Homer (Sc-8921; Santa Cruz), mGluR5 (Millipore), β3 tubulin (Abcam), Arc (Synaptic Systems), Map1b (gift from Dr. Itzhak Fischer, Drexel University), αCaMKII (Santa Cruz, sc-5391), actin (Millipore, MAB1501). For comparison of phosphoprotein levels across conditions or genotypes immunoreactive phosphoprotein bands were normalized to total protein levels from the same slice homogenates (e.g. P-mTOR/mTOR), each of which was first normalized to loading control (either tubulin or actin where indicated).

Coimmunoprecipitation

Hippocampus was lysed in co-immunoprecipitation buffer (50 mM Tris, pH 7.4, 120 mM NaCl, 0.5% NP40), and protein was tumbled overnight at 4°C

with 1 µg of antibody (either Homer (Santa Cruz, D-3), or eIF4G (Cell Signaling)). Protein A/G agarose bead slurry (Thermoscientific) was added for one additional hour and the beads were then washed with co-i.p. buffer. Western blotting was performed with the Homer (Santa Cruz, E-18 sc-8921), mGluR5 (Millipore), mGluR1 (BD Biosciences), Shank3 (gift from Paul Worley, John Hopkins University), EF2K (Cell Signalling), PIKE (Cell Signaling), eIF4E (Cell Signaling) or eIF4G (Cell Signaling).

Immunocytochemistry

All experiments were performed on at least three independent litter mate cultures with two to three different coverslips per condition. Neurons were fixed in 4% paraformaldehyde (37°C, 15 min) and permeabilized in 0.2% Triton X (10 min). Fixed cells were incubated in primary anti-mGluR5 (1:500; Millipore), primary anti-β3-tubulin (1:600; Abcam). Primary antibodies were detected with subsequent application of the appropriate Alexa Fluor 555 (AF555)-, AF546-, AF488-, or AF633-conjugated secondary antibody (Invitrogen). Fluorescence images were acquired on a Nikon TE2000 microscope with a cooled CCD camera (CoolSnap HQ; Roper Scientific) and quantified with MetaMorph Meta Imaging Series software (Molecular Devices) as described as in Niere et al. (2012).

Surface biotinylation of hippocampal slices

Hippocampal were prepared the same way as for LTD experiments. The slices recovered for 3.5-4 hours in ACSF at 32°C. Slices were transferred into cold

ACSF (2-4°C) with biotin and incubated for 10 minutes. Samples were kept at 4°C from this point on. Slices were washed 4 times with TBS for 3-4 minutes, then homogenized in 100 µl RIPA with protease inhibitors. Homogenates were rotated for 30-40 minutes, and then centrifuged for 5 minutes at 12,000 rpm. 100 µg of protein were tumbled with Avidin-bound Agarose beads for 2 hours.

Metabolic labeling of hippocampal slices

Hippocampal slices were prepared as described (Ronesi and Huber, 2008a), (Osterweil et al., 2010b). For these experiments (Fig. 3A-C) the most ventral slices (2 per hippocampus) were used since basal protein synthesis rates differ between dorsal and ventral hippocampal slices (Osterweil et al., 2010b). Slices recovered for 3.5 hours in ACSF at 32°C, and then were incubated in actinomycin D (25 µM) for 30 min. Slices were then incubated in actinomycin D and 10uCi/ml of ^{35}S labeled Methionine for 1hr. Where indicated, 20 µM U0126, or 10 µM MPEP was added at this step.

Neocortical Slice preparation and UP state recordings

UP state experiments in neocortical slices were performed and analyzed as described (Hays et al., 2011).

Audiogenic seizures

In order to evaluate audiogenic seizures, mice were placed in a plastic chamber (30X19X12cm) containing a 120 decibel siren (GE 50246 personal security alarm) and covered with a Styrofoam lid. A 120 dB siren was presented

to mice for 5 minutes. Mice were videotaped and scored for behavioral phenotype: 0=no response, 1=wild running, 2=tonic-clonic seizures, 3=status epilepticus/death as described (Dolen et al., 2007).

Behavioral measurements
Open field area experiments were performed as described in (Paylor et al., 1998).

Statistics:
Data plotted in the figures represents the mean ± SEM. Significant differences were determined using independent or paired t-tests between $mGluR5^{F/F}$ and $mGluR5^{R/R}$. For comparisons between $mGluR5^{F/F}$ and $mGluR5^{R/R}$ with or without drug a 2-way ANOVA and Bonferroni posttests were used. For comparisons between $mGluR5^{F/F}$, $mGluR5^{F/R}$ and $mGluR5^{R/R}$, for the UP states, a one-way ANOVA and Bonferroni multiple comparisions were used. Statistics on nominal data, such as seizure severity and incidence (Fig. 6A; Supplementary Table 3), a Chi squared (Fisher's Exact test) was used. Group data is presented in the figures as mean ±SEM. *$p< 0.05$; **$p< 0.01$; ***$p<0.001$.

Results
Characterization of the mGluR5F1128R knock-in mice.

To investigate if the altered mGluR5-Homer scaffolds contribute to the phenotypes observed in *Fmr1* KO mice, we utilized an mGluR5 knock-in mouse with a point mutation in the c-terminus tail from a phenylalanine (F) to arginine

(R) at amino acid position 1128, which disturbs the physical interaction between Homers and mGluR5. We first accessed the mGluR5$^{R/R}$ mice to make sure they are equivalent to wild types (WT) in measures of mGluR5 expression and trafficking, except for the binding of mGluR5 and Homer. Previous data has suggested that Homer can regulate mGluR5's trafficking, specifically out of the endoplasmic reticulum (Ango et al., 2000; Ciruela et al., 2000; Roche et al., 1999). Therefore we performed surface biotinylation on mGluR5$^{F/F}$ and mGluR5$^{R/R}$ slices and looked at total levels in fresh homogenates. The mGluR5$^{R/R}$ mice have normal total levels of mGluR5, Homer and FMRP (Fig. 1B,F), and the mutation has no effect on mGluR5 surface levels (Fig. 1 H,J). We also stained dissociated cortical cultures with mGluR5 and β-tubulin III to confirm mGluR5 localization and levels in the soma and dendrites. mGluR5 immunofluorescence shows normal expression in the soma and dendrites, which is confirmed by equal levels in the synaptoneurosomes (Fig. 1E,I). However, the mGluR5$^{R/R}$ mice have a 31% less mGluR5 in the postsynaptic density (PSD) (Fig. 1 A,D), which also occurs in the *Fmr1* KO mice (Giuffrida et al., 2005). The reduced mGluR5 levels in the PSD could be expected, since Homer scaffolds mGluR5 and stabilizes it in the PSD. Without the Homer scaffolding mGluR5 to the PSD, there should be less in the PSD. We importantly wanted to confirm that the mGluR5$^{R/R}$ mice have only altered mGluR5-Homer interactions, Co-immunoprecipitations were performed looking at Homer interactions with Homer's other binding partners.

The other Homer interacting proteins that we measured, such as Shank3 and PIKE, showed normal interactions except for mGluR1 ($mGluR5^{R/R}$: 68±4% of $mGluR5^{F/F}$, n=4; $p<0.005$; Fig. 1 C,G). mGluR1-Homer interactions may be reduced due to mGluR1 and mGluR5's ability to heterodimerize (Beqollari and Kammermeier, 2010), and it is unknown if one component of the heterodimer can affect the other. Overall, the $mGluR5^{R/R}$ mice appear to be very similar to WT mice except for the disrupted mGluR5-Homer interactions.

Disrupted mGluR-Homer interactions bidirectionally regulates group 1 mGluR signaling to translation machinery.

The rationale for this approach is based on data that *H1a*-bound mGluR5, which is increased in *Fmr1* KO, is functionally equivalent to mGluR5 that cannot interact with any Homer isoform (Ango et al., 2001; Tu et al., 1998; Xiao et al., 1998). *Fmr1* KO mice display a deficit in mGluR1/5 stimulation of protein synthesis which is rescued by H1a deletion may be a result of a specific alteration in mGluR5 interactions with Homer. Previously, we reported that using a peptide containing the Proline-rich motif (PPxxF) of the mGluR5 C-terminal tail that binds the EVH1 domain of Homer, mGluR5CT, (Mao et al., 2005; Ronesi and Huber, 2008b; Tu et al., 1998) disrupts mGluR5-Homer interactions and inhibits group 1 mGluR activation of PI3K-mTOR and translation initiation, but not ERK (Ronesi et al., 2012b; Ronesi and Huber, 2008b) in WT slices. To determine if specific disruption of mGluR5-Homer interactions causes altered mGluR

signaling, we measured mGluR signaling in the mGluR5$^{R/R}$ mice. Group 1 mGluR agonist, (RS)-3,5-Dihydroxyphenylglycine (DHPG; 100 µM; 5 min), induced activation was unable to activate the PI3K-mTOR pathway as measured by phosphorylation of mTOR (S2448) and S6K (Thr389) (P-mTOR: mGluR5$^{F/F}$: 245±52% of basal, n=12; mGluR5$^{R/R}$: 154±40% of basal, n=12; $p< 0.01$; P-S6K; mGluR5$^{F/F}$: 227±48% of basal, n=6; mGluR5$^{R/R}$: 77±22% of basal, n=6; $p< 0.05$; Fig. 2A-B) and had no effect on ERK activation (Thr202/Tyr204; P-ERK; mGluR5$^{F/F}$: 189±19% of basal, n=6; mGluR5$^{R/R}$: 228±31% of basal, n=6; n.s.; Fig. 2A,C) (Ronesi and Huber, 2008b). There was no difference in the total protein levels in the mGluR5$^{R/R}$ and DHPG did not affect total protein levels (Supplemental Table 1).

Homer and mGluR5 each directly interact with another translational regulatory factor, Elongation Factor 2 kinase (EF2K) (Park et al., 2008). Although phosphorylation of elongation factor 2 (EF2) by EF2K inhibits translation elongation globally, a moderate inhibition of elongation is thought to release translation factors that are then available for translational activation of poorly initiated transcripts such as *Arc* (activity-regulated cytoskeleton associated protein), and *αCaMKII* (Park et al., 2008). EF2 and EF2K are also FMRP targets and EF2 has been shown to be increased in *Fmr1* KO mice (Bhattacharya et al., 2012; Darnell et al., 2011). To determine if specific disruption of mGluR5-Homer

interactions causes enhanced EF2K signaling and not through FMRP regulation, we measured Group I mGluR stimulated EF2 phosphorylation. mGluR5$^{R/R}$ slices displayed a robust increase in phosphorylation of EF2 (T56) in response to DHPG (1128±345% of basal; n = 12 slices, Fig. 2A-B) in comparison to mGluR5$^{F/F}$ slices (215±31% of basal; n = 12; $p < 0.05$;. Fig. 2A-D). Taken together, our data suggest that Homer interactions facilitate mGluR activation of the PI3K-mTOR pathway to translation initiation, but dampen mGluR-induced phosphorylation of P-EF2 and thus restrain inhibition of global elongation rates. Consequently, disruption of mGluR5-Homer would be expected to block mRNA translation by blocking activation of the PI3K-mTOR pathway and translation initiation and enhancing inhibition of elongation to a level that may block elongation of all transcripts, including APP and Map1B. Consistent with this model, disrupting mGluR5-Homer interactions in hippocampal slices blocks DHPG-induced synthesis of APP (mGluR5$^{F/F}$: 131±13% of basal, n=10; mGluR5$^{R/R}$: 92±12% of basal, n=10; Fig. 2A,E) and Map1B (mGluR5$^{F/F}$: 175±23% of basal, n=10; mGluR5$^{R/R}$: 107±22% of basal, n=10; Fig. 2A,E) (Ronesi and Huber, 2008b). There is no difference in basal levels of APP and Map1B in the mGluR5$^{R/R}$ mice (Supplemental Table 1).

Altered mGluR-dependent LTD and translation of FMRP target mRNAs is attenuated in the mGluR5$^{R/R}$ mice.

In wildtype animals, mGluR-dependent long-term synaptic depression (mGluR-LTD) within the CA1 region of the hippocampus requires dendritic

protein synthesis Arc and MAP1b, whose mRNAs interact with FMRP (Luscher and Huber, 2010; Park et al., 2008; Waung et al., 2008). Although mGluR activation induces robust LTD in *Fmr1* KO mice, mGluR-induced rapid synthesis of Arc and MAP1b is deficient and LTD is independent of new protein synthesis (Luscher and Huber, 2010; Park et al., 2008). From this work it has been suggested that loss of FMRP-mediated translational suppression leads to enhanced steady state levels of "LTD proteins" allow mGluR-LTD to persist without new protein synthesis (Luscher and Huber, 2010). Consistent with this hypothesis, elevated levels of MAP1b and Arc have been reported in *Fmr1* KO brain (Luscher and Huber, 2010; Zalfa et al., 2003). Our previous work supports an essential role for FMRP interactions with its target mRNAs in mGluR-LTD and translational control of these mRNAs, and altered mGluR5-Homer scaffolds in the *Fmr1* KO mice do not mediate abnormal mGluR-LTD or altered translational control of specific FMRP target mRNAs (Bassell and Warren, 2008; Muddashetty et al., 2011; Ronesi et al., 2012b). Similarly, this view is also supported by our finding in the mGluR5$^{R/R}$ mice. We do not observe elevated steady state levels of LTD-promoting proteins or other FMRP target mRNAs as measured by western blots of MAP1b, and αCaMKII in hippocampal homogenates of mGluR5$^{F/F}$ and mGluR5$^{R/R}$ mice (Fig. 1B, Fig. 2A,E). Therefore, we did not expect the mGluR5$^{R/R}$ mice to have enhanced mGluR-LTD, like the *Fmr1* KO mice, but instead attenuated. mGluR-LTD was performed on acute

hippocampal slices from mGluR5$^{F/F}$ and mGluR5$^{R/R}$ mice, and showed the mGluR5$^{R/R}$ mice to have attenuated mGluR-LTD (mGluR5$^{F/F}$: 72±3% of baseline n=14 slices; mGluR5$^{R/R}$: 84±4% of baseline, n=11 slices; $p<0.05$; Fig. 2 F-G). The enhanced mGluR-LTD observed in the *Fmr1* KO is not mimicked in the mGluR5$^{R/R}$ mouse.

Basal translation rates are elevated in mGluR5$^{R/R}$ mice and rescued by inhibiting the ERK pathway

Although DHPG-induced translation is absent in *Fmr1* KO mice, basal translation rates are elevated (Bassell and Warren, 2008; Dolen et al., 2010; Gross et al., 2010; Osterweil et al., 2010b). Previously, we have shown enhanced protein synthesis rates in hippocampal slices are reversed by pharmacological blockade of mGluR5 or ERK activation, but not by an inhibitor of PI3K or mTOR (Osterweil et al., 2010b). Another consequence of disrupted mGluR5-Homer interaction is constitutive, or agonist-independent mGluR5 activity (Ango et al., 2001) which may drive translation rates through ERK activation, a pathway that remains intact in *Fmr1* KO mice and with Homer disruption (Osterweil et al., 2010b; Ronesi et al., 2012b; Ronesi and Huber, 2008a). Furthermore, we have shown acute peptide-mediated disruption of mGluR5-Homer interactions with mGluR5CT in WT slices is sufficient to mimic enhanced protein synthesis rates to that observed in *Fmr1* KO slices, with the peptide having no effect in *Fmr1* KO slices (Ronesi et al., 2012b). In the mGluR$^{R/R}$ mice, there are elevated basal protein synthesis rates similar to what is observed in the *Fmr1* KO mice

(Osterweil et al., 2010a; Ronesi et al., 2012b) (mGluR5$^{R/R}$ =135±10% of mGluR5$^{F/F}$, n= 17 slices from 5 mice; $p < 0.005$; Fig. 3A). Also as seen in the *Fmr1* KO mice (Osterweil et al., 2010a; Ronesi et al., 2012b), elevated basal protein synthesis rates in the mGluR5$^{R/R}$ are rescued by inhibiting the ERK pathway and normalized by inhibiting mGluR5 (Fig 3 B-C).

Translation initiation is the rate limiting step in translation (Proud, 2007). To determine if enhanced translation rates stem from disrupted mGluR5-Homer interactions enhanced initiation, we measured eIF4F translation initiation complex in hippocampal slices prepared from mGluR5$^{F/F}$ and mGluR5$^{R/R}$ mice. The eIF4F complex is composed of the 5' cap binding protein eIF4E, a scaffolding protein eIF4G, and the RNA helicase eIF4A (Proud, 2007). eIF4F complex assembly can be measured by co-immunoprecipitation of eIF4G and eIF4E (Banko et al., 2006). Previous reports show eIF4F complex levels are enhanced basally in *Fmr1* KO slices (Sharma et al., 2010), and we have shown eIF4F complex levels in *Fmr1* KO slices are restored to WT levels by *H1a* deletion (Ronesi et al., 2012b). The previous data suggests that elevated protein synthesis rates in *Fmr1* KO mice are due to enhanced translation initiation that is driven by disrupted mGluR5-Homer interactions causing increased eIF4E/4G association. However, in the mGluR5$^{R/R}$ mice, there is no change observed in the interaction between eIF4G and eIF4E (mGluR5$^{R/R}$: 86±14% of mGluR5$^{F/F}$, n=5; ns; Fig. 3F). The enhanced basal translation is not being driven by the increased association of eIF4E/4G like

previously believed. There must be other through which mGluR5 driven ERK pathway is increase basal translation as discussed below.

We previously showed phosphorylation of initiation factors known to be regulated by ERK enhanced *Fmr1* KO mice and rescued by deleting *H1a* (Ronesi et al., 2012b). ERK phosphorylates and activates MAPK-interacting kinase (Mnk) which in turn phosphorylates the cap-binding protein eIF4E (S209) (Proud, 2007). ERK also phosphorylates eIF4E binding protein (4EBP) at S65, a distinct site from mTOR regulated sites (T36/45) (Herbert et al., 2002). The ERK-dependent phosphorylation of eIF4E and 4EBP (S65) are associated with increased translation rates in neurons and other cell types (Banko et al., 2006; Kelleher et al., 2004). To determine if disrupted mGluR5-Homer interactions lead to enhanced signaling to translation downstream of ERK, we looked at hippocampal homogenates in mGluR5$^{F/F}$ and mGluR5$^{R/R}$ mice. P-4EBP and P-eIF4E levels were enhanced in hippocampal homogenates from mGluR5$^{R/R}$ mice (Fig. 3D-E). Just as what was previously reported in *Fmr1* KO mice (Osterweil et al., 2010b; Ronesi and Huber, 2008b) (Ronesi et al., 2012b), P-ERK levels were unchanged in mGluR5$^{R/R}$ lysates (Fig. 3D-E). Because P-ERK levels are not affected in mGluR5$^{R/R}$ mice, this suggests that mGluR5 may regulate accessibility or localization of eIF4E or 4EBP with ERK, as opposed to ERK activity per se.

Hyperexcitable neocortical circuit function in Fmr1 KO mice is mimicked in the mGluR5$^{R/R}$ mice.

FXS patients and *Fmr1* KO mice exhibit sensory hypersensitivity, epilepsy and/or audiogenic seizures suggestive of an underlying sensory circuit hyperexcitability (Berry-Kravis, 2002; Dolen et al., 2010). We recently discovered synaptic and circuit alterations indicative of hyperexcitability in slices and *in vivo* in the somatosensory, barrel neocortex of *Fmr1* KO mice. *Fmr1* KO mice have decreased excitatory drive onto layer IV fast-spiking interneurons and prolonged thalamically-evoked and spontaneously-occurring persistent activity, or UP, states (Gibson et al., 2008; Hays et al., 2011). UP states represent a normal physiological rhythm generated by the recurrent neocortical circuitry and is observed in alert and slow-wave sleep states *in vivo* as well as neocortical slice preparations (Haider and McCormick, 2009; Sanchez-Vives and McCormick, 2000). It has previously been reported (Gibson et al., 2008; Hays et al., 2011) that UP states are longer in slices of *Fmr1* KO mice in comparison to WT littermates. Importantly, genetic or pharmacological reduction of mGluR5 in *Fmr1* KO mice rescues the prolonged UP states in acute slices and *in vivo* (Hays et al., 2011). To determine if altered mGluR5-Homer interactions is sufficient to alter neocortical circuit function, we measured spontaneously occurring UP states in acute slices from mGluR5$^{R/R}$ mice in the somatosensory, barrel cortex using extracellular multiunit recordings (Sanchez-Vives and McCormick, 2000). mGluR5$^{R/R}$ mice have prolonged neocortical UP states, equivalent to the duration is seen in the

Fmr1 KO mice (mGluR5$^{F/F}$: 809.2±45.0 ms, n=21 slices; mGluR5$^{R/R}$: 1315±59.1 ms, n=26; Fig. 4). Also, the gene dosage has an additive effect as the mGluR5$^{F/R}$ have an intermediate duration (mGluR5$^{F/R}$: 1079±57.6 ms, n=22 slices; Fig. 4).

To better understand the pathways through which mGluR5 is driving the increased UP state durations, we tested the role of the ERK pathway plays. The ERK pathway is basal unregulated in the hippocampus (Fig. 3E) and drives the increased basal translation (Fig. 3C) (Osterweil et al., 2010a; Ronesi et al., 2012a). There is a role for disrupted mGluR5-Homer interactions in the neocortex (Fig. 4) (Ronesi et al., 2012a), so does ERK also contribute to this increase excitability phenotype? *Fmr1* KO and WT neocortical slices were treated for 45 min. with U0126, a MEK inhibitor, in the high activity buffer before recording. U0126 rescued the prolonged UP states in the *Fmr1* KO (*Fmr1* KO: 1519±112.0, n=11; *Fmr1* KO + U0126: 988±66.3, n=11; Fig. 5A,C). The MEK inhibitor had no effect on WT durations (WT: 1019±76.6, n=7; WT + U0126: 904±81.4, n=5; Fig. 5A,C). This experiment was repeated in the mGluR5$^{R/R}$ with the prediction that U0126 should rescue the prolonged neocortical UP states in this model as well. Unexpectedly, this result was not replicated in the mGluR5$^{R/R}$ with U0126 having no effect on the duration (mGluR5$^{R/R}$: 1306±59.3, n=23; mGluR5$^{R/R}$ + U0126: 1209±79.3, n=21; Fig. 5B). The reason for the difference between ERK's contribution to the prolonged UP

state duration the *Fmr1* KO and the mGluR5$^{R/R}$ is unknown. Possibilities are discussed below.

The mGluR5R/R mice have reduced audiogenic seizures and mimic the open field behavior in Fmr1 KO mice

To determine if mGluR5-Homer interactions mimicked any *in vivo* or behavioral phenotypes in *Fmr1* KO mice, we measured the incidence of audiogenic seizures and anxiety as measured using the open field activity test. We chose these phenotypes because they are robust in the C57BL6 strain of *Fmr1* KO mice and sensitive to mGluR5 antagonists (Dolen et al., 2010). The mGluR5$^{R/R}$ showed a reduced seizure rate to the *Fmr1* KO mice, while mGluR5$^{F/F}$ whom exhibited no incidence of seizure (Seizure score (0-3; 3 being most severe; see methods); mGluR5$^{F/F}$: 0.00±0.00, n = 27 mice; mGluR5$^{R/R}$: 0.38 ±0.18, n = 21; $p< 0.01$; Fig. 6C, Supplemental Table 2)). The date is consistent with our previous data in which deleting *H1a* partial rescues audiogenic seizures (Ronesi et al., 2012b) and what is observed with genetic reduction of mGluR5 in *Fmr1* KO mice (Dolen et al., 2007).

As previously reported, *Fmr1* KO mice spend more time in the center of a lit open field in comparison to WT littermates, which has been interpreted as reduced generalized anxiety in the mice(Liu and Smith, 2009). mGluR5$^{R/R}$ mice spend more time in the center, showing reduced anxiety similar to *Fmr1* KO mice (mGluR5$^{F/F}$: 0.336±0.009; n = 19; mGluR5$^{R/R}$: 0.381±0.017; n = 22, Fig. 6A).

There were no differences in locomotor activity between the mGluR5$^{R/R}$ and mGluR5$^{F/F}$ (Fig. 6B). Therefore, altered mGluR5-Homer interactions contribute to altered behavior in *Fmr1* KO mice and may be relevant for altered behaviors in FXS patients.

Discussion

Two mechanisms for mGluR dysfunction in Fragile X Syndrome

Here we demonstrate a single amino change in Homer binding domain of mGluR5, which disrupts mGluR5-Homer interactions, can mimic multiple phenotypes of a complex disease model. mGluR5 dysfunction in animal models of FXS is well established and genetic or pharmacological reduction of mGluR5 activity reduces or rescues many disease phenotypes in animal models (Dolen et al., 2010) and most recently in patients (Jacquemont et al., 2011). Our previous results in the *Fmr1/H1a* KO reveal two mechanisms for mGluR5 dysfunction in *Fmr1* KO mice. This study confirmed our previous results, showing disrupting mGluR5-Homer interactions are sufficient to cause some of the mGluR5 dysfunction. First, disrupting mGluR5-Homer interactions causes and mimics altered mGluR signaling, enhanced basal translation rates, neocortical hyperexcitability, audiogenic seizures and open field activity in the *Fmr1* KO mice. Second, disrupting mGluR5-Homer scaffolds does not lead to the enhanced mGluR-LTD in the *Fmr1* KO mice, implicating an essential role for

FMRP regulation of synaptic proteins in mGluR-LTD (Ronesi et al., 2012a). However, the study also leaves open the possibility of mGluR1 contributing caused by altered mGluR5 function. The discovery that simply altering mGluR5-Homer scaffolds can cause much of the complex dysfunction of mGluR5 in FXS will help provide insight into a complicated disease and help better understand what the underlying mechanisms that create the phenotypes seen in FXS.

Homer scaffolds coordinate mGluR regulation of translation

Our data demonstrate the role for specific Homer scaffolding to mGluR5 in coordinating mGluR-stimulated translation by activating the PI3K-mTOR pathway and translation initiation (Ronesi et al., 2012b; Ronesi and Huber, 2008a), as well as limiting activation of EF2K, which inhibits elongation (Fig. 2D). Homer scaffolds with the PI3K enhancer (PIKE), a small GTPase which binds and activates PI3K in response to mGluR activation (Shiraishi-Yamaguchi and Furuichi, 2007). The PI3K pathway stimulates mTOR and p70 S6K activating translation of 5' terminal oligopyrmidine tract (5' TOP) mRNAs that encode ribosomes and translation factors, thus increasing the translational capacity of the cell (Proud, 2007). mGluR activation of PI3K-mTOR-S6K pathway and stimulated protein synthesis is blocked in the mGluR5$^{R/R}$ indicating a key role for Homer scaffolds in mGluR-stimulated translation initiation (Ronesi et al., 2012b; Ronesi and Huber, 2008a).

Although somewhat counterintuitive, submaximal inhibition of global elongation may make poorly initiated mRNAs, like Arc, able to effectively compete for rate limiting translational factors (Scheetz et al., 2000). mGluRs stimulate phosphorylation of EF2, which in turn inhibits elongation rate (Park et al., 2008). Long Homer interactions limit EF2K activation by mGluRs promoting translation of poorly initiated mRNAs (Park et al., 2008). Disruption of mGluR5-Homer in the mGluR5$^{R/R}$ enhances EF2K activity (Fig. 2D) and would be expected to strongly inhibit elongation and block translational activation. Together the enhanced EF2K activity and reduced mTOR activity probably act together in the mGluR5$^{R/R}$ to block mGluR-induced synthesis of APP and Map1b (Fig. 2E) and mGluR-LTD (Fig. 2F) (Ronesi et al., 2012b; Ronesi and Huber, 2008a). However, previous results showed *H1a* deletion rescues mGluR-mediated translation initiation complex formation but not synthesis of Arc (Ronesi et al., 2012b), suggesting a requirement for both mGluR5-Homer scaffolds and FMRP in mGluR-triggered Arc translation. These results also indicate that mGluR5-Homer interactions are necessary to properly stimulate translation and induce LTD.

Altered mGluR5-Homer scaffolds increase translation rates

Although there is a deficit in mGluR agonist-stimulated translation in *Fmr1* KO mice, steady state translation rates and levels of specific proteins are elevated (Osterweil et al., 2010b; Sharma et al., 2010), thus reflecting the

complexity of translational control. Because one function of FMRP is to suppress translation of its mRNA targets (Bassell and Warren, 2008), an obvious possibility was that the elevated protein synthesis rates and levels directly result from loss of FMRP-mediated suppression of mRNA targets. However, elevated total protein synthesis rates are recapitulated in the mGluR5$^{R/R}$ mice (Fig. 3A), which still has normal FMRP levels. Thus, increased steady state translation rates in *Fmr1* KO tissue are a result of altered mGluR5-Homer scaffolds, a secondary consequence of FMRP loss. Elevated protein synthesis rates are reversed by the genetic reduction of mGluR5 (*Grm5het*), the mGluR5 inverse agonist MPEP, and inhibitors of ERK (Dolen et al., 2010; Osterweil et al., 2010b; Ronesi et al., 2012b) (Fig. 3B-C). In the *Fmr1* KO, there is enhanced phosphorylation of translation initiation factors that are downstream of ERK (eIF4E and 4EBP), which was reversed by *H1a* deletion (Ronesi et al., 2012b) and increased in the mGluR5$^{R/R}$ (Fig. 3D). Together these results suggest that constitutively active mGluR5 (Ango et al., 2001) drives ERK-dependent phosphorylation of eIF4E and 4EBP which enhances eIF4F initiation complex formation and translation rates. However, despite the increased phosphorylation of translation initiation factors, there is no basal increase in eIF4E/4G association (Fig. 3F). This suggests ERK must be regulating basal translation rates in the *Fmr1* KO through other pathways than cap dependent translation. One possible factor that may be altered is ribosomal activity. ERK regulates p90RSK, which phosphorylates rpS6 (Pende et

al., 2004; Roux et al., 2007). Phosphorylated rpS6 correlates with assembly of the translation pre-initiation complex and increased cap-dependent translation (Anjum and Blenis, 2008; Roux et al., 2007). Better understanding of alternative ERK regulation of translation and how it is regulated in the mGluR5R/R mice and will help increase the understanding for how basal translation is increased in the *Fmr1* KO.

An essential role for Homer in proper regulation of LTD

In the *Fmr1* KO mouse, there is enhanced mGluR-LTD, as well as, elevated steady state protein levels of FMRP target mRNAs, MAP1b and αCaMKII (Hou et al., 2006a; Huber et al., 2002; Niere et al., 2012). The enhanced mGluR-LTD in the *Fmr1* KO mice is protein synthesis independent (Iliff et al., 2013; Nosyreva and Huber, 2006). The enhanced mGluR-LTD and protein synthesis independent nature of the LTD in *Fmr1* KOs is thought to be due to increased levels of FMRP targets. The mGluR5$^{R/R}$ mice, steady state levels of FMRP target mRNAs are normal (Fig. 1B). Normally these proteins are synthesized after DHPG stimulation, but this does not occur in *Fmr1* KO or the mGluR5$^{R/R}$ mice (Hou et al., 2006) (Fig. 2E). Since there is no increase in FMRP targets and no mGluR-stimulated translation of these targets in the mGluR5$^{R/R}$ mice (Fig. 2B,E) , the proteins needed for the maintenance of mGluR-LTD are not synthesized causing attenuated mGluR-LTD. In contrast, the synaptic proteins are basally elevated in the *Fmr1* KO, the synaptic proteins are available for use,

therefore no longer require protein synthesis, and leading to the enhanced mGluR-LTD. This can account for the differential effect on mGluR-LTD observed in the *Fmr1* KO and mGluR5$^{R/R}$. However, disrupting mGluR5-Homer interactions increases basal protein synthesis rates, but does not increase mGluR-LTD like one may of predicted. Despite the increase in translation synaptic proteins, like MAP1b and CaMKII, are not basally increased in the mGluR5$^{R/R}$ mice (Fig 1B, 2A). This suggests that altered LTD and elevated Map1b and CaMKII are not a result of elevated protein synthesis rates in the *Fmr1* KO mice. This supports the hypothesis that the protein synthesis independence of mGluR-LTD in *Fmr1* KO mice is a result of loss of FMRP-mediated translational suppression of LTD promoting proteins, such as Map1b (Waung and Huber, 2009).

Altered mGluR5-Homer and neocortical network dysfunction

Altered neocortical circuit function and hyperexcitability have been predicted to contribute to cognitive disorders and autism (Rubenstein and Merzenich, 2003; Uhlhaas and Singer, 2006). The epilepsy and EEG abnormalities observed in FXS patients are indicative of brain hyperexcitability (Berry-Kravis, 2002; Dolen et al., 2010). Furthermore, FXS patients display hypersensitivity to sensory stimuli, and *Fmr1* KO mice have audiogenic seizures reflecting hyperexcitability of sensory circuits (Berry-Kravis, 2002; Dolen et al., 2010). Our previous findings indicate that the longer UP states in *Fmr1* KO neocortex are mediated by enhanced, likely constitutive, activity of H1a-bound

mGluR5 (Hays et al., 2011). These neocortical UP states have been rescued by mGluR5 inhibition, as well as, *H1a* deletion, and peptide-mediated disruption of mGluR5-Homer interactions prolongs UP states in WT, but not *Fmr1* KO, slices (Hays et al., 2011; Ronesi et al., 2012a). The mGluR5$^{R/R}$ also show prolonged neocortical UP states equivalent to *Fmr1* KO durations (Fig. 4). There is a gene dosage effect of the disrupted mGluR5-Homer interactions with the heterozygous having an intermediate phenotype (Fig. 4), which suggests that regulation of Homer scaffolds may regulate neocortical slow oscillations in the normal brain.

There is still little known about how mGluR5 activity leads to longer UP states. Prolonged UP states are not due to mGluR5-driven translation because the protein synthesis inhibitor, anisomycin, does not affect UP state duration in either WT or *Fmr1* KO slices (Hays et al., 2011). Therefore, mGluR5 activity likely leads to prolonged UP states through posttranslational regulation of the intrinsic excitability and/or synaptic function of neocortical neurons. mGluR5 has been shown to regulate the ERK pathway in the *Fmr1* KO (Ronesi et al., 2012b) and again in the mGluR5$^{R/R}$ (Fig. 3D). Inhibiting the ERK pathway rescues the prolonged neocortical UP states in the *Fmr1* KO (Fig. 4), but is unable to rescue them in the mGluR5$^{R/R}$ (Fig. 5). This data suggests that the prolonged neocortical UP states may be caused by a different mechanism in the mGluR5$^{R/R}$ than the *Fmr1* KO. One possible explanation is that there is a developmental difference between the *Fmr1* KO and the mGluR5$^{R/R}$. In the mGluR5$^{R/R}$ mouse, the

mGluR5-Homer interactions are disrupted embryonically. While it has been shown the mGluR5-Homer interactions are altered in the *Fmr1* KO mouse, there is no time course for when the disruption occurs (Giuffrida et al., 2005). The mGluR5-Homer interactions may not be disrupted all through development. Another possible explanation is possible morphological changes in the mGluR5$^{R/R}$ mouse not found in the *Fmr1* KO. mGluR5 has been shown to be involved in proper development of the barrel and in mGluR5 KO cells there is altered morphology and barrel structure (Ballester-Rosado et al., 2010; She et al., 2009; Wijetunge et al., 2008). mGluR5 is required for full polarization of layer IV spiny stellate neurons in the barrel cortex (She et al., 2009). If the loss of mGluR5 can cause altered morphology, it is therefore possible increased mGluR5 activity can also lead to altered morphology. The gross cortical morphology is normal in *Fmr1* KO mice, but there is a delay in circuit maturation (Till et al., 2012). Full polarization of layer IV neurons is delayed, along with barrel segregation, but both are normal in mature mice (Till et al., 2012).

Altered behavior in Fmr1 KO mice is mimicked by disrupting mGluR-Homer interactions

Genetic reduction of mGluR5 (heterozygosity), or *H1a* deletion, completely rescue neocortical hyperexcitability (e.g. long UP states) in *Fmr1* KO mice, but only partially rescue audiogenic seizures (Dolen et al., 2007; Hays et al., 2011; Ronesi et al., 2012b). Disrupting mGluR5-Homer interactions is able to

mimic neocortical hyperexcitability (Ronesi et al., 2012b) (Fig. 4) and partially mimic audiogenic seizures in the *Fmr1* KO (Fig. 5A). This suggests that hyperexcitability in other brain regions, such as the auditory brain stem, also contribute to audiogenic seizures in *Fmr1* KO mice, through mGluR5 independent mechanisms (Brown et al., 2010). Importantly, mGluR5 antagonism and *H1a* deletion rescued the increased open field activity in *Fmr1* KO mice (Ronesi et al., 2012b). Also the mGluR5$^{R/R}$ mice have decreased anxiety (Fig. 6B), suggesting that abnormal Homer scaffolds contribute to behavioral symptoms associated with FXS and may represent a new therapeutic target for the disease. In contrast to initial studies (Dolen et al., 2010; Dolen et al., 2007; Osterweil et al., 2010b), recent reports have failed to rescue some *Fmr1* KO mouse behaviors by reduction of mGluR5 activity (Thomas et al., 2011a; Thomas et al., 2011b), suggesting mGluR5-independent mechanisms in FXS pathology. Interestingly, in these studies inhibition of mGluR1 proved efficacious in reducing some *Fmr1* KO phenotypes (Thomas et al., 2011a; Thomas et al., 2011b). MGluR1a, is a Homer binding protein, and mGluR1a-Homer scaffolds may also be affected in *Fmr1* KO mice. Disrupted mGluR1a-Homer interactions seen in the mGluR5$^{R/R}$ (Fig. 1C,G) suggest a possible role for mGluR1 in *Fmr1* KO mice. This study did not look at the contribution of mGluR1 to the phenotypes, but in future it may be important to understand their individual contributions. The heterodimers comprised of mGluR5 and mGluR1 may be able

to alter the signaling of its counterpart (Goudet et al., 2005). mGluR5 antagonism has proven effective in some FXS patients (Jacquemont et al., 2011) and may also be acting indirectly on mGluR1 as well. The understanding of mGluR5 and mGluR1 function in the normal brain and its dysfunction in FXS may provide additional and more targeted treatments for the disease and provide insight into autism.

Figure 3.1: Reduced mGluR5 levels in the PSD and disrupted mGluR1-Homer interactions of the mGluR5$^{R/R}$ mice.

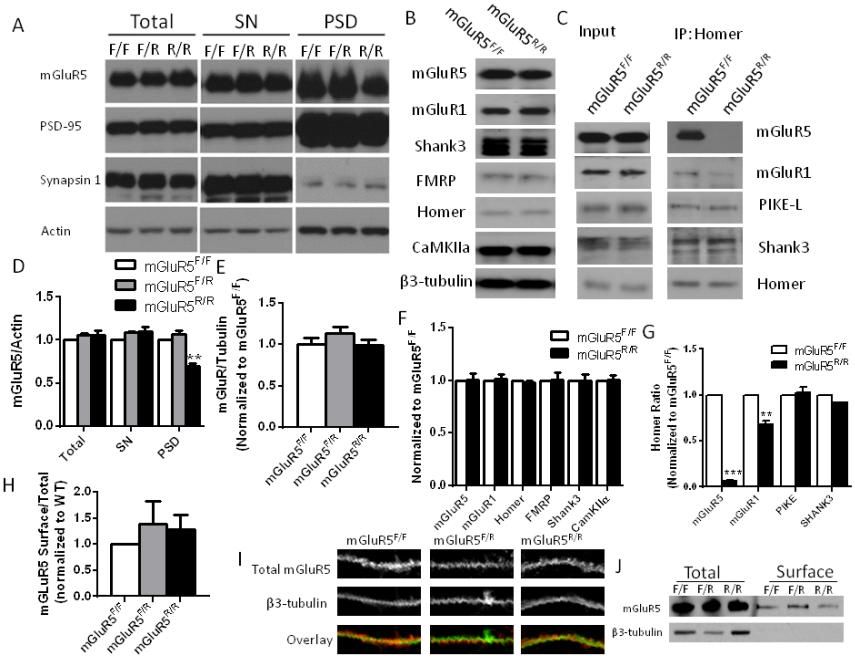

Figure 3.1: Reduced mGluR5 levels in the PSD and disrupted mGluR1-Homer interactions of the mGluR5$^{R/R}$ mice. A. The mGluR5$^{R/R}$ mice show normal total levels of mGluR5 compared to mGluR5$^{F/F}$ mice. Synpatoneurosome (SN) fractions also show normal levels of mGluR5 in the FR. The PSD fraction shows a reduced amount of mGluR5 in only the mGluR5$^{R/R}$ mice. The reduced amount of mGluR5 in the PSD is similar to what is seen in the *Fmr1* KO mice**. B.** The mGluR5$^{R/R}$ mice have normal levels of mGluR1, Homer, FMRP and FMRP targets, like CaMKIIα. **C.** Homer interacting proteins have normal interactions except for mGluR1 in the mGluR5$^{R/R}$ mice. **D.** Graphical analysis of A. **E.** Dendritic analysis of mGluR5 levels in dissociated cortical cultures shows no change in the mGluR5$^{R/R}$ mice compare to mGluR5$^{F/F}$. **F-G.** Graphical analysis of B-C. **H.** The mGluR5$^{R/R}$ mice do not have altered surface mGluR5 levels, measure by surface biotinylation. **I.** Representative images of mGluR5 and β-tubulin III staining in dendrites. **J.** Representative blots of mGluR5 surface biotinylation levels. For this figure and all subsequent figures, *p< 0.05; **p < 0.01, ***p<0.005.

Figure 3.2. mGluR5$^{R/R}$ mice have attenuated mGluR-LTD, but the same altered group 1 mGluR activation of translational control pathways as *Fmr1* KO mice.

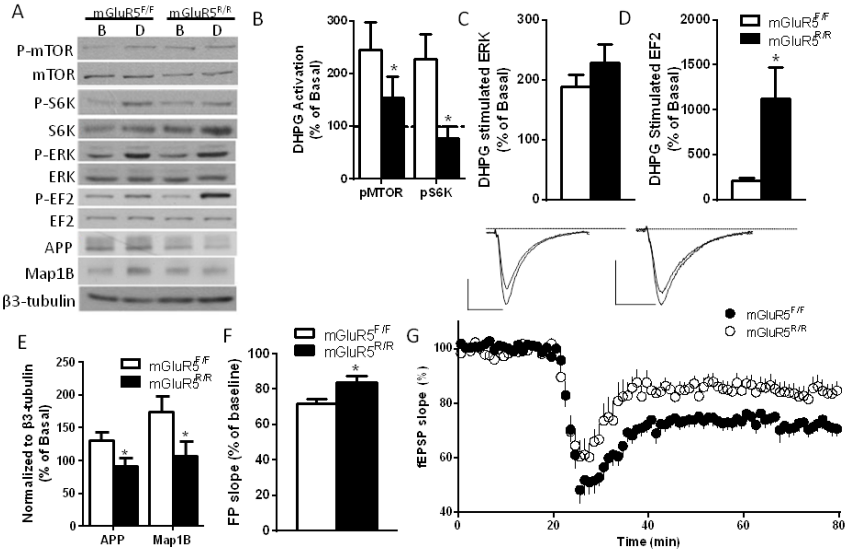

Figure 3.2. mGluR5$^{R/R}$ mice have attenuated mGluR-LTD, but the same altered group 1 mGluR activation of translational control pathways as *Fmr1* KO mice. A. Acute hippocampal slices from mGluR5$^{R/R}$ mice stimulated with the group 1 mGluR agonist DHPG (D; 100 μM; 5 min) have a deficiency in phosphorylation of p70S6K and enhanced EF2 phosphorylation compared to mGluR5$^{F/F}$ slices. In contrast, DHPG-induced phosphorylation of ERK was unaffected. There was a deficiency in mGluR-induced synthesis of APP have a deficiency in phosphorylation of p70S6K (T389) and enhanced EF2 phosphorylation compared to WT slices. **B-D.** Analysis of phosphorylated mTOR, S6K, EF2, or ERK with DHPG (D) treated slices normalized to untreated slices (basal or B). Group data is expressed as phosphorylated to total mTOR, S6K, EF2 or ERK (each normalized to a β-tubulin III loading control) in untreated or DHPG treated slices. **E.** Analysis of APP and Map1B synthesis normalized to basal. **F.** mGluR5$^{R/R}$ have attenuated mGluR-LTD compared to mGluR5$^{F/F}$ littermates. **G.** Example traces and average plots of F. *p< 0.05, **p< 0.01; ***p<0.001.

Figure 3.3: Enhanced, ERK-dependent translation rates are observed in hippocampal slices from mGluR5$^{R/R}$ mice.

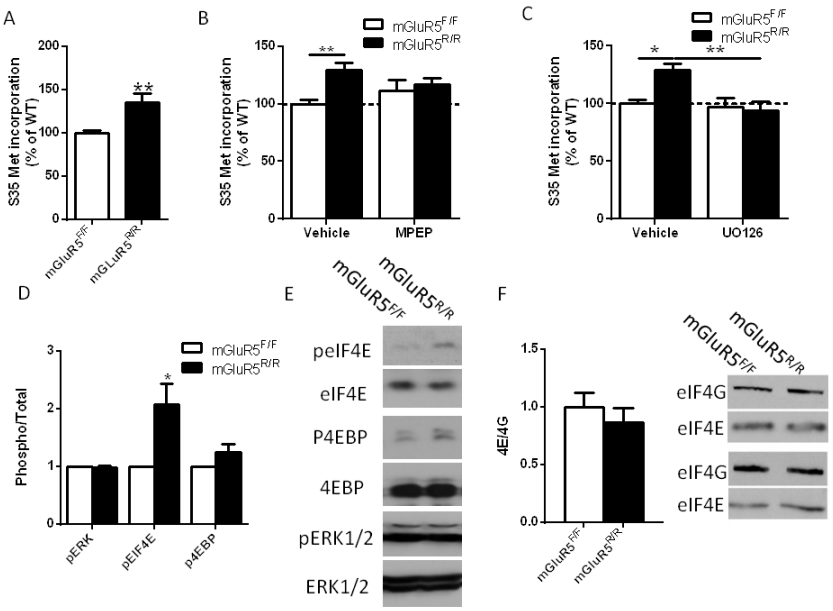

Figure 3.3: Enhanced, ERK-dependent translation rates are observed in hippocampal slices from mGluR5$^{R/R}$ mice. A. Acute hippocampal slices from mGluR5$^{R/R}$ mice display elevated protein synthesis rate in comparison to mGluR5$^{F/F}$ littermates as measured by incorporation of ^{35}S Met/Cys into total protein. **B.** MPEP, mGluR5 reverse antagonist, equalizes protein synthesis rates between mGluR5$^{F/F}$ and mGluR5$^{R/R}$ slices. **C.** Inhibition of the ERK pathway rescues protein synthesis rates in mGluR5$^{R/R}$ slices to mGluR5$^{F/F}$ levels. **D.** Representative western blots of phospho- and total ERK and translation initiation factors that are regulated by ERK, (phospho- and total eIF4E and 4EBP) from hippocampal homogenates in each genotype. **E**. Quantified group data reveals elevated P-4EBP and P-eIF4E in mGluR5$^{R/R}$ brains as compared to mGluR5$^{F/F}$. P-ERK levels were not different across any genotype (n = 5-7 mice per genotype). **F.** Right: Quantified group data of the levels of eIF4E that coimmunoprecipitated with eIF4G (eIF4E/4G) show no change in mGluR5$^{R/R}$ hippocampal lysates (normalized to the levels of eIF4E/4G in mGluR5$^{F/F}$) N = 6 mice per genotype. Left: Representative western blots of eIF4E that co-immunoprecipitated with eIF4G from mGluR5$^{F/F}$ and mGluR5$^{R/R}$ *p< 0.05; **p< 0.01; ***p<0.001.

Figure 3.4. Disruption of mGluR5-Homer interactions mediates prolonged neocortical UP states in *Fmr1* KO mice.

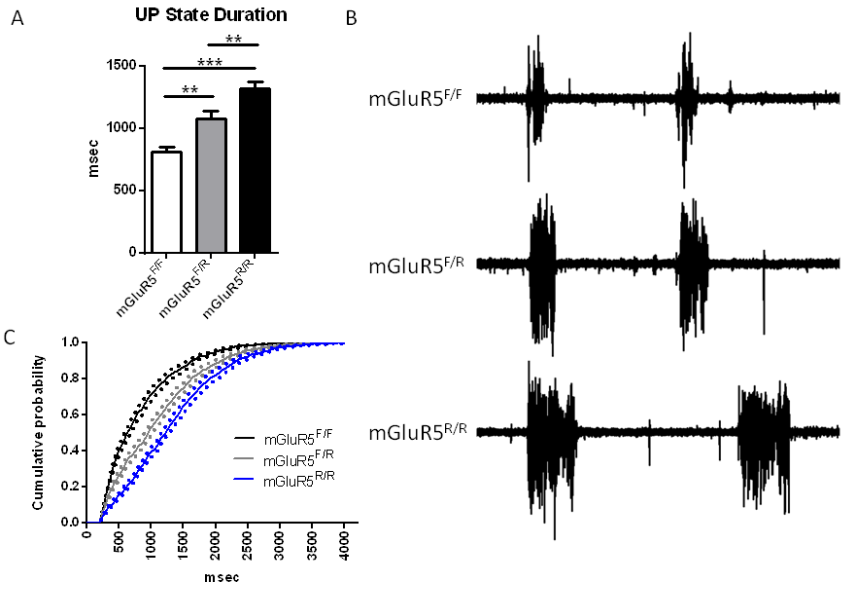

Figure 3.4. Disruption of mGluR5-Homer interactions mediates prolonged neocortical UP states in *Fmr1* KO mice. A. In 3 week old mice, UP states are longer in the mGluR5$^{R/R}$ mice similar to *Fmr1* KO mice and mGluR5$^{F/R}$ have an intermediate duration. **B.** Representative extracellular multiunit recordings of spontaneous, persistent activity or UP states from layer 4 of somatosensory, barrel neocortical slices from each genotype. Scale bar = 50 µV / 1 sec. **C.** The cumulative distribution of average duration (normalized for each slice and averaged over slices; same data set as A) was evenly shifted to the right for the mGluR5$^{R/R}$. Outer dashed lines represent the standard error. **p< 0.01; ***p<0.001.

Figure 3.5. Inhibiting the ERK pathway rescues prolonged neocortical UP states in *Fmr1* KO, but not the mGluR5$^{R/R}$ mice.

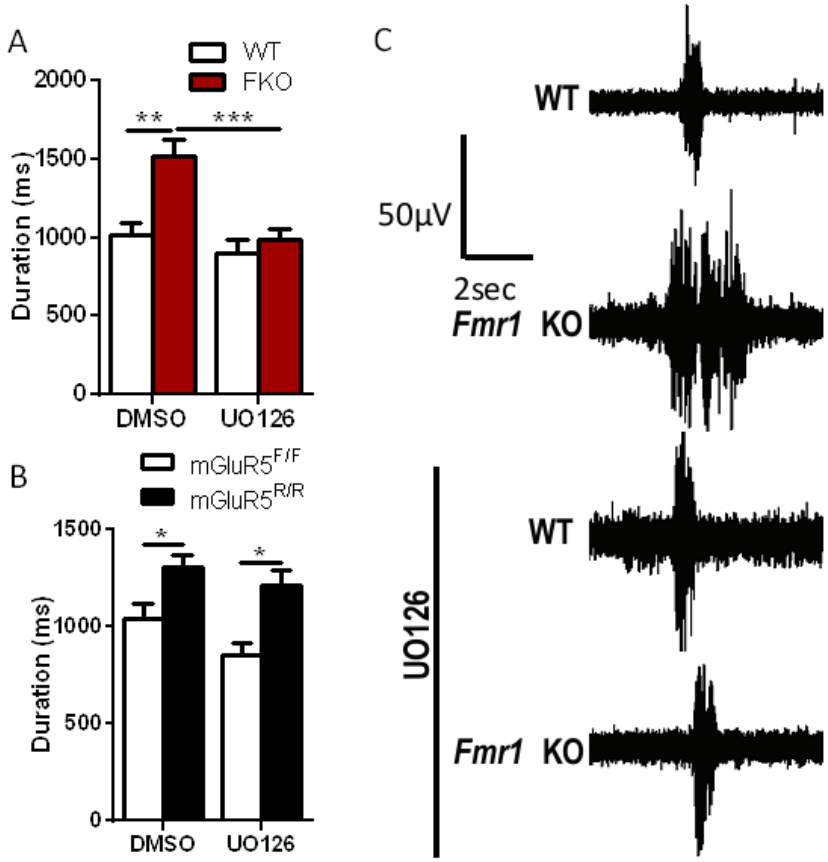

Figure 3.5. Inhibiting the ERK pathway rescues prolonged neocortical UP states in *Fmr1* KO, but not the mGluR5$^{R/R}$ mice. A. UP states are longer in the *Fmr1* KO mice and rescued to WT levels when treated with an MEK inhibitor, U0126 (20µM). **B.** UP states are longer in the mGlur5$^{R/R}$ mice, but U0126 has no effect on their duration. **C.** Representative recordings of UP states from WT and *Fmr1* KO slices in vehicle and U0126. Scale bar = 50 µV / 2 sec. *p< 0.05; **p< 0.01; ***p<0.001.

Figure 3.6. Altered mGluR5-Homer scaffolds in mGluR5$^{R/R}$ mice partially mimic audiogenic seizures and mimics open field activity.

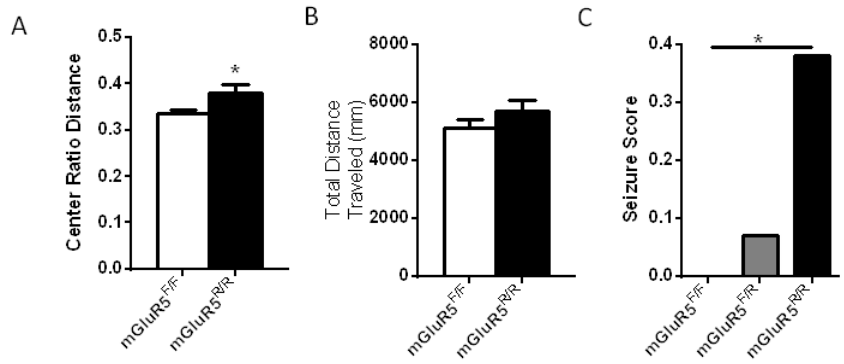

Figure 3.6. Altered mGluR5-Homer scaffolds in mGluR5$^{R/R}$ mice partially mimic audiogenic seizures and mimics open field activity. A. Open field activity, measured as a ratio of the distance travelled in the center to total distance travelled of an open arena, was increased in mGluR5$^{R/R}$ mice. **B.** Total distance travelled by the mice in the open field arena is not different between genotypes. **C.** mGluR5$^{F/F}$, mGluR5$^{F/R}$ and mGluR5$^{R/R}$ litters mates were subjected to a 120 dB for 5 minutes. Mice were scored for the severity of seizure (0-no siezure, 1-wild running, 2-clonic/tonic, 3-status epilepticus). mGluR5$^{F/F}$ did not seize, while 20% of the mGluR5$^{R/R}$ seized, a third of the 60% seizure rate seen in the *Fmr1* KO mice. *$p<0.05$

Supplementary Table 3.1: mGluR5$^{R/R}$ genotype does not affect basal levels total or phosphorylated levels of proteins.

	mGluR5$^{R/R}$		
% of WT	**Mean**	**SEM**	**n**
T-EF2	95	10	19
T-ERK	103	15	6
T-p70S6K	114	15	8
T-mTOR	108	17	25
P-EF2	98	30	19
P-ERK	89	11	6
P-p70S6K	167	54	8
P-mTOR*	242	61	25
APP	115	21	11
Map1B	159	38	17

	mGluR5$^{F/F}$			mGluR5$^{R/R}$		
% of basal	DHPG			DHPG		
	Mean	SEM	n	Mean	SEM	n
T-EF2	105	9	19	96	11	18
T-ERK	102	5	6	89	6	6
T-p70S6K	96	7	9	137	35	7
T-mTOR	105	9	24	112	16	24

Supplementary Table 3.1: mGluR5$^{R/R}$ genotype does not affect basal levels total or phosphorylated levels of proteins. Upper: Basal levels of phosphorylated or total EF2, p70S6K, and ERK are not different in acute hippocampal slices across genotypes (mGluR5$^{F/F}$ and mGluR5$^{R/R}$). Total mTOR levels are not different, but there is an increase in basal phospho-mTOR levels in the mGluR5$^{R/R}$. Data is normalized to levels in slices from mGluR5$^{F/F}$ littermates and expressed as the mean ± SEM; n = # slices. Lower: There is no effect of genotype or DHPG treatment on total EF2, p70S6K, ERK, and mTOR levels in acute hippocampal slices. Data is normalized to levels from untreated slices and expressed as the mean ± SEM; n = # slices.

Supplementary Table 3.2. Seizure occurrence and severity in mGluR5$^{F/F}$, mGluR5$^{F/R}$, and mGluR5$^{R/R}$ genotypes.

	Wild running	Seizure (clonic/tonic)	Status Epilepticus	% Incidence
mGluR5$^{F/F}$	0/27	0/27	0/27	0%
mGluR5$^{F/R}$	0/28	1/28	0/28	3.6%
mGluR5$^{R/R}$	0/21	4/21	0/21	19.0%

Supplementary Table 3.3. Seizure occurrence and severity in mGluR5$^{F/F}$, mGluR5$^{F/R}$, and mGluR5$^{R/R}$ genotypes. * $p < 0.05$ Fisher's Exact test. Related to Fig. 3.6.

CHAPTER FOUR

Results

Elevated CaMKIIα levels in the *Fmr1* KO contribute to disrupted mGluR5-Homer interactions and mGluR5 dysfunction.

This chapter contains data that was collected as a collaborative effort between a Dr. Weirui Guo, a postdoc in the lab, and me. I originally piloted the study, before handing it off to a post doctorate in the lab, who has fully dissected the role of CaMKIIα. I contributed the basal protein synthesis and the UP states. However, the other data described in this chapter is important in understanding the contribution of CaMKIIα to disrupted Homer-mGluR scaffold in the *Fmr1*.

Summary

Enhanced mGluR5 function is causally associated with the pathophysiology of Fragile X Syndrome (FXS), a leading inherited cause of intellectual disability and autism. Here we provide evidence that altered mGluR5-Homer scaffolds contribute to mGluR5 dysfunction and phenotypes in the FXS mouse model, *Fmr1* KO. In *Fmr1* KO mice mGluR5 is less associated with long Homer isoforms, but more associated with the short Homer1a. Phosphorylation of Homer by CaMKIIα disrupts mGluR5-Homer interactions, and CaMKIIα, an FMRP target, is elevated in the *Fmr1* KO mouse. Increased phosphorylation of Homer at CamKIIα sites disrupts mGluR5-Homer interactions. Inhibiting CaMKIIα is able to basal translational rates and neocortical circuit dysfunction.

Our findings reveal novel mechanism of mGluR5-Homer disruption by elevated CaMKIIα in Fragile X disease.

Introduction

Fragile X Syndrome (FXS) is the most common form of mental retardation and autism, which affects approximately 1:4000 males and 1:8000 females (O'Donnell and Warren, 2002). Fragile X patients exhibit multiple neurological deficits, including mental retardation, seizures during childhood, visual spatial defects, learning difficulties and other characteristics of autism. FXS is caused by the loss of function of the Fragile X mental retardation protein (FMRP), due to the silencing of its encoding gene, Fragile X mental retardation 1 (*Fmr1*) (Abrahams and Geschwind, 2008; Bassell and Warren, 2008; O'Donnell and Warren, 2002).

FMRP is an RNA-binding protein that associates with small messenger ribonucleoprotein complexes (mRNP) and regulates translation both in soma and dendrites (Bassell and Warren, 2008). Although FMRP is recognized as a translational suppressor, it is also observed to be associated with actively translating polyribosomes, suggesting that FMRP may bi-directionally regulate the translation of its targeted mRNAs, possibly depending on the phosphorylation status of the protein (Ceman et al., 2003; Corbin et al., 1997; Feng et al., 1997; Stefani et al., 2004).

Most people with FXS show many neurological deficits, including low intelligence quotient, seizures, sensory hypersensitivity, social anxiety, hyperactivity and other characteristics of autism. We discovered enhanced Group 1 mGluR dependent synaptic plasticity, as well as altered mGluR5 signaling in the Fragile X mouse and proposed that mGluR5 antagonists would be novel therapeutic targets for the disease (Bear et al., 2004; Huber et al., 2002). Remarkably, pharmacological and genetic reduction of mGluR5 ameliorates the behavioral symptoms of Fragile X in animal models of the disease (Dolen et al., 2007; McBride et al., 2005; Yan et al., 2005) and in patients (Jacquemont et al., 2011). We have continued to work to understand why mGluR5 is overactive in FXS. Most recently we have discovered a molecular basis for mGluR5 dysfunction in *Fmr1* KO mice-altered association of mGluR5 with the scaffolding protein Homer (Giuffrida et al., 2005; Ronesi et al., 2012a). In the brains of *Fmr1* KO mice there is a reduced interaction of mGluR5 with a scaffolding protein called Homer, which normally keeps mGluR5 inactive and regulates mGluR5 responses to glutamate. Homer binds to the intracellular C-terminal tail of group 1 mGluRs and form multi-protein signaling complexes at the postsynaptic density with mGluRs and their downstream effectors (Park et al., 2008; Rong et al., 2003). All Homer isoforms share a common EVH1 domain at the N-terminus, which binds to mGluR1a, mGluR5, PI3 Kinase enhancer (PIKE), IP3 receptor, SHANK and others. Long, constitutively expressed forms of Homer (Homer1, 2

and 3) multimerize through their C-terminal coiled-coil domain and localize mGluRs to the PSD through interactions with SHANK, as well as scaffold mGluRs to signaling pathways through Homer interactions with the PI3 Kinase enhancer (PIKE), Elongation Factor 2 kinase (EF2K) and the IP3 receptor (Shiraishi-Yamaguchi and Furuichi, 2007; Worley et al., 2007). Homer1a (H1a), a short, activity-inducible, form of Homer lacks the coiled-coiled domain and cannot multimerize with other Homers. Consequently, H1a disrupts mGluR5-long Homer complexes, alters mGluR signaling and causes constitutive, agonist-independent activity of mGluR1/5 (Ango et al., 2001). In *Fmr1* KO mice mGluR5 is less associated with long Homer isoforms and more associated with H1a (Giuffrida et al., 2005; Ronesi et al., 2012a).

Our recent findings showed that genetic deletion of H1a restores mGluR5-Homer scaffolds and corrects multiple aberrant phenotypes in *Fmr1* KO mice (Ronesi et al., 2012a). Furthermore, acute, peptide-mediated disruption of mGluR5-Homer scaffolds in wildtype brain mimics phenotypes of the *Fmr1* KO mouse (Ronesi et al., 2012a). Therefore, many biochemical, neurophysiological and behavioral phenotypes in *Fmr1 KO* mice result from a shift in the balance of short and long Homers bound to mGluR5 and likely to the constitutive activity of mGluR5.

The mechanisms that lead to decreased mGluR5-Homer interactions in FXS are unknown. Protein levels of H1a, long Homers and mGluR5 are normal in *Fmr1* KO mice (Dolen et al., 2007; Giuffrida et al., 2005; Ronesi et al., 2011). However, several have reported increased CaMKIIα levels in the *Fmr1* KO mouse (Hou et al., 2006b; Osterweil et al., 2010a; Zalfa et al., 2003). Ca2+-calmodulin dependent protein kinase 2 (CaMKIIα), Akt, and ERK phosphorylate Homer and decrease Homer interactions with its effectors (Huang et al., 2008a; Mizutani et al., 2008). The loss of FMRP's regulation of CaMKIIα may be leading to the disrupted mGluR5-Homer interactions and mGluR5 dysfunction. In this study, we show increased phosphorylation of long Homers in the *Fmr1* KO mouse. We also show increased CaMKIIα levels and subsequently increased phospho-CaMKIIα levels contribute to the decreased mGluR5-Homer interactions and mGluR5 dysfunction. By blocking CaMKIIα, we were able to restore the balance of mGluR5-Homer interactions and rescue *Fmr1* KO phenotpyes, including increased neocortical excitability and increased basal translation rates. This study brings to light the direct role FMRP is plays in causing mGluR5 dysfunction.

Methods

Animals

Congenic *Fmr1* KO mice (Consortium, 1994) were bred on the C57/BL6J background. Congenic mGluR5F1128R Knock-in mice were generated as

described (Cozzoli et al., 2009) and backcrossed at least 5 generations onto the C57/Bl6J mice from the UT Southwestern mouse breeding core facility. All experiments were performed on littermate controls and blind to mouse genotype. The animal use protocols used in this manuscript were approved by the UT Southwestern IACUC committee.

Reagents

KN-93 was prepared as stocks and stored at -20°C and used within two weeks. KN-93 were purchased from Tocris Bioscience and prepared as described (Gao et al., 2006).

Western blotting

Western blotting on slices was performed as described (Ronesi and Huber, 2008a). Blotting membranes were incubated with the following antibodies according to the manufacturer's instructions: Homer (Sc-8921; Santa Cruz), mGluR5 (Millipore), β3 tubulin (Abcam), CaMKIIα (Santa Cruz, sc-5391), phosphor-Homer 3 S120, S159 and S176 (gift from Mikoshiba's lab). For comparison of phosphoprotein levels across conditions or genotypes immunoreactive phosphoprotein bands were normalized to total protein levels from the same slice homogenates (P-CaMKIIα/CaMKIIα), each of which was first normalized to loading control (β3 tubulin).

Coimmunoprecipitation

Hippocampus was lysed in co-immunoprecipitation buffer (50 mM Tris, pH 7.4, 120 mM NaCl, 0.5% NP40), and protein was tumbled overnight at 4°C

with 1 µg of antibody (Homer (Santa Cruz, D-3). Protein A/G agarose bead slurry (Thermoscientific) was added for one additional hour and the beads were then washed with co-i.p. buffer. Western blotting was performed with the Homer (Santa Cruz, E-18 sc-8921) and mGluR5 (Millipore).

Metabolic labeling of hippocampal slices

Hippocampal slices were prepared as described(Ronesi and Huber, 2008a), (Osterweil et al., 2010b). For these experiments (Fig. 3) the most ventral slices (2 per hippocampus) were used since basal protein synthesis rates differ between dorsal and ventral hippocampal slices (Osterweil et al., 2010b). Slices recovered for 3.5 hours in ACSF at 32°C, and then were incubated in actinomycin D (25 µM) for 30 min. Slices were then incubated in actinomycin D and 10uCi/ml of ^{35}S labeled Methionine for 1hr. Where indicated, 10 µM KN-93 was added at this step.

Neocortical Slice preparation and UP state recordings

UP state experiments in neocortical slices were performed and analyzed as described (Hays et al., 2011). ACSF containing vehicle or KN-93 was perfused onto the slices in the interface chamber for 45 minutes prior to recording.

Statistics:

Data plotted in the figures represents the mean ± SEM. Significant differences were determined using independent or paired t-tests. For comparisons between

WT and *Fmr1* KO or mGluR5$^{R/R}$ ± KN-93 a 2-way ANOVA and Bonferroni posttests were used. *p< 0.05; **p< 0.01; ***p<0.001.

Results

Increased CaMKIIα regulates mGluR5-Homer interactions in Fmr1 KO

The *Fmr1* KO mice, several have reported increased CaMKIIα levels (Hou et al., 2006b; Osterweil et al., 2010a; Zalfa et al., 2003). We also see these increased CaMKIIα levels, as well as, increased phosphor-CaMKIIα levels with no change in the ratio of phospho to total (Fig. 1A). CaMKIIα has been shown to phosphorylate Homer and decrease Homer interactions with its effectors (Huang et al., 2008a; Mizutani et al., 2008). Therefore it would be expected that there are increased Homer phosphorylation at CaMKIIα sites. In *Fmr1* KO mice there is increased phosphorylation of Homer 3 at CaMKIIα sites (Fig. 1B). CaMKIIα phosphorylation has been implicated in regulating Homer binding, so inhibiting it may rescue the mGluR5-Homer ineractions (Mizutani et al., 2008). Inhibiting CaMKIIα with KN-93, is able to rescue the disrupted mGluR5-Homer interactions in the *Fmr1* KO mice (Fig. 1C). However, inhibiting MEK, PI3K, or PKC had no effect on mGluR5-Homer interactions suggesting a specific role for CaMKIIα phosphorylation (Fig. 1C). This suggests most mGluR5 dysfunction may link back to one single FMRP target, CaMKIIα.

Inhibiting CaMKIIα rescues enhanced translation rates in Fmr1 KO

Basal translation rates in brain are elevated in *Fmr1* KO (Bassell and Warren, 2008; Dolen et al., 2010; Gross et al., 2010; Osterweil et al., 2010b). Enhanced protein synthesis in hippocampal slices is reversed by pharmacological blockade of mGluR5 (Osterweil et al., 2010b), and restoring mGluR5-Homer scaffolds, by deleting *H1a,* rescues enhanced protein synthesis (Ronesi et al., 2012b). Artificially disrupting mGluR5-Homer interactions with a peptide of the Homer binding domain of mGluR5 in wild type slices causes increased basal protein synthesis rates, however, it has no effect on *Fmr1* KO slices (Ronesi et al., 2012b). Increased CaMKIIα levels in *Fmr1* KO mice drive the altered mGluR5-Homer interactions (Fig. 1A) and therefore likely plays a role in the increased basal translation rates. In support of this hypothesis, inhibiting CaMKIIα rescues enhanced translation rates as measured by ^{35}S Met incorporation in hippocampal slice proteins (*Fmr1* KO 144±13% of WT, n=12 slices from 6 mice; WT + KN-93 111±10% of WT, n=12 slices from 6 mice; *Fmr1* KO + KN-93 111±11% of WT, n=12 slices from 6 mice; Fig. 2). This data suggests the increased CaMKIIα levels contribute to the enhanced basal protein synthesis rates. This experiments needs to be repeated in the mGluR5F1128R mice, which contain a mutation in mGluR5 disrupting Homer binding (Cozzoli et al., 2009; Tu et al., 1998). This would show CaMKIIα rescues the enhanced basal protein synthesis rates through the restoration of the mGluR5-Homer interactions.

Inhibiting CaMKIIα rescues hyperexcitable neocortical circuits in Fmr1 KO

FXS patients and *Fmr1* KO mice exhibit sensory hypersensitivity, epilepsy and/or audiogenic seizures suggestive of an underlying sensory circuit hyperexcitability (Berry-Kravis, 2002; Dolen et al., 2010). We recently discovered synaptic and circuit alterations indicative of hyperexcitability in the somatosensory, barrel neocortex of *Fmr1* KO mice. Neocortical slices of *Fmr1* KO mice have decreased excitatory drive onto layer IV fast-spiking interneurons and prolonged thalamically-evoked and spontaneously-occurring persistent activity, or UP, states (Gibson et al., 2008; Hays et al., 2011). UP states represent a normal physiological rhythm generated by the recurrent neocortical synaptic connections and is observed in alert and slow-wave sleep states *in vivo* as well as neocortical slice preparations (Haider and McCormick, 2009; Sanchez-Vives and McCormick, 2000). Importantly, genetic or pharmacological reduction of mGluR5 in *Fmr1* KO mice rescues the prolonged UP states in acute slices and *in vivo* (Hays et al., 2011). Also, rescuing mGluR5-Homer interactions by deleting *H1a* rescues the prolonged neocortical UP states (Ronesi et al., 2012a). Since inhibiting CaMKIIα rescues the mGluR5-Homer interactions like *H1a* deletion, inhibiting CaMKIIα would be predicted to rescue prolonged UP states in the *Fmr1* KO. To determine if increased CaMKIIα activity contribute to altered neocortical circuit function and hyperexcitability in *Fmr1* KO mice, we measured

spontaneously occurring UP states in acute slices from somatosensory, barrel cortex using extracellular multiunit recordings (Sanchez-Vives and McCormick, 2000). As previously reported (Gibson et al., 2008; Hays et al., 2011), UP states are longer in slices of *Fmr1* KO mice in comparison to WT littermates (WT: 912.3±82.4 ms, n=8 slices; *Fmr1*-KO: 1527.6±134.2 ms, n=7; Fig. 3A,C). In support for a role for CaMKIIα regulating UP state duration, it was shortened to WT levels by inhibiting CaMKIIα with KN-93 (*Fmr1* KO + KN-93: 1060.9±52.1 ms, n=11; Fig. 3A,C). KN-93 alone does not affect UP states, ruling out general alterations in excitability (WT + KN-93: 993.7±82.4 ms, n=9; Fig. 3A,C). To confirm the mechanism which CaMKIIα rescues through, we utilized a knock-in mouse with a mutation in mGluR5. The mGluR5F1128R ($mGluR5^{R/R}$) mutation prevents mGluR5 from interacting with Homer (Cozzoli et al., 2009; Tu et al., 1998). The $mGluR5^{R/R}$ have a similar duration to what is seen in the *Fmr1* KO mouse ($mGluR5^{F/F}$: 998.3±92.8 ms, n=16; $mGluR5^{R/R}$: 1325.9±60.5 ms, n=24; Fig. 3B). $mGluR5^{R/R}$ slices were treated with KN-93 the same way as *Fmr1* KO, but KN-93 had no effect on prolonged duration in the $mGluR5^{R/R}$ ($mGluR5^{F/F}$ + KN-93: 962.2±68.0 ms, n=12; $mGluR5^{R/R}$ + KN-93: 1291.1±77.8 ms, n=16; Fig. 3B). This data suggests the prolonged neocortical UP states in the *Fmr1* KO are driven by increased CaMKIIα levels disrupting mGluR5-Homer interactions.

CaMKIIα is activated by calcium, so it would be predicted that inhibiting calcium channels would also rescue mGluR5-Homer interactions and the

prolonged UP states in the *Fmr1* KO. Inhibiting L-type calcium channels with nifedipine (50μM), was able to rescue mGluR5-Homer interactions (Fig. 4A). However nifedipine only normalized the UP state durations in the WT and *Fmr1* KO with little effect on the *Fmr1* KO durations (*Fmr1* KO + nifedipine: 1565.3±122.3 ms, n=19; Fig. 4B,C). Nifedipine alone appears to increase WT durations, but has no significant effect (WT + nifedipine: 1468.6±212.3 ms, n=17; Fig. 4B,C). While inhibiting L-type calcium channels with nifedipine is able to rescue mGluR5-Homer interactions, it does not have much effect on UP states like expected. This suggests that the L-type calcium channels are having some other effect on the UP states. What is interesting about this data is that nifedipine has different effects in WT and FMr1 KO and therefore normalizes the up states. Therefore, altered Ca2+ signaling through L-type Ca2+ channels could be involved in the pathology of the UP states.

Discussion

Increased Homer Phosphorylation causes disrupted mGluR5-Homer interactions

Here we demonstrate a causative role for reduced Homer scaffolds in mGluR5 dysfunction in a model of human neurological disease. mGluR5 dysfunction in animal models of FXS is well established and genetic or

pharmacological reduction of mGluR5 activity reduces or rescues many disease phenotypes in animal models (Dolen et al., 2010) and most recently in patients (Jacquemont et al., 2011). Our previous results in the *Fmr1/H1a* KO reveal mechanisms for mGluR5 dysfunction in *Fmr1* KO mice (Ronesi et al., 2012a). An imbalance of mGluR5 interactions from long to short Homer1a isoforms, leads to altered mGluR5 signaling, enhanced basal translation rates, neocortical hyperexcitability, audiogenic seizures and open field activity. However, a direct role FMRP plays in disrupting the mGluR5-Homer interactions has been unknown. For the first time, we demonstrated that FMRP's regulation of CaMKIIα is important in regulating the mGluR5 Homer interactions (Fig. 1C). The increased phosphorylation of Homer at CaMKIIα sites in the *Fmr1* KO mouse causes the disrupted mGluR5-Homer interactions, and therefore mGluR5 dysfunction.

Altered mGluR5-Homer scaffolds increase translation rates

Although there is a deficit in mGluR agonist-stimulated translation in *Fmr1* KO mice, steady state translation rates and levels of specific proteins are elevated (Osterweil et al., 2010b; Sharma et al., 2010), thus reflecting the complexity of translational control. Because one function of FMRP is to suppress translation of its mRNA targets (Bassell and Warren, 2008), an obvious possibility was that the elevated protein synthesis rates and levels directly result from loss of FMRP-mediated suppression of mRNA targets. In support of this

hypothesis, *H1a* deletion does not reverse enhanced protein levels of Map1b and CaMKIIα (Ronesi et al., 2012b). However, elevated total protein synthesis rates are recapitulated WT type slices with the CT peptide (Ronesi et al., 2012b). Thus, increased steady state translation rates in *Fmr1* KO tissue are a result of altered mGluR5-Homer scaffolds that are a secondary consequence of FMRP loss. Elevated protein synthesis rates in *Fmr1* KO hippocampal slices are reversed by the genetic reduction of mGluR5 (*Grm5het*), the mGluR5 inverse agonist MPEP (Dolen et al., 2010; Osterweil et al., 2010b; Ronesi et al., 2012b). Rescuing the mGluR5-Homer interactions by inhibiting CaMKIIα is able to rescue the increased basal protein synthesis rates (Fig. 2). Disrupted mGluR5-Homer interactions clearly increases basal protein synthesis rates in the *Fmr1* KO, which caused by the loss of FMRP's translation suppression of CaMKIIα.

Altered mGluR5-Homer and neocortical network dysfunction

Altered neocortical circuit function and hyperexcitability have been predicted to contribute to cognitive disorders and autism (Rubenstein and Merzenich, 2003; Uhlhaas and Singer, 2006). The epilepsy and EEG abnormalities observed in FXS patients are indicative of brain hyperexcitability (Berry-Kravis, 2002; Dolen et al., 2010). Furthermore, FXS patients display hypersensitivity to sensory stimuli, and *Fmr1* KO mice have audiogenic seizures reflecting hyperexcitability of sensory circuits (Berry-Kravis, 2002; Dolen et al., 2010). Although UP states are a normal physiological rhythm and are not

epileptiform activity, they provide an effective readout of the state of circuit function and excitability (Sanchez-Vives and McCormick, 2000). Furthermore, UP states underlie the slow oscillations that occur during slow wave sleep and are implicated in memory consolidation as well as sensory processing in waking states (Haider and McCormick, 2009). Therefore, altered neocortical UP states in the *Fmr1* KO (Gibson et al., 2008; Hays et al., 2011) may be relevant to the sensory processing and cognitive abnormalities in FXS patients.

Our findings indicate that the longer UP states in *Fmr1* KO neocortex are mediated by enhanced, likely constitutive, activity of H1a-bound mGluR5 (Hays et al., 2011). These neocortical UP states have been rescued by mGluR5 inhibition, as well as, *H1a* deletion, and peptide-mediated disruption of mGluR5-Homer interactions prolongs UP states in WT, but not *Fmr1* KO, slices (Hays et al., 2011; Ronesi et al., 2012a). Inhibiting CaMKIIα rescued the prolonged neocortical UP states in the *Fmr1* KO mice. Inhibiting CaMKIIα rescues the UP state durations through restoring the scaffolds as the mGluR5$^{R/R}$, which show prolonged neocortical UP states equivalent to *Fmr1* KO, was not altered by KN-93 (Fig. 2). CaMKIIα is a potentially novel target for fragile X patients and possibly in other autistic patients. Pregnant rats given valproic acid mimic the effects of valproic acid have on human developing fetus, a form of autism spectrum disorder (Wegner and Nau, 1991). The valproic acid model of autism has been also shown to have increased CaMKIIα levels (Kim et al., 2013).

Interestingly, Angelman syndrome has also been shown to have increased phospho-CaMKIIα levels at Thr305 and Thr306, which inhibits CaMKIIα (van Woerden et al., 2007; Weeber et al., 2003). Increases and decreases of CaMKIIα phosphorylation both seem to play role in autism. CaMKIIα offers a potential therapeutic target for autistic patients.

Figure 4.1: CaMKIIα regulates mGluR5-Homer interactions in *Fmr1* KO mice via Homer phosphorylation.

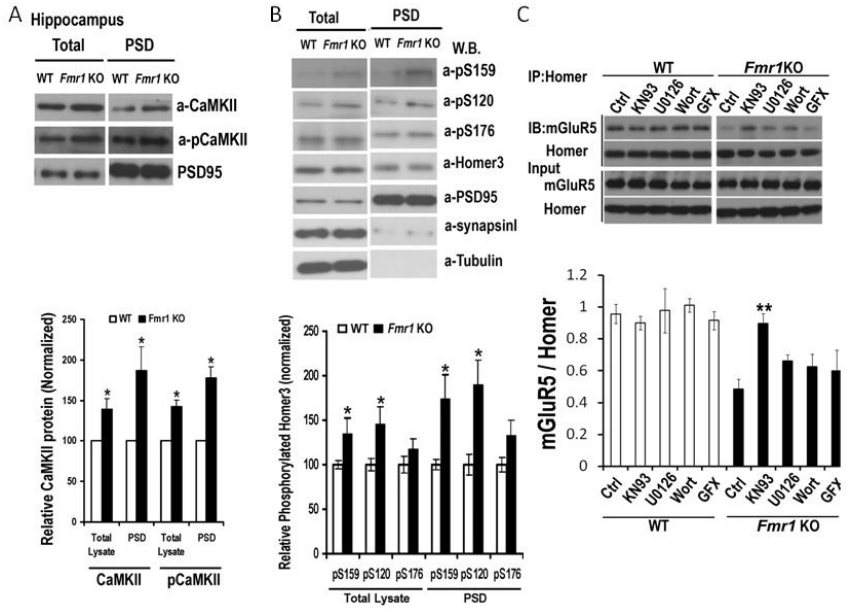

Figure 4.1: CaMKIIα regulates mGluR5-Homer interactions in *Fmr1* KO mice via Homer phosphorylation. A. Increased CamKIIα and pCaMKIIα levels in hippocampal total lysates and postsynaptic density (PSD) fractions of *Fmr1* KO mice. **B.** Homer3 phosphorylation at CaMKIIα sites S120 and S159 are increased in *Fmr1* KO hippocampal total lysates and postsynaptic density (PSD) fractions in comparison to WT littermates. **C.** Inhibition of CaMKIIα by KN-93 restores mGluR5-long Homer interaction in *Fmr1* KO neocortical neurons. The specific inhibitors: CaMKIIα: KN-93; PI3K, upstream kinase of AKT: wortmannin; ERK: U0126; PKC: GF109203X(GFX). *p< 0.05; **p< 0.01

Figure 4.2: Inhibiting CaMKIIα rescues enhanced basal translation rates in hippocampal slices from *Fmr1* KO mice.

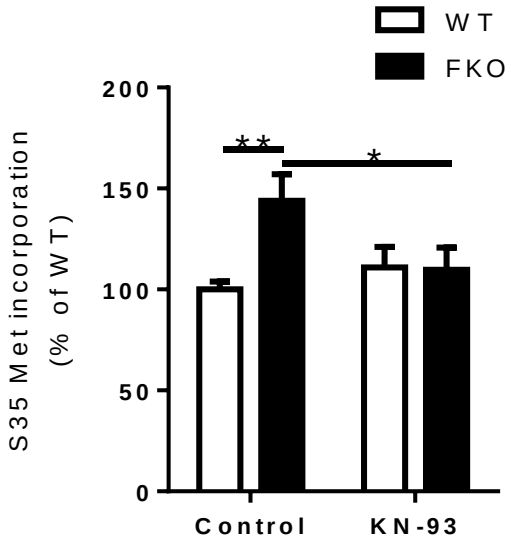

Figure 4.2: Inhibiting CaMKIIα rescues enhanced basal translation rates in hippocampal slices from *Fmr1* KO mice. Acute hippocampal slices from *Fmr1* KO mice display elevated protein synthesis rate in comparison to WT littermates as measured by incorporation of ^{35}S Met/Cys into total protein. Inhibition of CaMKIIα rescues protein synthesis rates in *Fmr1* KO slices to WT levels. *p< 0.05; **p< 0.01; ***p<0.001.

Figure 4.3. Inhibiting CaMKIIα rescues prolonged neocortical UP states in *Fmr1* KO, but not the mGluR5$^{R/R}$ mice.

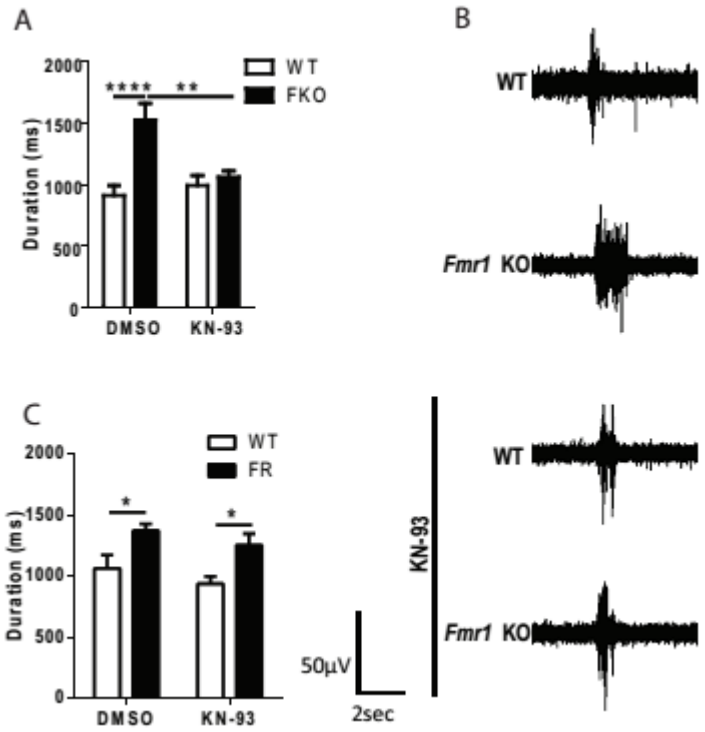

Figure 4.3. Inhibiting CaMKIIα rescues prolonged neocortical UP states in *Fmr1* KO, but not the mGluR5$^{R/R}$ mice. **A.** UP states are longer in the *Fmr1* KO mice and rescued to WT levels when treated with a CaMKIIα inhibitor, KN-93 (5µM). **B.** Representative recordings of UP states from WT and *Fmr1* KO slices in vehicle and KN-93. Scale bar = 50 µV / 2 sec. **C.** UP states are longer in the mGluR5$^{R/R}$ mice, but KN-93 has no effect on their duration. *p< 0.05; **p< 0.01; ***p<0.001.

Figure 4.4. Inhibiting L-type Ca channels rescues mGluR5-Homer interactions but not UP states in the *Fmr1* KO.

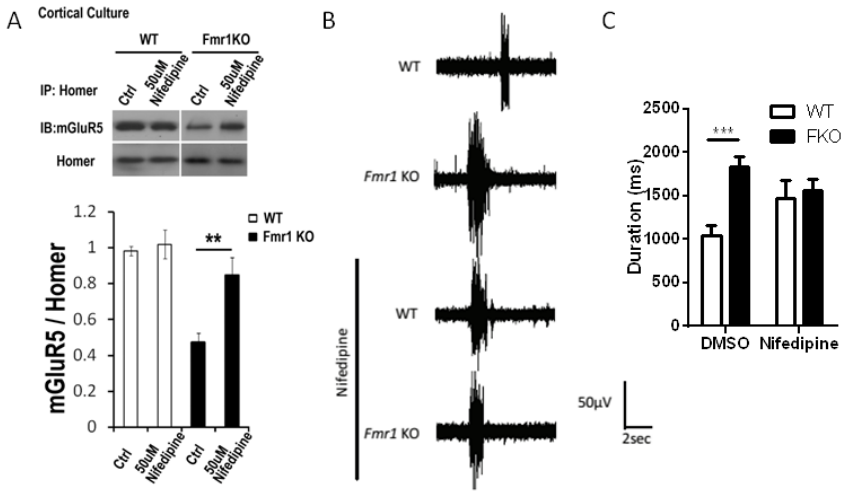

Figure 4.4. Inhibiting L-type Ca channels rescues mGluR5-Homer interactions but not UP states in the *Fmr1* KO. A. mGluR5-Homer interactions in the *Fmr1* KO are rescued to WT levels when treated with an L-type Ca channel inhibitor, Nifedipine (50µM). **B.** Representative recordings of UP states from WT and *Fmr1* KO slices in vehicle and Nifedipine. **C.** UP states in WT and *Fmr1* KO slices are normalized when treated with Nifedipine (50µM). Scale bar = 50 µV / 2 sec. *p< 0.05; **p< 0.01; ***p<0.001.

CHAPTER FIVE

Results

mGluR5 dysfunction in the PTEN conditional knockout model of autism

This chapter contains data that was collected as a collaborative effort between several colleagues. I contributed the the UP states. However, the other data described in this chapter is important in understanding the contribution disrupted Homer-mGluR5 scaffold in the PTEN conditional KO mice.

Summary

Enhanced mGluR5 function is causally associated with the pathophysiology of Fragile X Syndrome (FXS), a leading inherited cause of intellectual disability and autism. Other autism models have also been shown to be responsive to mGluR5 inhibition. Altered mGluR5-Homer scaffolds have been shown to contribute to mGluR5 dysfunction, and Homer's binding to mGluR5 has been shown to be regulated by AKT. Recently a link between PTEN mutations and children with ASD and macrocephaly has been found. Mouse models with PTEN deleted, also display macrocephaly as well as enlarged neurons and dendrites. In this study, we show PTEN cKO mice also have disrupted mGluR5-Homer interactions. The PTEN cKO mice also have neocortical circuit dysfunction, which can be rescued by inhibiting mGluR5. Our findings reveal a common mechanism of mGluR5-Homer disruption in autism models leading to increased excitability.

Introduction

Recently a link between PTEN mutations and children with ASD and macrocephaly has been found (Butler et al., 2005; Herman et al., 2007). About 5% of children diagnosed with ASD and macrocephaly have a mutation in PTEN (McBride et al., 2010). Children with the PTEN mutations have macrocephaly, which is an enlarged head. Mouse models with PTEN deleted, also display macrocephaly as well as enlarged neurons and dendrites (Kwon et al., 2006a; Kwon et al., 2001). PTEN has also been linked to seizures, which can be found in some ASD patients (Backman et al., 2001; Kwon et al., 2006a; Ogawa et al., 2007). Kwon et al. have also shown PTEN conditional KO (cKO) mice, with deletion in layers III-V of the cortex and the dendate in the hippocampus, display altered social interactions (Kwon et al., 2006b).

PTEN is a is a tumor suppressor gene, frequently mutated in human cancers, and plays an important role in brain development (Endersby and Baker, 2008; Li et al., 1997). PTEN is important for embryonic development as the complete KO mice are embryonic lethal (Suzuki et al., 1998). PTEN is a negative regulator of PI3K. The PI3K/mTOR pathway is involved in cell survival, cell proliferation, cell growth, angiogenesis and cellular metabolism (Manning and Cantley, 2007). The vast many cellular functions PTEN regulates through the PI3K/mTOR pathway make it an important gene and easy to understand why it

underlies so many disease, like ASD, intellectual disability, childhood seizures and highly prevelant in cancers (Ali et al., 1999; Backman et al., 2001; Butler et al., 2005; Endersby and Baker, 2008; Rosen and She, 2006).

The PTEN cKO mice have increased phosphorylation of downstream proteins of the PI3K/mTOR pathway (Kwon et al., 2006a; Kwon et al., 2001).

AKT can regulate Homer interaction in T cells, and inhibiting AKT increases Homer binding to its target (Huang et al., 2008a). AKT phosphorylation is increased in the PTEN cKO mice and possible that mGluR5-Homer interactions are disrupted in the PTEN cKO mice, and mGluR5 may be contributing to some of its phenotypes (Kwon et al., 2006a; Kwon et al., 2001). Inhibiting mGluR5 in other autism mouse models had improved behavioral phenotypes, so there could be a common link between autism models (Hays et al., 2011; Silverman et al., 2010; Thomas et al., 2012). In this study, we show the PTEN cKO mice have disrupted mGluR5-Homer interactions and mGluR5 regulates increased neocortical excitability. A commonality in disrupted mGluR5-Homer interactions between autism models and mGluR5 regulation of phenotypes leaves the possibility for a common treatment of autism.

Methods

Animals

$PTEN^{flox/flox}$ mice were crossed to Neuron-specific enolase Cre mice on the C57/BL6J background (Kwon et al., 2006a; Kwon et al., 2006b). All

experiments were performed on littermate controls and blind to mouse genotype. The animal use protocols used in this manuscript were approved by the UT Southwestern IACUC committee.

Reagents

MPEP was prepared as freshly each time. MPEP was purchased from Tocris Bioscience and prepared as described (Thomas et al., 2012).

Western blotting

Western blotting on slices was performed as described (Ronesi and Huber, 2008a). Blotting membranes were incubated with the following antibodies according to the manufacturer's instructions: Homer (Sc-8921; Santa Cruz), mGluR5 (Millipore).

Coimmunoprecipitation

Hippocampus was lysed in co-immunoprecipitation buffer (50 mM Tris, pH 7.4, 120 mM NaCl, 0.5% NP40), and protein was tumbled overnight at 4°C with 1 µg of antibody (Homer (Santa Cruz, D-3). Protein A/G agarose bead slurry (Thermoscientific) was added for one additional hour and the beads were then washed with co-i.p. buffer. Western blotting was performed with the Homer (Santa Cruz, E-18 sc-8921) and mGluR5 (Millipore).

Neocortical Slice preparation and UP state recordings

UP state experiments in neocortical slices were performed and analyzed as described (Hays et al., 2011). For MPEP experiments, an intraperitoneal injection of 5 mg/kg was given to the mice 2 hours before slicing. Control mice were given

saline (0.9% NaCl) injections 2 hrs prior instead. ACSF also contained saline or MPEP

Statistics:

Data plotted in the figures represents the mean ± SEM. Significant differences were determined using independent or paired t-tests. For comparisons between WT and PTEN cKO ± MPEP a 2-way ANOVA and Bonferroni posttests were used. *p< 0.05; **p< 0.01; ***p<0.001.

Results

Increased PI3K signaling regulates mGluR5-Homer interactions.

The PTEN cKO mice have increased phosphorylation of downstream proteins of the PI3K/mTOR pathway (Kwon et al., 2006a; Kwon et al., 2001).

AKT can regulate Homer interaction in T cells, and inhibiting AKT increases Homer binding to its target (Huang et al., 2008a). There are three sites found on Homer which can be phosphorylated by AKT, Thr36, Ser38, and Ser52. We mutated the three AKT sites to alanines (Thr36Ala, Ser38Ala, and Ser52Ala) to prevent phosphorylation of the sites. The sites were also mutated to mimic the phosphorylation sites (Thr36E, Ser38D, and Ser52D). The constructs were transfected into cells along with mGluR5 and then coimmunoprecipitated. The dephosphomimic Homer had no effect on mGluR5-Homer interactions compared to a control Homer (Fig. 1C-D). The phosphomimic Homer showed a reduced interaction with mGluR5 (Fig. 1C-D), confirming AKT can regulate Homer

binding. It also shows AKT can regulate mGluR5-Homer interactions, not just NFAT-Homer interactions. AKT phosphorylation is increased in the PTEN cKO (Kwon et al., 2006a), so neurons were transfected with a constiutively acitive AKT. Neurons transfected with the constiutively acitive AKT showed reduced mGluR5-Homer interactions (Fig. 1B). AKT phosphorylation is increased in the PTEN cKO mice, and therefore it is possible that mGluR5-Homer interactions are disrupted in the PTEN cKO mice, (Kwon et al., 2006a; Kwon et al., 2001). Co-IPs were performed on fresh cortical tissue from PTEN cKO mice. PTEN cKO mice showed decreased mGluR5-Homer interactions compared to floxed littermates without Cre (Fig. 1E-F). Therefore, disrutped mGluR5-Homer scaffolds may be contributing to some of the phenotypes in PTEN cKO mice.

Increased hyperexcitable neocortical circuits in PTEN cKO mice

UP states represent a normal physiological rhythm generated by the recurrent neocortical synaptic connections and is observed in alert and slow-wave sleep states *in vivo* as well as neocortical slice preparations (Haider and McCormick, 2009; Sanchez-Vives and McCormick, 2000). We recently discovered synaptic and circuit alterations indicative of hyperexcitability in the somatosensory, barrel neocortex of Fragile X syndrome mice, or *Fmr1* KO mice. Neocortical slices of *Fmr1* KO mice have prolonged thalamically-evoked and spontaneously-occurring persistent activity, or UP, states (Gibson et al., 2008;

Hays et al., 2011). Rescuing mGluR5-Homer interactions by deleting *H1a* rescues the prolonged neocortical UP states, and inhibiting mGluR5 can also rescue them (Hays et al., 2011; Ronesi et al., 2012a). Because the evidence suggests disrupted mGluR5-Homer interactions regulate the prolonged neocortical UP states in the *Fmr1* KO, it is possible that the PTEN cKO mice also have prolonged neocortical UP states.

PTEN cKO mice have altered electromyogram and electroencephalographic (EEG), with normal EEG background activity often interrupted by epileptiform activity that indicates subclinical electrographic seizures (Ljungberg et al., 2009; Ogawa et al., 2007). The PTEN cKO mice also experience spontaneous seizures which become more frequent with age (Amiri et al., 2012; Kwon et al., 2006a; Ogawa et al., 2007). To determine if the PTEN cKO mice have altered neocortical circuit function and hyperexcitability, we measured spontaneously occurring UP states in acute slices from somatosensory, barrel cortex using extracellular multiunit recordings (Sanchez-Vives and McCormick, 2000). Floxing the *PTEN* gene shows a trend towards prolonged UP states, but no significant difference from WT littermates ($PTEN^{+/+}$ $Cre^{-/-}$: 789.8±60.2 ms, n=22 slices; $PTEN^{f/+}$ $Cre^{-/-}$: 1068±58 ms, n=13 slices; $PTEN^{f/f}$ $Cre^{-/-}$: 1019±75 ms, n=21 slices; Fig. 2). UP states are longer in slices of PTEN cKO mice in comparison to WT littermates ($PTEN^{f/f}$ $Cre^{-/-}$: 1019±75 ms, n=21 slices; $PTEN^{f/f}$ $Cre^{+/-}$: 1431±177 ms, n=17; Fig. 2B-C). Heterozyogous mice also

showed the same prolonged duration as the homozygous mice (*PTEN*$^{f/+}$ Cre$^{-/-}$: 1068±58 ms, n=13 slices; *PTEN*$^{f/+}$ Cre$^{+/-}$: 1563±133 ms, n=14; Fig. 2A,C). Cre alone had no effect on the UP state duration (*PTEN*$^{+/+}$ Cre$^{+/-}$: 674.6±88.1 ms, n=10 slices; Fig. 2D). This data suggests that a heterozygous deletion of PTEN is sufficient to cause the prolonged neocortical UP state duration. Since the heterozygous deletion is sufficient to cause the phenotype and also more relevant to the patients, because they only have one gene mutated (Butler et al., 2005; Buxbaum et al., 2007; Fombonne et al., 1999), therefore we only used the heterozygous mice for further experiments. Since mGluR5 regulated the prolonged neocortical UP states in the *Fmr1* KO mouse, we wanted to know if mGluR5 also regulates the phenotype in the PTEN cKO mice. Because the PTEN cKO mice have disrupted mGluR5-Homer interactions, like the *Fmr1* KO mice, we predict that mGluR5 plays a role in the prolonged UP state durations in the PTEN cKO mice. Mice were given an IP injection of saline or MPEP two hrs prior to slicing. Inhibition of mGluR5 was maintained with MPEP in the ACSF, and the rest of the experiment was performed the same way as the previous UP state experiments. Inhibiting mGluR5 rescued the prolonged neocortical UP states in the PTEN cKO mice (*PTEN*$^{f/+}$ Cre$^{+/-}$ + Saline: 1467.6±107.6 ms, n=18 slices; *PTEN*$^{f/+}$ Cre$^{+/-}$ + MPEP: 1128.3±75.6 ms, n=19; Fig. 3A-B). MPEP had no effect on the duration of UP states in WT slices (*PTEN*$^{f/+}$ Cre$^{-/-}$ + Saline: 1023.8±78.8 ms, n=14 slices; *PTEN*$^{f/+}$ Cre$^{-/-}$ + MPEP: 988.1±73.2 ms, n=17; Fig.

3A-B). This data suggests that the prolonged neocortical UP states in the PTEN cKO mice is regulated by mGluR5, like seen in the *Fmr1* KO mice (Hays et al., 2011). It is also possible that the UP states in the PTEN cKO mice are regulated by the disrupted mGluR5-Homer interactions like seen in the *Fmr1* KO mice (Ronesi et al., 2011).

The original study in the *Fmr1* KO mice was not done with IP injections of MPEP. The results seen by Hays et al. (2011) were replicated with the altered method. Inhibiting mGluR5 rescued the prolonged neocortical UP states in the *Fmr1* KO mice (*Fmr1* KO + Saline: 1979.3±158.3 ms, n=20 slices; *Fmr1* KO + MPEP: 1504.0±135.7 ms, n=18; Fig. 3C). MPEP had no effect on the duration of UP states in WT slices (WT + Saline: 1283.6±134.4 ms, n=14 slices; WT + MPEP: 1140.7±100.0 ms, n=14; Fig. 3C).

Discussion

Autism is still largely diagnosed based on behavioral criteria. Autism spectrum disorders (ASD), as defined by the DSM-V criteria, is characterized by exhibiting repetitive behaviors, social anxiety and verbal and non-verbal communication. ASD has a wide range of symptoms from sensory hyper sensation, seizures, intellectual disability to savant. All with this wide range of symptoms are a wide range of causes and genes making the disease more complicated to treat and understand (Klauck, 2006; Newschaffer et al., 2007).

Because of the large diversity between autistic patients, this can cause the need for different treatments for different types of ASD. Therefore, finding common links between these many different forms can improve our understanding of the disease and lead to a more uniform treatment.

This study demonstrated a common link between two different autism models, Fragile X Syndrome and PTEN mutation. Other studies have shown that inhibiting mGluR5 can rescue autistic mouse models, including Fragile X mice (Silverman et al., 2010; Thomas et al., 2011b). AKT has been shown to regulate Homer interactions in T cells and there is increased in AKT phosphorylation in the PTEN cKO mice (Kwon et al., 2006a; Ogawa et al., 2007). We demonstrated that AKT can also regulate mGluR5-Homer interactions in neurons with a constutively active AKT (Fig. 1B), as well as by using phosphomimics of AKT phosphorylation sites (Fig. 1A,C-D). Because there is increased AKT phosphorylation, we predicted mGluR5-Homer interactions would be disrupted, and that is what is seen in the PTEN cKO mice (Fig. 1E-F). This discovery shows that other autism models other than the Fragile X mice have disrupted mGluR5-Homer interactions (Giuffrida et al., 2005; Ronesi et al., 2012a). This data presents a novel link between autism models, which may be present in other autism model as well. If other autism models have altered mGluR5-Homer interactions as well, this could allow for other similar treatments to be used on these patients.

PTEN cKO have previously been shown to have increased excitability. PTEN cKO mice have altered electromyogram and electroencephalographic (EEG), with normal EEG background activity often interrupted by epileptiform activity that indicates subclinical electrographic seizures (Ljungberg et al., 2009; Ogawa et al., 2007). The PTEN cKO mice also experience spontaneous seizures which become more frequent with age (Amiri et al., 2012; Kwon et al., 2006a; Ogawa et al., 2007). Knocking out PTEN increases the number of mature spines, which could cause increase excitability (Haws et al., 2013). In primary neuron cultures, when PTEN is inhibited with a dominate negative, there is an increase in miniature amplitude and frequency (Moult et al., 2010). In the primary somatosenory cortex, the PTEN ckO have prolonged UP states that suggests increased circuit excitability, supporting previous data (Fig. 2). The heterozygous mice have the same prolonged neocortical UP states as the homozygous mice showing deletion of a single PTEN gene is sufficient to cause the excitability. The increase in circuit excitability was not unexpected with the PTEN cKO displaying spontaneous seizures; however, the excitability was seen at three weeks while the seizures don't start till thirteen weeks of age (Ogawa et al., 2007). This suggests the altered circuit excitability occurs long before the seizures occur. The seizure frequency increases from thirteen to thirty-three weeks, which makes it possible for the circuit excitability to also increase over time as well. The UP state duration in the PTEN cKO could become more

prolonged at older ages. The increased circuit excitability in the PTEN cKO is regulated by mGluR5, as inhibiting mGluR5 rescues the prolonged UP states to WT levels (Fig. 3). The sensitivity of the prolonged neocortical UP states to mGluR5 inhibitors in the PTEN cKO is the same as what is seen in the *Fmr1* KO mice (Hays et al., 2011). It also possible the spontaneous seizures in the PTEN cKO mice could be due to the increased circuit excitability, and the seizures may be sensitive to MPEP as well. MPEP can rescue the audiogenic seizures in the *Fmr1* KO, so it stands to reason MPEP may be able to rescue the spontaneous seizures (Thomas et al., 2011b). The MPEP rescue of the prolonged UP state suggests a common mechanism cause increased excitability in the autism models through mGluR5. mGluR5-Homer interactions are disrupted in both of these models, and the rescue of mGluR5-Homer interactions was shown to rescue the prolonged neocortical UP states (Ronesi et al., 2012a). Rescuing mGluR5-Homer interactions in the PTEN cKO may also be able to rescue the prolonged neocortical UP states. This would give us a greater insight into the cause of the increased excitability.

With so many different proteins involved in autism, the disease is a very complicated one with each gene being studied outside the context of the others. This study presents one of the first common mechanisms between autistic models of altered mGluR5 function through disrupted mGluR5-Homer interactions.

Better understanding of this disease allows for the possibility of common mechanisms leading to autistic phenotypes and the future for common treatments.

Figure 5.1. AKT regulates mGluR5-Homer interactions and PTEN conditional KO mice (cKO) have disrupted mGluR5-Homer interactions.

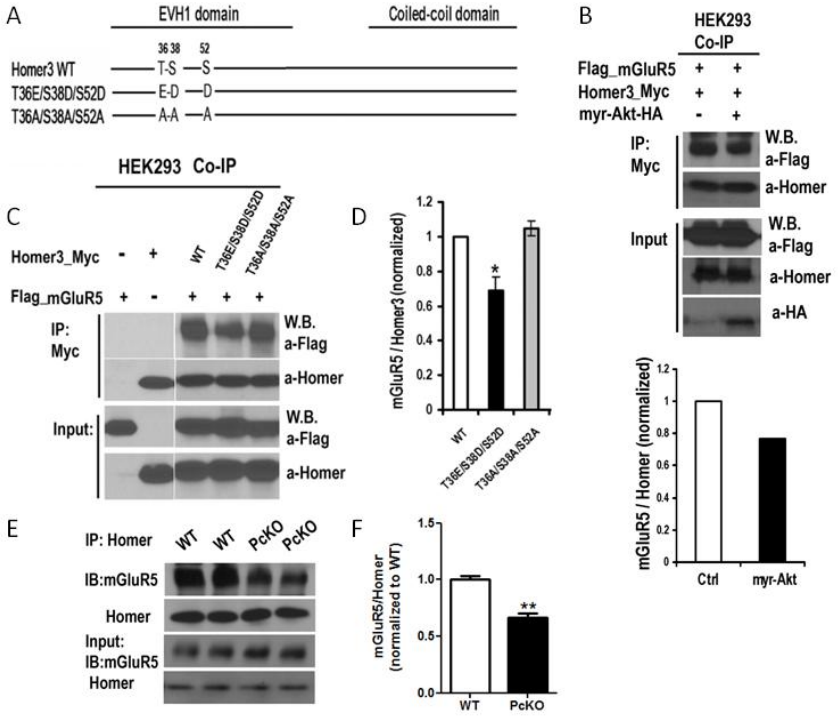

Figure 5.1. AKT regulates mGluR5-Homer interactions and PTEN conditional KO mice (cKO) have disrupted mGluR5-Homer interactions. A. Schematic of Homer and mutated AKT phosphorylation at sites Thr36, Ser38, and Ser52. **B.** Cells were transfected with the various Homer constructs and mGluR5 and then coimmunoprecipitated. Representative blots of mGluR5-Homer interactions with mutated Homers **C.** The phospho-mimic Homer binds significantly less to mGluR5 than the unmutated Homer. **D.** Neurons were transfected with a constitutive active form of AKT. Top: Representative blots of mGluR5-Homer interactions. Bottom: Analysis of mGluR5-Homer interactions shows a decrease in binding when a constitutive active AKT is expressed. **E.** Coimmunoprecipitation of mGluR5 and Homer from hippocampal homogenates demonstrate reduced interactions in $PTEN^{f/f}$ $Cre^{+/-}$ in comparison to $PTEN^{f/f}$ (no Cre) littermates. Protein samples in the input were immunoprecipitated with anti-panHomer and western blot using anti-mGluR5 and anti-panHomer. **F.** Quantification of co-immunoprecipiated mGluR5 with Homer (normalized to $PTEN^{f/f}$). *p< 0.05; **p< 0.01.

Figure 5.2. The PTEN cKO mice have prolonged neocortical UP states.

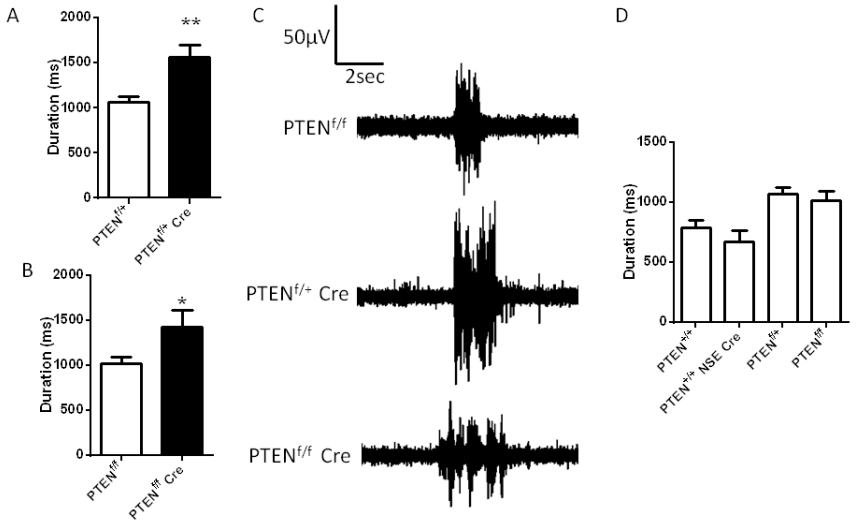

Figure 5.2. The PTEN cKO mice have prolonged neocortical UP states. A. In 3 week old mice, PTEN$^{f/+}$ Cre$^{+/-}$ mice have prolonged neocortical UP states compared to PTEN$^{f/+}$ littermates. **B.** PTEN$^{f/+}$ UP states in the PTEN$^{f/f}$ Cre$^{+/-}$ mice are prolonged in comparison to PTEN$^{f/f}$ mice. **C.** Representative extracellular multiunit recordings of spontaneous, persistent activity or UP states from layer 4 of somatosensory, barrel neocortical slices from each genotype. **D.** UP state durations from floxed controls and NSE Cre mice are not significantly different from WT littermates. *p< 0.05; **p< 0.01.

Figure 5.3. Inhibiting mGluR5 rescues prolonged neocortical UP states in the PTEN cKO.

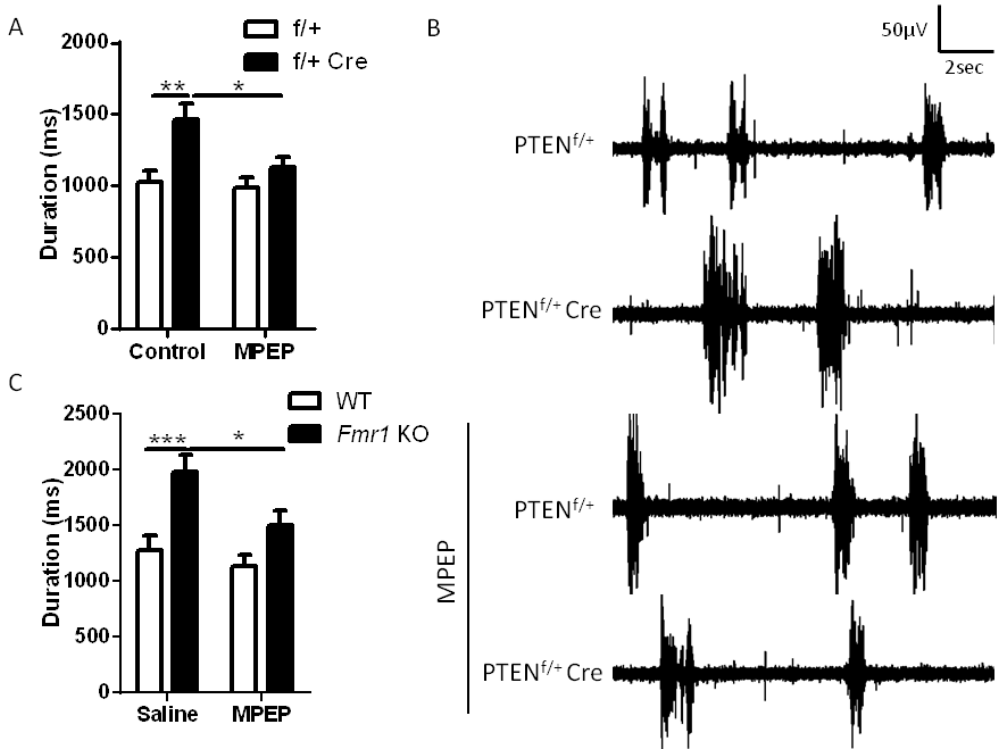

Figure 5.3. Inhibiting mGluR5 rescues prolonged neocortical UP states in the PTEN cKO. A. UP states in PTEN cKO slices are rescued to WT levels when mice are give an IP injection of MPEP (5mg/kg). **B.** Representative recordings of UP states from WT and PTEN cKO slices from vehicle and MPEP mice. Scale bar = 50 µV / 2 sec. **C.** UP states in *Fmr1* KO slices are rescued to WT levels when mice are give an IP injection of MPEP. *p< 0.05; **p< 0.01.

CHAPTER SIX

Discussion

Concluding Remarks and Recommendations for Future Studies

Summary

Here we demonstrate a causative role for reduced Homer scaffolds in mGluR5 dysfunction in a model of human neurological disease. mGluR5 dysfunction in animal models of FXS is well established and genetic or pharmacological reduction of mGluR5 activity reduces or rescues many disease phenotypes in animal models (Dolen et al., 2010) and most recently in patients (Jacquemont et al., 2011). Our previous results reveal an imbalance of mGluR5 interactions from long to short Homer1a isoforms leading to altered mGluR5 signaling, enhanced basal translation rates, neocortical hyperexcitability, audiogenic seizures and open field activity. Disrupted Homer scaffolds in *Fmr1* KO mice cannot account for altered mGluR-LTD or abnormal translational control of FMRP target mRNAs and implicate an essential role for FMRP binding to and translational regulation of specific mRNAs in mGluR-LTD (Ronesi et al., 2012a). My data confirms our previous results, showing disrupting mGluR5-Homer interactions are sufficient to cause some of the mGluR5 dysfunction, but leaves open the possibility of mGluR1 contribution. We also show the mechanism which causes the disrupted mGluR5-Homer interactions is due to loss

of translation suppression of CaMKIIα by FMRP. Increased CaMKIIα levels leads to increased Homer phosphorylation and disrupted mGluR5-Homer interactions. The disrupted mGluR5-Homer interactions are a common dysfunction in autism models, also seen in the PTEN cKO mice.

Disrupted mGluR5-Homer interactions regulate majority of mGluR5 dysfunction in the *Fmr1* KO

How is ERK regulating translation?

In *Fmr1* KO mice, steady state translation rates and levels of specific proteins are elevated (Osterweil et al., 2010b; Sharma et al., 2010), thus reflecting the complexity of translational control. However, increased steady state translation rates in *Fmr1* KO tissue are a result of altered mGluR5-Homer scaffolds that are a secondary consequence of FMRP loss. Elevated protein synthesis rates in *Fmr1* KO hippocampal slices are reversed by the genetic reduction of mGluR5, the mGluR5 inverse agonist MPEP, and inhibitors of ERK (Dolen et al., 2010; Osterweil et al., 2010b; Ronesi et al., 2012b). In *Fmr1* KO cortical lysates, there is enhanced phosphorylation of translation initiation factors that are downstream of ERK (eIF4E and 4EBP) which was reversed by *H1a* deletion (Ronesi et al., 2012b), and enhanced in mGluR5$^{R/R}$ mice. However, despite the increased phosphorylation of translation initiation factors, there is no basal increase in eIF4E/4G association in the mGluR5$^{R/R}$ mice. This suggests ERK must be regulating basal translation rates in the *Fmr1* KO through other pathways than cap dependent translation. One possible factor that may be altered

is the ribosomes themselves. ERK regulates p90RSK, which phosphorylates rpS6 (Pende et al., 2004; Roux et al., 2007), which correlates with assembly of the translation pre-initiation complex and increased cap-dependent translation (Anjum and Blenis, 2008; Roux et al., 2007). Better understanding of alternative ERK regulation of translation and how it is regulated in the mGluR5$^{R/R}$ mice and will help increase the understanding for how basal translation is increased in the *Fmr1* KO.

In *Fmr1* KO, there is an increased association of eIF4E and eIF4G (Sharma et al., 2010). In *Fmr1* KO cortical lysates, there is enhanced phosphorylation of translation initiation factors that are downstream of ERK (eIF4E and 4EBP) which was reversed by *H1a* deletion (Ronesi et al., 2012b), and enhanced in mGluR5$^{R/R}$ mice. However, despite the increased phosphorylation of translation initiation factors, there is no basal increase in eIF4E/4G association in the mGluR5$^{R/R}$ mice. So what is driving the increase in eIF4E/4G association in the *Fmr1* KO mice? PIKE-L is elevated in the *Fmr1* KO which leads to increased PI3K activity and increased basal phosphorylation of the PI3K/mTOR pathway (Gross et al., 2010; Sharma et al., 2010). When 4E-BP is phosphorylated by mTOR, and ERK1/2, 4E-BP dissociates from eIF4E and allows eIF4E to bind with eIF4G, increasing translation (Brunn et al., 1997; Gingras et al., 1999; Gingras et al., 2001). It is not known if either the mTOR or ERK pathway are regulating the eIF4E/4G association in the *Fmr1* KO. The role

the increased eIF4E/4G association in the *Fmr1* KO is very unclear, but overexpression of eIF4E is able to recapitulate some Fragile X phenotypes, so altered eIF4E/4G association may yet still be involved (Santini et al., 2013).

Proteomic study of mGluR-LTD

In the *Fmr1* KO mouse, there is enhanced mGluR-LTD, as well as, elevated steady state protein levels of FMRP target mRNAs, MAP1b and αCaMKII (Huber et al., 2002). However, in the mGluR5$^{R/R}$ mice, steady state levels of FMRP target mRNAs are normal and there is attenuated mGluR-LTD. Since there is no increase in FMRP targets and no mGluR-stimulated translation of these targets, the proteins needed for the maintenance of mGluR-LTD are not synthesized and therefore attenuated mGluR-LTD. Now that we have these two mice models with bidirectional mGluR-LTD compared to WT, this may allow us to determine which protein are involved in mGluR-LTD. A proteomic study could be performed on WT, mGluR5$^{R/R}$, and *Fmr1* KO looking for proteins involved in mGluR-LTD. Candidates would be expected to be less in the mGluR5$^{R/R}$ compared to WT and increased in the *Fmr1* KO mice. Then siRNA could be used to test the validity of the promising candidates. Performing a proteomic study may provide insight and novel proteins involved in mGluR-LTD.

What is the difference between the mGluR5$^{R/R}$ and Fmr1 KO UP states?

Altered neocortical circuit function and hyperexcitability have been predicted to contribute to cognitive disorders and autism (Rubenstein and

Merzenich, 2003; Uhlhaas and Singer, 2006). The epilepsy and EEG abnormalities observed in FXS patients are indicative of brain hyperexcitability (Berry-Kravis, 2002; Dolen et al., 2010). Furthermore, FXS patients display hypersensitivity to sensory stimuli, and *Fmr1* KO mice have audiogenic seizures reflecting hyperexcitability of sensory circuits (Berry-Kravis, 2002; Dolen et al., 2010). UP states underlie the slow oscillations that occur during slow wave sleep and are implicated in memory consolidation as well as sensory processing in waking states (Haider and McCormick, 2009). Our findings indicate that the longer UP states in *Fmr1* KO neocortex are mediated by enhanced, likely constitutive, activity of H1a-bound mGluR5 (Hays et al., 2011). These neocortical UP states have been rescued by mGluR5 inhibition, as well as, *H1a* deletion, and peptide-mediated disruption of mGluR5-Homer interactions prolongs UP states in WT, but not *Fmr1* KO, slices (Hays et al., 2011; Ronesi et al., 2012a). The mGluR5$^{R/R}$ also show prolonged neocortical UP states equivalent to *Fmr1* KO durations. Inhibiting the ERK pathway rescues the prolonged neocortical UP states in the *Fmr1* KO, but is unable to rescue them in the mGluR5$^{R/R}$ (Fig. 4). This data suggests that the prolonged neocortical UP states may be caused by a different mechanism in the mGluR5$^{R/R}$ than the *Fmr1* KO. One possible explanation is that there is a developmental difference between the *Fmr1* KO and the mGluR5$^{R/R}$. In the mGluR5$^{R/R}$ mouse, the mGluR5-Homer interactions are disrupted embryonically. While it has been shown the mGluR5-

Homer interactions are altered in the *Fmr1* KO mouse, there is no time course for when the disruption occurs (Giuffrida et al., 2005). The mGluR5-Homer interactions may not be disrupted all through development. Another possible explanation is possible morphological changes in the mGluR5$^{R/R}$ mouse not found in the *Fmr1* KO. mGluR5 has been shown to be involved in proper development of the barrel and in mGluR5 KO cells there is altered morphology and barrel structure (Ballester-Rosado et al., 2010; She et al., 2009; Wijetunge et al., 2008). mGluR5 is required for full polarization of layer IV spiny stellate neurons in the barrel cortex (She et al., 2009). If the loss of mGluR5 can cause altered morphology, it is therefore possible increased mGluR5 activity can also lead to altered morphology. The gross cortical morphology is normal in *Fmr1* KO mice, but there is a delay in circuit maturation (Till et al., 2012). Full polarization of layer IV neurons is delayed, along with barrel segregation, but both are normal in mature mice (Till et al., 2012). A full understanding of the differences between what causes the prolonged UP states in mGluR5$^{R/R}$ and *Fmr1* KO could help us better understand what drives the increased excitability in the *Fmr1* KO.

Inhibiting the ERK pathway rescues the prolonged neocortical UP states in the *Fmr1* KO, but does not rescue the mGluR5-Homer interactions. ERK regulation of the prolonged UP states must be downstream of the disrupted mGluR5-Homer interactions. ERK has been shown to regulate Voltage-gated potassium channel subunit Kv4.2. Functionally, Kv4.2 is the major component

of A-type potassium current, a transient, subthreshold current that serves to oppose depolarization (Guan et al., 2011; Hoffman et al., 1997; Norris and Nerbonne, 2010). Phosphorylation of Kv4.2 by ERK at site Thr607 decreases the current (Schrader et al., 2006). A decrease in potassium current would cause the membrane potential to be more depolarized and increasing the excitability of the cell. A more excitable cell or potentially circuit could account for the prolonged UP states in the *Fmr1* KO mice. FMRP also directly interacts with the mRNA for Kv4.2; however, regulation of Kv4.2 in the *Fmr1* KO is unclear. One study reports an increase in Kv4.2 expression, while a different group reports reduction in Kv4.2 expression (Gross et al., 2011; Lee et al., 2011). An increase in Kv4.2 expression seems likely, since FMRP is a translational repressor, but a decrease in Kv4.2 expression fits more with the functional data. However, if ERK regulation of Kv4.2 is increased in the *Fmr1* KO, an increase in Kv4.2 levels could still lead to increased excitability with an increase in phosphorylated Kv4.2.

What causes increased ERK activity?

With so many phenotypes in the *Fmr1* KO being regulated by the ERK pathway, including UP states and basal translation (Osterweil et al., 2013; Osterweil et al., 2010a; Ronesi et al., 2012a), it is interesting that there is no change in basal ERK phosphorylation. Our previous data has implicated increased mGluR5 activity due to altered long Homer binding causes increase basal phosphorylation of ERK substrates (Ronesi et al., 2012a). If ERK

phosphorylation is not increased in the *Fmr1* KO mice, then what is leading to this increased basal phosphorylation of ERK substrates? One potential explanation is ERK subcellular localization is altered in the Fragile X mice. Altered ERK localization may lead to increase the availability of ERK's substrates, and therefore increased activity of downstream proteins. Another potential explanation is altered ERK binding to scaffoldings, or even mGluR5. ERK forms complexes with scaffolds and its effecter proteins, allowing for efficient signaling specificity (Shaul and Seger, 2007). If ERK is more bound to these scaffolds and complexes, small activation of ERK would be more amplified and therefore an increase in phosphorylation of ERK substrates. Both of these are possible and may give us better insight into how ERK is regulating so many processes in the *Fmr1* KO mice.

Homer Phosphorylation altered in Fragile X

Here we demonstrate a causative role for reduced Homer scaffolds in mGluR5 dysfunction in a model of human neurological disease. mGluR5 dysfunction in animal models of FXS is well established and genetic or pharmacological reduction of mGluR5 activity reduces or rescues many disease phenotypes in animal models (Dolen et al., 2010) and most recently in patients (Jacquemont et al., 2011). Our previous results in the *Fmr1/H1a* KO reveal mechanisms for mGluR5 dysfunction in *Fmr1* KO mice (Ronesi et al., 2012a).

An imbalance of mGluR5 interactions from long to short Homer1a isoforms, leads to altered mGluR5 signaling, enhanced basal translation rates, neocortical hyperexcitability, audiogenic seizures and open field activity. However, a direct role FMRP plays in disrupting the mGluR5-Homer interactions has been unknown. For the first time, we demonstrated that FMRP's regulation of CaMKIIα is important in regulating the mGluR5 Homer interactions. The increased phosphorylation of Homer at CaMKIIα sites in the *Fmr1* KO mouse causes the disrupted mGluR5-Homer interactions, and therefore mGluR5 dysfunction. The increased steady state translation rates in *Fmr1* KO tissue are a result of altered mGluR5-Homer scaffolds that are a secondary consequence of FMRP loss. Rescuing the mGluR5-Homer interactions by inhibiting CaMKIIα is able to rescue the increased basal protein synthesis rates. Disrupted mGluR5-Homer interactions clearly increases basal protein synthesis rates in the *Fmr1* KO, which caused by the loss of FMRP's translation suppression of CaMKIIα. Our findings also indicate that the longer UP states in *Fmr1* KO neocortex are mediated by enhanced, likely constitutive, activity of H1a-bound mGluR5 (Hays et al., 2011). Inhibiting CaMKIIα rescued the prolonged neocortical UP states in the *Fmr1* KO mice. Inhibiting CaMKIIα rescues the UP state durations through restoring the scaffolds as the mGluR5$^{R/R}$, which show prolonged neocortical UP states equivalent to *Fmr1* KO, was not altered by KN-93.

Increased Homer phosphorylation in other autism models?

CaMKIIα is a potentially novel target for fragile X patients and possibly in other autistic patients. Pregnant rats given valproic acid mimic the effects of valproic acid have on human developing fetus, a form of autism spectrum disorder (Wegner and Nau, 1991). The valproic acid model of autism has been also shown to have increased CaMKIIα levels (Kim et al., 2013). Angelman syndrome has also been shown to have increased phospho-CaMKIIα levels, and reducing CaMKIIα levels rescues behavioral phenotypes (van Woerden et al., 2007). CaMKIIα offers a potential therapeutic target for autistic patients.

PTEN cKO mice also have mGluR5 dysfunction

CaMKIIα is not the only kinase that can phosphorylate Homer, AKT can as well. This study demonstrated a common link between two different autism models, Fragile X Syndrome and PTEN mutation. Other studies have shown that inhibiting mGluR5 can rescue autistic mouse models, including Fragile X mice (Silverman et al., 2010; Thomas et al., 2011b). AKT has been shown to regulate Homer interactions in T cells and there is increased in AKT phosphorylation in the PTEN cKO mice (Kwon et al., 2006a; Ogawa et al., 2007). We showed disrupted mGluR5-Homer interactions in the PTEN cKO mice. This discovery shows that other autism models other than the Fragile X mice have disrupted mGluR5-Homer interactions (Giuffrida et al., 2005; Ronesi et al., 2012a).

PTEN cKO have previously been shown to have increased excitability. The PTEN cKO mice experience spontaneous seizures which become more frequent with age (Amiri et al., 2012; Kwon et al., 2006a; Ogawa et al., 2007). In the primary somatosenory cortex, the PTEN ckO have prolonged UP states that suggests increased circuit excitability, supporting previous data (Fig. 2). The heterozygous mice have the same prolonged neocortical UP states as the homozygous mice showing deletion of a single PTEN gene is sufficient to cause the excitability. The increase in circuit excitability was not unexpected with the PTEN cKO displaying spontaneous seizures; however, the excitability was seen at three weeks while the seizures don't start till thirteen weeks of age (Ogawa et al., 2007). This suggests the altered circuit excitability occurs long before the seizures occur. The seizure frequency increases from thirteen to thirty-three weeks, which makes it possible for the circuit excitability to also increase over time as well. The UP state duration in the PTEN cKO could become more prolonged at older ages. The increased circuit excitability in the PTEN cKO is regulated by mGluR5, as inhibiting mGluR5 rescues the prolonged UP states to WT levels (Fig. 2). The sensitivity of the prolonged neocortical UP states to mGluR5 inhibitors in the PTEN cKO is the same as what is seen in the *Fmr1* KO mice (Hays et al., 2011). It also possible the spontaneous seizures in the PTEN cKO mice could be due to the increased circuit excitability and the seizures may be sensitive to MPEP as well. MPEP can rescue the audiogenic seizures in the

Fmr1 KO, so it stands to reason MPEP may be able to rescue the spontaneous seizures (Thomas et al., 2011b). The MPEP rescue of the prolonged UP state suggests a common mechanism cause increased excitability in the autism models through mGluR5.

Potential mGluR5 regulation of other PTEN cKO phenotypes

mGluR5 may be regulating other phenotypes in the PTEN cKO, like behavior. PTEN cKO mice did not display social preference by spending equal time with an inanimate object and mouse. The PTEN cKO mice could also not recognize the difference between a novel mouse and a familiar mouse (Kwon et al., 2006a). This study also showed the PTEN cKO mice had a problem with learning and memory in the Morris water maze, which is consistant with patients having intellectual disability (McBride et al., 2010; Varga et al., 2009). It would be informative to know if inhibiting mGluR5 with MPEP is able to rescue these phenotypes and would provide a new target of treatment for PTEN patients. AFQ056, a selective mGluR5 antagonist, is in clinical trials with promising results in Fragile X patients (Jacquemont et al., 2011). If MPEP rescues any of these phenotypes, AFQ056 could potentially be used on the patients, and would not require as much approval for use if things continue favorably in the clinical trial.

mGluR5-Homer interactions are disrupted in both PTEN and Fragile X models, and the rescue of mGluR5-Homer interactions was shown to rescue the

prolonged neocortical UP states in the *Fmr1* KO mouse (Ronesi et al., 2012a). Rescuing mGluR5-Homer interactions in the PTEN cKO by deleting Homer 1a may also be able to rescue the prolonged neocortical UP states and other potential mGluR5 regulated phenotypes. This would give us a greater insight into the cause of the increased excitability. This data presents a novel link between autism models, which may be present in other autism model as well. If other autism models have altered mGluR5-Homer interactions as well, this could allow for other similar treatments to be used on these patients.

Potential for Homer screening in autism patients

This data provides potential use for patients. AFQ056, a selective mGluR5 antagonist, is in clinical trials with promising results (Jacquemont et al., 2011). However, AFQ056 only has promising results with patients with a complete loss of FMRP. It is unknown if a complete loss of FMRP is required for disrupted mGluR5-Homer interactions. Small amounts of FMRP may be enough to keep levels of CaMKIIα low enough to prevent increased phosphorylation of Homer. If it were possible to understand why AFQ056 works on some patients and not others, it may allow a way to screen patients. It is not possible to get brain tissue from living patients to look at mGluR5-Homer interactions and mGluR5 is not found in the blood, therefore another way must be found. AKT has been shown to regulate NFAT-Homer interactions in T cells (Huang et al., 2008a). CaMKIIα,

FMRP, ERK and AKT, all the proteins which regulate Homer binding are all found in T cells (Bui et al., 2000; Mizutani et al., 2008; Ravindran et al., 2005). It is unknown if Homer binding to Nuclear factor of activated T-cells (NFAT) is altered in Fragile X. If NFAT-Homer interactions show the same alteration as mGluR5-Homer interactions, NFAT-Homer interactions and/or Homer phosphorylation levels can be compared to Fragile X patients' responsiveness to AFQ056. If NFAT-Homer interactions and/or Homer phosphorylation levels have predictive powers over the drug's effectiveness, then it may be utilized to screen other autistic patients and determine if they may be candidates for the drug working.

Conclusions

With so many different proteins involved in autism, the disease is a very complicated one with each gene being studied outside the context of the others. This study presents one of the first common mechanisms between autistic models of altered mGluR5 function through disrupted mGluR5-Homer interactions. Better understanding of this disease allows for the possibility of common mechanisms leading to autistic phenotypes and the future for common treatments.

BIBLIOGRAPHY

(2007). Prevalence of autism spectrum disorders--autism and developmental disabilities monitoring network, 14 sites, United States, 2002. MMWR Surveill Summ *56*, 12-28.

Abe, T., Sugihara, H., Nawa, H., Shigemoto, R., Mizuno, N., and Nakanishi, S. (1992). Molecular characterization of a novel metabotropic glutamate receptor mGluR5 coupled to inositol phosphate/Ca2+ signal transduction. J Biol Chem *267*, 13361-13368.

Abrahams, B.S., and Geschwind, D.H. (2008). Advances in autism genetics: on the threshold of a new neurobiology. Nat Rev Genet *9*, 341-355.

Ali, I.U., Schriml, L.M., and Dean, M. (1999). Mutational spectra of PTEN/MMAC1 gene: a tumor suppressor with lipid phosphatase activity. J Natl Cancer Inst *91*, 1922-1932.

Amiri, A., Cho, W., Zhou, J., Birnbaum, S.G., Sinton, C.M., McKay, R.M., and Parada, L.F. (2012). Pten deletion in adult hippocampal neural stem/progenitor cells causes cellular abnormalities and alters neurogenesis. J Neurosci *32*, 5880-5890.

Ango, F., Pin, J.P., Tu, J.C., Xiao, B., Worley, P.F., Bockaert, J., and Fagni, L. (2000). Dendritic and axonal targeting of type 5 metabotropic glutamate receptor is regulated by homer1 proteins and neuronal excitation. J Neurosci *20*, 8710-8716.

Ango, F., Prezeau, L., Muller, T., Tu, J.C., Xiao, B., Worley, P.F., Pin, J.P., Bockaert, J., and Fagni, L. (2001). Agonist-independent activation of metabotropic glutamate receptors by the intracellular protein Homer. Nature *411*, 962-965.

Anjum, R., and Blenis, J. (2008). The RSK family of kinases: emerging roles in cellular signalling. Nat Rev Mol Cell Biol *9*, 747-758.

Antion, M.D., Hou, L., Wong, H., Hoeffer, C.A., and Klann, E. (2008). mGluR-dependent long-term depression is associated with increased phosphorylation of S6 and synthesis of elongation factor 1A but remains expressed in S6K-deficient mice. Mol Cell Biol *28*, 2996-3007.

Atkinson, P.J., Young, K.W., Ennion, S.J., Kew, J.N., Nahorski, S.R., and Challiss, R.A. (2006). Altered expression of G(q/11alpha) protein shapes mGlu1 and mGlu5 receptor-mediated single cell inositol 1,4,5-trisphosphate and Ca(2+) signaling. Mol Pharmacol *69*, 174-184.

Auerbach, B.D., Osterweil, E.K., and Bear, M.F. (2011). Mutations causing syndromic autism define an axis of synaptic pathophysiology. Nature *480*, 63-68.

Backman, S.A., Stambolic, V., Suzuki, A., Haight, J., Elia, A., Pretorius, J., Tsao, M.S., Shannon, P., Bolon, B., Ivy, G.O., *et al.* (2001). Deletion of Pten in mouse brain causes seizures, ataxia and defects in soma size resembling Lhermitte-Duclos disease. Nat Genet *29*, 396-403.

Ballester-Rosado, C.J., Albright, M.J., Wu, C.S., Liao, C.C., Zhu, J., Xu, J., Lee, L.J., and Lu, H.C. (2010). mGluR5 in cortical excitatory neurons exerts both cell-autonomous and -nonautonomous influences on cortical somatosensory circuit formation. J Neurosci *30*, 16896-16909.

Bangash, M.A., Park, J.M., Melnikova, T., Wang, D., Jeon, S.K., Lee, D., Syeda, S., Kim, J., Kouser, M., Schwartz, J., *et al.* (2011a). Enhanced Polyubiquitination of Shank3 and NMDA Receptor in a Mouse Model of Autism. Cell.

Bangash, M.A., Park, J.M., Melnikova, T., Wang, D., Jeon, S.K., Lee, D., Syeda, S., Kim, J., Kouser, M., Schwartz, J., *et al.* (2011b). Enhanced polyubiquitination of Shank3 and NMDA receptor in a mouse model of autism. Cell *145*, 758-772.

Banko, J.L., Hou, L., Poulin, F., Sonenberg, N., and Klann, E. (2006). Regulation of eukaryotic initiation factor 4E by converging signaling pathways during metabotropic glutamate receptor-dependent long-term depression. J Neurosci *26*, 2167-2173.

Barbaresi, W.J., Katusic, S.K., Colligan, R.C., Weaver, A.L., and Jacobsen, S.J. (2005). The incidence of autism in Olmsted County, Minnesota, 1976-1997: results from a population-based study. Arch Pediatr Adolesc Med *159*, 37-44.

Bassell, G.J., and Warren, S.T. (2008). Fragile X syndrome: loss of local mRNA regulation alters synaptic development and function. Neuron *60*, 201-214.

Batchelor, A.M., Madge, D.J., and Garthwaite, J. (1994). Synaptic activation of metabotropic glutamate receptors in the parallel fibre-Purkinje cell pathway in rat cerebellar slices. Neuroscience *63*, 911-915.

Bateup, H.S., Takasaki, K.T., Saulnier, J.L., Denefrio, C.L., and Sabatini, B.L. (2011). Loss of Tsc1 in vivo impairs hippocampal mGluR-LTD and increases excitatory synaptic function. J Neurosci *31*, 8862-8869.

Baude, A., Nusser, Z., Roberts, J.D., Mulvihill, E., McIlhinney, R.A., and Somogyi, P. (1993). The metabotropic glutamate receptor (mGluR1 alpha) is concentrated at perisynaptic membrane of neuronal subpopulations as detected by immunogold reaction. Neuron *11*, 771-787.

Bazhenov, M., Lonjers, P., Skorheim, S., Bedard, C., and Dstexhe, A. (2011). Non-homogeneous extracellular resistivity affects the current-source density profiles of up-down state oscillations. Philos Trans A Math Phys Eng Sci *369*, 3802-3819.

Bear, M.F., Huber, K.M., and Warren, S.T. (2004). The mGluR theory of fragile X mental retardation. Trends Neurosci *27*, 370-377.

Benoist, M., Palenzuela, R., Rozas, C., Rojas, P., Tortosa, E., Morales, B., Gonzalez-Billault, C., Avila, J., and Esteban, J.A. (2013). MAP1B-dependent Rac activation is required for AMPA receptor endocytosis during long-term depression. EMBO J *32*, 2287-2299.

Beqollari, D., and Kammermeier, P.J. (2010). Venus Fly Trap Domain of mGluR1 Functions as a Dominant Negative Against Group I mGluR Signaling. Journal of Neurophysiology *104*, 439-448.

Berg, J.M., and Geschwind, D.H. (2012). Autism genetics: searching for specificity and convergence. Genome Biol *13*, 247.

Berry-Kravis, E. (2002). Epilepsy in fragile X syndrome. Dev Med Child Neurol *44*, 724-728.

Berry-Kravis, E., Raspa, M., Loggin-Hester, L., Bishop, E., Holiday, D., and Bailey, D.B. (2010). Seizures in fragile X syndrome: characteristics and comorbid diagnoses. Am J Intellect Dev Disabil *115*, 461-472.

Bhattacharya, A., Kaphzan, H., Alvarez-Dieppa, A.C., Murphy, J.P., Pierre, P., and Klann, E. (2012). Genetic removal of p70 S6 kinase 1 corrects molecular, synaptic, and behavioral phenotypes in fragile X syndrome mice. Neuron *76*, 325-337.

Billuart, P., Bienvenu, T., Ronce, N., des Portes, V., Vinet, M.C., Zemni, R., Roest Crollius, H., Carrie, A., Fauchereau, F., Cherry, M., *et al.* (1998). Oligophrenin-1 encodes a rhoGAP protein involved in X-linked mental retardation. Nature *392*, 923-926.

Brakeman, P.R., Lanahan, A.A., O'Brien, R., Roche, K., Barnes, C.A., Huganir, R.L., and Worley, P.F. (1997). Homer: a protein that selectively binds metabotropic glutamate receptors. Nature *386*, 284-288.

Brock, C., Schaefer, M., Reusch, H.P., Czupalla, C., Michalke, M., Spicher, K., Schultz, G., and Nurnberg, B. (2003). Roles of G beta gamma in membrane recruitment and activation of p110 gamma/p101 phosphoinositide 3-kinase gamma. J Cell Biol *160*, 89-99.

Brown, M.R., Kronengold, J., Gazula, V.R., Chen, Y., Strumbos, J.G., Sigworth, F.J., Navaratnam, D., and Kaczmarek, L.K. (2010). Fragile X mental retardation protein controls gating of the sodium-activated potassium channel Slack. Nat Neurosci *13*, 819-821.

Brown, V., Jin, P., Ceman, S., Darnell, J.C., O'Donnell, W.T., Tenenbaum, S.A., Jin, X., Feng, Y., Wilkinson, K.D., Keene, J.D., *et al.* (2001). Microarray identification of FMRP-associated brain mRNAs and altered mRNA translational profiles in fragile X syndrome. Cell *107*, 477-487.

Brunn, G.J., Hudson, C.C., Sekulic, A., Williams, J.M., Hosoi, H., Houghton, P.J., Lawrence, J.C., Jr., and Abraham, R.T. (1997). Phosphorylation of the translational repressor PHAS-I by the mammalian target of rapamycin. Science *277*, 99-101.

Bui, J.D., Calbo, S., Hayden-Martinez, K., Kane, L.P., Gardner, P., and Hedrick, S.M. (2000). A role for CaMKII in T cell memory. Cell *100*, 457-467.

Bureau, I., Shepherd, G.M., and Svoboda, K. (2008). Circuit and plasticity defects in the developing somatosensory cortex of FMR1 knock-out mice. J Neurosci *28*, 5178-5188.

Butler, M.G., Dasouki, M.J., Zhou, X.P., Talebizadeh, Z., Brown, M., Takahashi, T.N., Miles, J.H., Wang, C.H., Stratton, R., Pilarski, R., *et al.* (2005). Subset of individuals with autism spectrum disorders and extreme macrocephaly associated with germline PTEN tumour suppressor gene mutations. J Med Genet *42*, 318-321.

Buxbaum, J.D., Cai, G., Chaste, P., Nygren, G., Goldsmith, J., Reichert, J., Anckarsater, H., Rastam, M., Smith, C.J., Silverman, J.M., *et al.* (2007). Mutation screening of the PTEN gene in patients with autism spectrum disorders and macrocephaly. Am J Med Genet B Neuropsychiatr Genet *144B*, 484-491.

Ceman, S., O'Donnell, W.T., Reed, M., Patton, S., Pohl, J., and Warren, S.T. (2003). Phosphorylation influences the translation state of FMRP-associated polyribosomes. Hum Mol Genet *12*, 3295-3305.

Chen, L., and Toth, M. (2001). Fragile X mice develop sensory hyperreactivity to auditory stimuli. Neuroscience *103*, 1043-1050.

Chevaleyre, V., and Castillo, P.E. (2003). Heterosynaptic LTD of hippocampal GABAergic synapses: a novel role of endocannabinoids in regulating excitability. Neuron *38*, 461-472.

Chuang, S.C., Zhao, W., Bauchwitz, R., Yan, Q., Bianchi, R., and Wong, R.K. (2005). Prolonged epileptiform discharges induced by altered group I metabotropic glutamate receptor-mediated synaptic responses in hippocampal slices of a fragile X mouse model. J Neurosci *25*, 8048-8055.

Ciruela, F., Soloviev, M.M., Chan, W.Y., and McIlhinney, R.A. (2000). Homer-1c/Vesl-1L modulates the cell surface targeting of metabotropic glutamate receptor type 1alpha: evidence for an anchoring function. Mol Cell Neurosci *15*, 36-50.

Comery, T.A., Harris, J.B., Willems, P.J., Oostra, B.A., Irwin, S.A., Weiler, I.J., and Greenough, W.T. (1997). Abnormal dendritic spines in fragile X knockout mice: maturation and pruning deficits. Proc Natl Acad Sci U S A *94*, 5401-5404.

Conn, P.J., and Pin, J.P. (1997). Pharmacology and functions of metabotropic glutamate receptors. Annu Rev Pharmacol Toxicol *37*, 205-237.

Consortium, T.D.-B.F.X. (1994). Fmr1 knockout mice: a model to study fragile X mental retardation. . Cell *78*, 23-33.

Corbin, F., Bouillon, M., Fortin, A., Morin, S., Rousseau, F., and Khandjian, E.W. (1997). The fragile X mental retardation protein is associated with poly(A)+ mRNA in actively translating polyribosomes. Hum Mol Genet *6*, 1465-1472.

Cozzoli, D.K., Goulding, S.P., Zhang, P.W., Xiao, B., Hu, J.H., Ary, A.W., Obara, I., Rahn, A., Abou-Ziab, H., Tyrrel, B., *et al.* (2009). Binge drinking upregulates accumbens mGluR5-Homer2-PI3K signaling: functional implications for alcoholism. J Neurosci *29*, 8655-8668.

Dansie, L.E., Phommahaxay, K., Okusanya, A.G., Uwadia, J., Huang, M., Rotschafer, S.E., Razak, K.A., Ethell, D.W., and Ethell, I.M. (2013). Long-lasting effects of minocycline on behavior in young but not adult Fragile X mice. Neuroscience *246*, 186-198.

Darnell, J.C., Van Driesche, S.J., Zhang, C., Hung, K.Y., Mele, A., Fraser, C.E., Stone, E.F., Chen, C., Fak, J.J., Chi, S.W., *et al.* (2011). FMRP stalls ribosomal translocation on mRNAs linked to synaptic function and autism. Cell *146*, 247-261.

Davidkova, G., and Carroll, R.C. (2007). Characterization of the role of microtubule-associated protein 1B in metabotropic glutamate receptor-mediated endocytosis of AMPA receptors in hippocampus. J Neurosci *27*, 13273-13278.

De Boulle, K., Verkerk, A.J., Reyniers, E., Vits, L., Hendrickx, J., Van Roy, B., Van den Bos, F., de Graaff, E., Oostra, B.A., and Willems, P.J. (1993). A point mutation in the FMR-1 gene associated with fragile X mental retardation. Nat Genet *3*, 31-35.

de Vrij, F.M., Levenga, J., van der Linde, H.C., Koekkoek, S.K., De Zeeuw, C.I., Nelson, D.L., Oostra, B.A., and Willemsen, R. (2008). Rescue of behavioral phenotype and neuronal protrusion morphology in Fmr1 KO mice. Neurobiol Dis *31*, 127-132.

Dictenberg, J.B., Swanger, S.A., Antar, L.N., Singer, R.H., and Bassell, G.J. (2008). A direct role for FMRP in activity-dependent dendritic mRNA transport links filopodial-spine morphogenesis to fragile X syndrome. Dev Cell *14*, 926-939.

Dolan, B.M., Duron, S.G., Campbell, D.A., Vollrath, B., Shankaranarayana Rao, B.S., Ko, H.Y., Lin, G.G., Govindarajan, A., Choi, S.Y., and Tonegawa, S. (2013). Rescue of fragile X syndrome phenotypes in Fmr1 KO mice by the small-molecule PAK inhibitor FRAX486. Proc Natl Acad Sci U S A *110*, 5671-5676.

Dolen, G., Carpenter, R.L., Ocain, T.D., and Bear, M.F. (2010). Mechanism-based approaches to treating fragile X. Pharmacol Ther *127*, 78-93.

Dolen, G., Osterweil, E., Rao, B.S., Smith, G.B., Auerbach, B.D., Chattarji, S., and Bear, M.F. (2007). Correction of Fragile X Syndrome in Mice. Neuron *56*, 955-962.

Dupre, D.J., Robitaille, M., Rebois, R.V., and Hebert, T.E. (2009). The role of Gbetagamma subunits in the organization, assembly, and function of GPCR signaling complexes. Annu Rev Pharmacol Toxicol *49*, 31-56.

Endersby, R., and Baker, S.J. (2008). PTEN signaling in brain: neuropathology and tumorigenesis. Oncogene *27*, 5416-5430.

Feng, Y., Absher, D., Eberhart, D.E., Brown, V., Malter, H.E., and Warren, S.T. (1997). FMRP associates with polyribosomes as an mRNP, and the I304N mutation of severe fragile X syndrome abolishes this association. Mol Cell *1*, 109-118.

Fombonne, E., Roge, B., Claverie, J., Courty, S., and Fremolle, J. (1999). Microcephaly and macrocephaly in autism. J Autism Dev Disord *29*, 113-119.

Frankland, P.W., Wang, Y., Rosner, B., Shimizu, T., Balleine, B.W., Dykens, E.M., Ornitz, E.M., and Silva, A.J. (2004). Sensorimotor gating abnormalities in young males with fragile X syndrome and Fmr1-knockout mice. Mol Psychiatry *9*, 417-425.

Gallagher, S.M., Daly, C.A., Bear, M.F., and Huber, K.M. (2004). Extracellular signal-regulated protein kinase activation is required for metabotropic glutamate receptor-dependent long-term depression in hippocampal area CA1. J Neurosci *24*, 4859-4864.

Ganz, M.L. (2007). The lifetime distribution of the incremental societal costs of autism. Arch Pediatr Adolesc Med *161*, 343-349.

Gao, L., Blair, L.A., and Marshall, J. (2006). CaMKII-independent effects of KN93 and its inactive analog KN92: reversible inhibition of L-type calcium channels. Biochem Biophys Res Commun *345*, 1606-1610.

Gao, Y., Vasilyev, D.V., Goncalves, M.B., Howell, F.V., Hobbs, C., Reisenberg, M., Shen, R., Zhang, M.Y., Strassle, B.W., Lu, P., *et al.* (2010). Loss of retrograde endocannabinoid signaling and reduced adult neurogenesis in diacylglycerol lipase knock-out mice. J Neurosci *30*, 2017-2024.

Garber, K.B., Visootsak, J., and Warren, S.T. (2008). Fragile X syndrome. Eur J Hum Genet *16*, 666-672.

Gibson, J.R., Bartley, A.F., Hays, S.A., and Huber, K.M. (2008). Imbalance of neocortical excitation and inhibition and altered UP states reflect network hyperexcitability in the mouse model of fragile X syndrome. J Neurophysiol *100*, 2615-2626.

Gingras, A.C., Gygi, S.P., Raught, B., Polakiewicz, R.D., Abraham, R.T., Hoekstra, M.F., Aebersold, R., and Sonenberg, N. (1999). Regulation of 4E-BP1 phosphorylation: a novel two-step mechanism. Genes Dev *13*, 1422-1437.

Gingras, A.C., Raught, B., Gygi, S.P., Niedzwiecka, A., Miron, M., Burley, S.K., Polakiewicz, R.D., Wyslouch-Cieszynska, A., Aebersold, R., and Sonenberg, N. (2001). Hierarchical phosphorylation of the translation inhibitor 4E-BP1. Genes Dev *15*, 2852-2864.

Giuffrida, R., Musumeci, S., D'Antoni, S., Bonaccorso, C.M., Giuffrida-Stella, A.M., Oostra, B.A., and Catania, M.V. (2005). A reduced number of metabotropic glutamate subtype 5 receptors are associated with constitutive homer proteins in a mouse model of fragile X syndrome. J Neurosci *25*, 8908-8916.

Godfraind, J.M., Reyniers, E., De Boulle, K., D'Hooge, R., De Deyn, P.P., Bakker, C.E., Oostra, B.A., Kooy, R.F., and Willems, P.J. (1996). Long-term potentiation in the hippocampus of fragile X knockout mice. Am J Med Genet *64*, 246-251.

Goebel-Goody, S.M., Wilson-Wallis, E.D., Royston, S., Tagliatela, S.M., Naegele, J.R., and Lombroso, P.J. (2012). Genetic manipulation of STEP reverses behavioral abnormalities in a fragile X syndrome mouse model. Genes Brain Behav *11*, 586-600.

Gonzalez, M.I., Susarla, B.T., Fournier, K.M., Sheldon, A.L., and Robinson, M.B. (2007). Constitutive endocytosis and recycling of the neuronal glutamate transporter, excitatory amino acid carrier 1. J Neurochem *103*, 1917-1931.

Goudet, C., Kniazeff, J., Hlavackova, V., Malhaire, F., Maurel, D., Acher, F., Blahos, J., Prezeau, L., and Pin, J.P. (2005). Asymmetric functioning of dimeric metabotropic glutamate receptors disclosed by positive allosteric modulators. J Biol Chem *280*, 24380-24385.

Gray, N.W., Fourgeaud, L., Huang, B., Chen, J., Cao, H., Oswald, B.J., Hemar, A., and McNiven, M.A. (2003). Dynamin 3 is a component of the postsynapse, where it interacts with mGluR5 and Homer. Curr Biol *13*, 510-515.

Gross, C., Nakamoto, M., Yao, X., Chan, C.B., Yim, S.Y., Ye, K., Warren, S.T., and Bassell, G.J. (2010). Excess phosphoinositide 3-kinase subunit synthesis and activity as a novel therapeutic target in fragile X syndrome. J Neurosci *30*, 10624-10638.

Gross, C., Yao, X., Pong, D.L., Jeromin, A., and Bassell, G.J. (2011). Fragile X mental retardation protein regulates protein expression and mRNA translation of the potassium channel Kv4.2. J Neurosci *31*, 5693-5698.

Guan, D., Horton, L.R., Armstrong, W.E., and Foehring, R.C. (2011). Postnatal development of A-type and Kv1- and Kv2-mediated potassium channel currents in neocortical pyramidal neurons. J Neurophysiol *105*, 2976-2988.

Guhan, N., and Lu, B. (2004). Homer-PIKE complex: a novel link between mGluRI and PI 3-kinase. Trends Neurosci *27*, 645-648.

Hagerman, R. (2002). The physical and behavioral phenotype. In Fragile X Syndrome: Diagnosis, Treatment, and Research, R. Hagerman, and P. Hagerman, eds. (Baltimore, The Johns Hopkins University Press), pp. 3-109.

Hagerman, R.J., Chudley, A.E., Knoll, J.H., Jackson, A.W., 3rd, Kemper, M., and Ahmad, R. (1986). Autism in fragile X females. Am J Med Genet *23*, 375-380.

Hagerman, R.J., and Hagerman, P.J. (2002). The fragile X premutation: into the phenotypic fold. Curr Opin Genet Dev *12*, 278-283.
Hagerman, R.J., Ono, M.Y., and Hagerman, P.J. (2005). Recent advances in fragile X: a model for autism and neurodegeneration. Curr Opin Psychiatry *18*, 490-496.
Haider, B., Duque, A., Hasenstaub, A.R., and McCormick, D.A. (2006). Neocortical network activity in vivo is generated through a dynamic balance of excitation and inhibition. J Neurosci *26*, 4535-4545.
Haider, B., and McCormick, D.A. (2009). Rapid neocortical dynamics: cellular and network mechanisms. Neuron *62*, 171-189.
Haws, M.E., Jaramillo, T.C., Espinosa-Becerra, F., Widman, A., Stuber, G.D., Sparta, D.R., Tye, K.M., Russo, S.J., Parada, L.F., Kaplitt, M., *et al.* (2013). PTEN knockdown alters dendritic spine/protrusion morphology, not density. J Comp Neurol.
Hayashi, M.K., Tang, C., Verpelli, C., Narayanan, R., Stearns, M.H., Xu, R.M., Li, H., Sala, C., and Hayashi, Y. (2009). The postsynaptic density proteins Homer and Shank form a polymeric network structure. Cell *137*, 159-171.
Hays, S.A., Huber, K.M., and Gibson, J.R. (2011). Altered neocortical rhythmic activity states in Fmr1 KO mice are due to enhanced mGluR5 signaling and involve changes in excitatory circuitry. J Neurosci *31*, 14223-14234.
Henderson, C., Wijetunge, L., Kinoshita, M.N., Shumway, M., Hammond, R.S., Postma, F.R., Brynczka, C., Rush, R., Thomas, A., Paylor, R., *et al.* (2012). Reversal of disease-related pathologies in the fragile X mouse model by selective activation of GABAB receptors with arbaclofen. Sci Transl Med *4*, 152ra128.
Herbert, T.P., Tee, A.R., and Proud, C.G. (2002). The extracellular signal-regulated kinase pathway regulates the phosphorylation of 4E-BP1 at multiple sites. J Biol Chem *277*, 11591-11596.
Herman, G.E., Henninger, N., Ratliff-Schaub, K., Pastore, M., Fitzgerald, S., and McBride, K.L. (2007). Genetic testing in autism: how much is enough? Genet Med *9*, 268-274.
Hermans, E., and Challiss, R.A. (2001). Structural, signalling and regulatory properties of the group I metabotropic glutamate receptors: prototypic family C G-protein-coupled receptors. Biochem J *359*, 465-484.
Hoeffer, C.A., Sanchez, E., Hagerman, R.J., Mu, Y., Nguyen, D.V., Wong, H., Whelan, A.M., Zukin, R.S., Klann, E., and Tassone, F. (2012). Altered mTOR signaling and enhanced CYFIP2 expression levels in subjects with fragile X syndrome. Genes Brain Behav *11*, 332-341.
Hoffman, D.A., Magee, J.C., Colbert, C.M., and Johnston, D. (1997). K+ channel regulation of signal propagation in dendrites of hippocampal pyramidal neurons. Nature *387*, 869-875.
Holz, M.K., Ballif, B.A., Gygi, S.P., and Blenis, J. (2005). mTOR and S6K1 mediate assembly of the translation preinitiation complex through dynamic protein interchange and ordered phosphorylation events. Cell *123*, 569-580.
Hou, L., Antion, M.D., Hu, D., Spencer, C.M., Paylor, R., and Klann, E. (2006a). Dynamic Translational and Proteasomal Regulation of Fragile X Mental

Retardation Protein Controls mGluR-Dependent Long-Term Depression. Neuron *51*, 441-454.

Hou, L., Antion, M.D., Hu, D., Spencer, C.M., Paylor, R., and Klann, E. (2006b). Dynamic translational and proteasomal regulation of fragile X mental retardation protein controls mGluR-dependent long-term depression. Neuron *51*, 441-454.

Hou, L., and Klann, E. (2004). Activation of the phosphoinositide 3-kinase-Akt-mammalian target of rapamycin signaling pathway is required for metabotropic glutamate receptor-dependent long-term depression. J Neurosci *24*, 6352-6361.

Hu, J.H., Park, J.M., Park, S., Xiao, B., Dehoff, M.H., Kim, S., Hayashi, T., Schwarz, M.K., Huganir, R.L., Seeburg, P.H., *et al.* (2010). Homeostatic scaling requires group I mGluR activation mediated by Homer1a. Neuron *68*, 1128-1142.

Hu, J.H., Yang, L., Kammermeier, P.J., Moore, C.G., Brakeman, P.R., Tu, J., Yu, S., Petralia, R.S., Li, Z., Zhang, P.W., *et al.* (2012). Preso1 dynamically regulates group I metabotropic glutamate receptors. Nat Neurosci *15*, 836-844.

Huang, G.N., Huso, D.L., Bouyain, S., Tu, J., McCorkell, K.A., May, M.J., Zhu, Y., Lutz, M., Collins, S., Dehoff, M., *et al.* (2008a). NFAT binding and regulation of T cell activation by the cytoplasmic scaffolding Homer proteins. Science *319*, 476-481.

Huang, J., Dibble, C.C., Matsuzaki, M., and Manning, B.D. (2008b). The TSC1-TSC2 complex is required for proper activation of mTOR complex 2. Mol Cell Biol *28*, 4104-4115.

Huber, K.M., Gallagher, S.M., Warren, S.T., and Bear, M.F. (2002). Altered synaptic plasticity in a mouse model of fragile X mental retardation. Proc Natl Acad Sci U S A *99*, 7746-7750.

Huber, K.M., Kayser, M.S., and Bear, M.F. (2000). Role for rapid dendritic protein synthesis in hippocampal mGluR-dependent long-term depression. Science *288*, 1254-1257.

Huber, K.M., Roder, J.C., and Bear, M.F. (2001). Chemical induction of mGluR5- and protein synthesis--dependent long-term depression in hippocampal area CA1. J Neurophysiol *86*, 321-325.

Hubert, G.W., Paquet, M., and Smith, Y. (2001). Differential subcellular localization of mGluR1a and mGluR5 in the rat and monkey Substantia nigra. J Neurosci *21*, 1838-1847.

Igal, R.A., Caviglia, J.M., de Gomez Dumm, I.N., and Coleman, R.A. (2001). Diacylglycerol generated in CHO cell plasma membrane by phospholipase C is used for triacylglycerol synthesis. J Lipid Res *42*, 88-95.

Iliff, A.J., Renoux, A.J., Krans, A., Usdin, K., Sutton, M.A., and Todd, P.K. (2013). Impaired activity-dependent FMRP translation and enhanced mGluR-dependent LTD in Fragile X premutation mice. Hum Mol Genet *22*, 1180-1192.

Irie, K., Nakatsu, T., Mitsuoka, K., Miyazawa, A., Sobue, K., Hiroaki, Y., Doi, T., Fujiyoshi, Y., and Kato, H. (2002). Crystal structure of the Homer 1 family conserved region reveals the interaction between the EVH1 domain and own proline-rich motif. J Mol Biol *318*, 1117-1126.

Irwin, S.A., Galvez, R., and Greenough, W.T. (2000). Dendritic spine structural anomalies in fragile-X mental retardation syndrome. Cereb Cortex *10*, 1038-1044.

Jacquemont, S., Curie, A., des Portes, V., Torrioli, M.G., Berry-Kravis, E., Hagerman, R.J., Ramos, F.J., Cornish, K., He, Y., Paulding, C., *et al.* (2011). Epigenetic modification of the FMR1 gene in fragile X syndrome is associated with differential response to the mGluR5 antagonist AFQ056. Sci Transl Med *3*, 64ra61.

Jakkamsetti, V., Tsai, N.P., Gross, C., Molinaro, G., Collins, K.A., Nicoletti, F., Wang, K.H., Osten, P., Bassell, G.J., Gibson, J.R., *et al.* (2013). Experience-induced Arc/Arg3.1 primes CA1 pyramidal neurons for metabotropic glutamate receptor-dependent long-term synaptic depression. Neuron *80*, 72-79.

Jarbrink, K., and Knapp, M. (2001). The economic impact of autism in Britain. Autism *5*, 7-22.

Johansen, T., Bjorkoy, G., Overvatn, A., Diaz-Meco, M.T., Traavik, T., and Moscat, J. (1994). NIH 3T3 cells stably transfected with the gene encoding phosphatidylcholine-hydrolyzing phospholipase C from Bacillus cereus acquire a transformed phenotype. Mol Cell Biol *14*, 646-654.

Jong, Y.-J.I., Kumar, V., and O'Malley, K.L. (2009). Intracellular Metabotropic Glutamate Receptor 5 (mGluR5) Activates Signaling Cascades Distinct from Cell Surface Counterparts. Journal of Biological Chemistry *284*, 35827-35838.

Jung, K.M., Sepers, M., Henstridge, C.M., Lassalle, O., Neuhofer, D., Martin, H., Ginger, M., Frick, A., DiPatrizio, N.V., Mackie, K., *et al.* (2012). Uncoupling of the endocannabinoid signalling complex in a mouse model of fragile X syndrome. Nat Commun *3*, 1080.

Kammermeier, P.J. (2006). Surface clustering of metabotropic glutamate receptor 1 induced by long Homer proteins. BMC Neurosci *7*, 1.

Kammermeier, P.J., Xiao, B., Tu, J.C., Worley, P.F., and Ikeda, S.R. (2000). Homer proteins regulate coupling of group I metabotropic glutamate receptors to N-type calcium and M-type potassium channels. J Neurosci *20*, 7238-7245.

Kano, M., Ohno-Shosaku, T., Hashimotodani, Y., Uchigashima, M., and Watanabe, M. (2009). Endocannabinoid-mediated control of synaptic transmission. Physiol Rev *89*, 309-380.

Katritch, V., Cherezov, V., and Stevens, R.C. (2013). Structure-function of the G protein-coupled receptor superfamily. Annu Rev Pharmacol Toxicol *53*, 531-556.

Kaufmann, W.E., Cortell, R., Kau, A.S., Bukelis, I., Tierney, E., Gray, R.M., Cox, C., Capone, G.T., and Stanard, P. (2004). Autism spectrum disorder in fragile X syndrome: communication, social interaction, and specific behaviors. Am J Med Genet A *129A*, 225-234.

Kelleher, R.J., 3rd, Govindarajan, A., Jung, H.Y., Kang, H., and Tonegawa, S. (2004). Translational Control by MAPK Signaling in Long-Term Synaptic Plasticity and Memory. Cell *116*, 467-479.

Kim, K.C., Kim, P., Go, H.S., Choi, C.S., Park, J.H., Kim, H.J., Jeon, S.J., Dela Pena, I.C., Han, S.H., Cheong, J.H., *et al.* (2013). Male-specific alteration in excitatory

post-synaptic development and social interaction in pre-natal valproic acid exposure model of autism spectrum disorder. J Neurochem *124*, 832-843.
Kim, S.H., Markham, J.A., Weiler, I.J., and Greenough, W.T. (2008). Aberrant early-phase ERK inactivation impedes neuronal function in fragile X syndrome. Proc Natl Acad Sci U S A *105*, 4429-4434.
Kim, Y.S., Leventhal, B.L., Koh, Y.J., Fombonne, E., Laska, E., Lim, E.C., Cheon, K.A., Kim, S.J., Kim, Y.K., Lee, H., *et al.* (2011). Prevalence of autism spectrum disorders in a total population sample. Am J Psychiatry *168*, 904-912.
Klauck, S.M. (2006). Genetics of autism spectrum disorder. Eur J Hum Genet *14*, 714-720.
Kotecha, S.A., Jackson, M.F., Al-Mahrouki, A., Roder, J.C., Orser, B.A., and MacDonald, J.F. (2003). Co-stimulation of mGluR5 and N-methyl-D-aspartate receptors is required for potentiation of excitatory synaptic transmission in hippocampal neurons. J Biol Chem *278*, 27742-27749.
Kuwajima, M., Dehoff, M.H., Furuichi, T., Worley, P.F., Hall, R.A., and Smith, Y. (2007). Localization and expression of group I metabotropic glutamate receptors in the mouse striatum, globus pallidus, and subthalamic nucleus: regulatory effects of MPTP treatment and constitutive Homer deletion. J Neurosci *27*, 6249-6260.
Kwon, C.H., Luikart, B.W., Powell, C.M., Zhou, J., Matheny, S.A., Zhang, W., Li, Y., Baker, S.J., and Parada, L.F. (2006a). Pten regulates neuronal arborization and social interaction in mice. Neuron *50*, 377-388.
Kwon, C.H., Zhou, J., Li, Y., Kim, K.W., Hensley, L.L., Baker, S.J., and Parada, L.F. (2006b). Neuron-specific enolase-cre mouse line with cre activity in specific neuronal populations. Genesis *44*, 130-135.
Kwon, C.H., Zhu, X., Zhang, J., Knoop, L.L., Tharp, R., Smeyne, R.J., Eberhart, C.G., Burger, P.C., and Baker, S.J. (2001). Pten regulates neuronal soma size: a mouse model of Lhermitte-Duclos disease. Nat Genet *29*, 404-411.
Lafourcade, C.A. (2009). Presynaptic mechanisms of endocannabinoid-mediated long-term depression in the hippocampus. J Neurophysiol *102*, 2009-2012.
Lawrence, J.C., Jr., and Abraham, R.T. (1997). PHAS/4E-BPs as regulators of mRNA translation and cell proliferation. Trends Biochem Sci *22*, 345-349.
Lea, P.M.t., Movsesyan, V.A., and Faden, A.I. (2005). Neuroprotective activity of the mGluR5 antagonists MPEP and MTEP against acute excitotoxicity differs and does not reflect actions at mGluR5 receptors. Br J Pharmacol *145*, 527-534.
Lee, H.Y., Ge, W.P., Huang, W., He, Y., Wang, G.X., Rowson-Baldwin, A., Smith, S.J., Jan, Y.N., and Jan, L.Y. (2011). Bidirectional regulation of dendritic voltage-gated potassium channels by the fragile X mental retardation protein. Neuron *72*, 630-642.
Lee, J.O., Yang, H., Georgescu, M.M., Di Cristofano, A., Maehama, T., Shi, Y., Dixon, J.E., Pandolfi, P., and Pavletich, N.P. (1999). Crystal structure of the PTEN tumor suppressor: implications for its phosphoinositide phosphatase activity and membrane association. Cell *99*, 323-334.
Levenga, J., Hayashi, S., de Vrij, F.M., Koekkoek, S.K., van der Linde, H.C., Nieuwenhuizen, I., Song, C., Buijsen, R.A., Pop, A.S., Gomezmancilla, B., *et al.*

(2011). AFQ056, a new mGluR5 antagonist for treatment of fragile X syndrome. Neurobiol Dis *42*, 311-317.
Li, J., Yen, C., Liaw, D., Podsypanina, K., Bose, S., Wang, S.I., Puc, J., Miliaresis, C., Rodgers, L., McCombie, R., *et al.* (1997). PTEN, a putative protein tyrosine phosphatase gene mutated in human brain, breast, and prostate cancer. Science *275*, 1943-1947.
Li, Y., Krogh, K.A., and Thayer, S.A. (2012). Epileptic stimulus increases Homer 1a expression to modulate endocannabinoid signaling in cultured hippocampal neurons. Neuropharmacology *63*, 1140-1149.
Li, Z., Zhang, Y., Ku, L., Wilkinson, K.D., Warren, S.T., and Feng, Y. (2001). The fragile X mental retardation protein inhibits translation via interacting with mRNA. Nucleic Acids Res *29*, 2276-2283.
Liu, Z.H., and Smith, C.B. (2009). Dissociation of social and nonsocial anxiety in a mouse model of fragile X syndrome. Neurosci Lett *454*, 62-66.
Ljungberg, M.C., Sunnen, C.N., Lugo, J.N., Anderson, A.E., and D'Arcangelo, G. (2009). Rapamycin suppresses seizures and neuronal hypertrophy in a mouse model of cortical dysplasia. Dis Model Mech *2*, 389-398.
Lopez-Bendito, G., Shigemoto, R., Fairen, A., and Lujan, R. (2002). Differential distribution of group I metabotropic glutamate receptors during rat cortical development. Cereb Cortex *12*, 625-638.
Lujan, R., Nusser, Z., Roberts, J.D., Shigemoto, R., and Somogyi, P. (1996). Perisynaptic location of metabotropic glutamate receptors mGluR1 and mGluR5 on dendrites and dendritic spines in the rat hippocampus. Eur J Neurosci *8*, 1488-1500.
Luscher, C., and Huber, K.M. (2010). Group 1 mGluR-dependent synaptic long-term depression: mechanisms and implications for circuitry and disease. Neuron *65*, 445-459.
Lv, J.W., Cheng, T.L., Qiu, Z.L., and Zhou, W.H. (2013). Role of the PTEN signaling pathway in autism spectrum disorder. Neurosci Bull *29*, 773-778.
Maccarrone, M., Rossi, S., Bari, M., De Chiara, V., Rapino, C., Musella, A., Bernardi, G., Bagni, C., and Centonze, D. (2010). Abnormal mGlu 5 receptor/endocannabinoid coupling in mice lacking FMRP and BC1 RNA. Neuropsychopharmacology *35*, 1500-1509.
Mackiewicz, M., Paigen, B., Naidoo, N., and Pack, A.I. (2008). Analysis of the QTL for sleep homeostasis in mice: Homer1a is a likely candidate. Physiol Genomics *33*, 91-99.
Maehama, T., and Dixon, J.E. (1998). The tumor suppressor, PTEN/MMAC1, dephosphorylates the lipid second messenger, phosphatidylinositol 3,4,5-trisphosphate. J Biol Chem *273*, 13375-13378.
Manning, B.D., and Cantley, L.C. (2007). AKT/PKB signaling: navigating downstream. Cell *129*, 1261-1274.
Mao, L., Yang, L., Tang, Q., Samdani, S., Zhang, G., and Wang, J.Q. (2005). The scaffold protein Homer1b/c links metabotropic glutamate receptor 5 to extracellular signal-regulated protein kinase cascades in neurons. J Neurosci *25*, 2741-2752.
Marrion, N.V. (1997). Control of M-current. Annu Rev Physiol *59*, 483-504.

McBride, K.L., Varga, E.A., Pastore, M.T., Prior, T.W., Manickam, K., Atkin, J.F., and Herman, G.E. (2010). Confirmation study of PTEN mutations among individuals with autism or developmental delays/mental retardation and macrocephaly. Autism Res *3*, 137-141.

McBride, S.M., Choi, C.H., Wang, Y., Liebelt, D., Braunstein, E., Ferreiro, D., Sehgal, A., Siwicki, K.K., Dockendorff, T.C., Nguyen, H.T., *et al.* (2005). Pharmacological rescue of synaptic plasticity, courtship behavior, and mushroom body defects in a Drosophila model of fragile X syndrome. Neuron *45*, 753-764.

McCudden, C.R., Hains, M.D., Kimple, R.J., Siderovski, D.P., and Willard, F.S. (2005). G-protein signaling: back to the future. Cell Mol Life Sci *62*, 551-577.

Merenstein, S.A., Sobesky, W.E., Taylor, A.K., Riddle, J.E., Tran, H.X., and Hagerman, R.J. (1996). Molecular-clinical correlations in males with an expanded FMR1 mutation. Am J Med Genet *64*, 388-394.

Merlin, L.R., and Wong, R.K. (1997). Role of group I metabotropic glutamate receptors in the patterning of epileptiform activities in vitro. J Neurophysiol *78*, 539-544.

Miller, L.J., McIntosh, D.N., McGrath, J., Shyu, V., Lampe, M., Taylor, A.K., Tassone, F., Neitzel, K., Stackhouse, T., and Hagerman, R.J. (1999). Electrodermal responses to sensory stimuli in individuals with fragile X syndrome: a preliminary report. Am J Med Genet *83*, 268-279.

Minakami, R., Kato, A., and Sugiyama, H. (2000). Interaction of Vesl-1L/Homer 1c with syntaxin 13. Biochem Biophys Res Commun *272*, 466-471.

Mizutani, A., Kuroda, Y., Futatsugi, A., Furuichi, T., and Mikoshiba, K. (2008). Phosphorylation of Homer3 by calcium/calmodulin-dependent kinase II regulates a coupling state of its target molecules in Purkinje cells. J Neurosci *28*, 5369-5382.

Moult, P.R., Cross, A., Santos, S.D., Carvalho, A.L., Lindsay, Y., Connolly, C.N., Irving, A.J., Leslie, N.R., and Harvey, J. (2010). Leptin regulates AMPA receptor trafficking via PTEN inhibition. J Neurosci *30*, 4088-4101.

Muddashetty, R.S., Kelic, S., Gross, C., Xu, M., and Bassell, G.J. (2007). Dysregulated metabotropic glutamate receptor-dependent translation of AMPA receptor and postsynaptic density-95 mRNAs at synapses in a mouse model of fragile X syndrome. J Neurosci *27*, 5338-5348.

Muddashetty, R.S., Nalavadi, V.C., Gross, C., Yao, X., Xing, L., Laur, O., Warren, S.T., and Bassell, G.J. (2011). Reversible Inhibition of PSD-95 mRNA Translation by miR-125a, FMRP Phosphorylation, and mGluR Signaling. Mol Cell *42*, 673-688.

Nalavadi, V.C., Muddashetty, R.S., Gross, C., and Bassell, G.J. (2012). Dephosphorylation-induced ubiquitination and degradation of FMRP in dendrites: a role in immediate early mGluR-stimulated translation. J Neurosci *32*, 2582-2587.

Narayanan, U., Nalavadi, V., Nakamoto, M., Thomas, G., Ceman, S., Bassell, G.J., and Warren, S.T. (2008). S6K1 phosphorylates and regulates fragile X mental retardation protein (FMRP) with the neuronal protein synthesis-dependent mammalian target of rapamycin (mTOR) signaling cascade. J Biol Chem *283*, 18478-18482.

Newschaffer, C.J., Croen, L.A., Daniels, J., Giarelli, E., Grether, J.K., Levy, S.E., Mandell, D.S., Miller, L.A., Pinto-Martin, J., Reaven, J., *et al.* (2007). The epidemiology of autism spectrum disorders. Annu Rev Public Health *28*, 235-258.

Nielsen, D.M., Derber, W.J., McClellan, D.A., and Crnic, L.S. (2002). Alterations in the auditory startle response in Fmr1 targeted mutant mouse models of fragile X syndrome. Brain Res *927*, 8-17.

Niere, F., and Huber, K.M. (2010). Dephosphorylation of FMRP by PP2A is required for Group 1 mGluR-induced LTD and increases in dendritic Arc protein. Paper presented at: Society For Neuroscience (San Diego, CA).

Niere, F., Wilkerson, J.R., and Huber, K.M. (2012). Evidence for a fragile X mental retardation protein-mediated translational switch in metabotropic glutamate receptor-triggered Arc translation and long-term depression. J Neurosci *32*, 5924-5936.

Nimchinsky, E.A., Oberlander, A.M., and Svoboda, K. (2001). Abnormal development of dendritic spines in FMR1 knock-out mice. J Neurosci *21*, 5139-5146.

Nishimura, Y., Martin, C.L., Vazquez-Lopez, A., Spence, S.J., Alvarez-Retuerto, A.I., Sigman, M., Steindler, C., Pellegrini, S., Schanen, N.C., Warren, S.T., *et al.* (2007). Genome-wide expression profiling of lymphoblastoid cell lines distinguishes different forms of autism and reveals shared pathways. Hum Mol Genet *16*, 1682-1698.

Norris, A.J., and Nerbonne, J.M. (2010). Molecular dissection of I(A) in cortical pyramidal neurons reveals three distinct components encoded by Kv4.2, Kv4.3, and Kv1.4 alpha-subunits. J Neurosci *30*, 5092-5101.

Nosyreva, E.D., and Huber, K.M. (2005). Developmental switch in synaptic mechanisms of hippocampal metabotropic glutamate receptor-dependent long-term depression. J Neurosci *25*, 2992-3001.

Nosyreva, E.D., and Huber, K.M. (2006). Metabotropic receptor-dependent long-term depression persists in the absence of protein synthesis in the mouse model of fragile X syndrome. J Neurophysiol *95*, 3291-3295.

O'Donnell, W.T., and Warren, S.T. (2002). A decade of molecular studies of fragile X syndrome. Annu Rev Neurosci *25*, 315-338.

O'Leary, D.M., Movsesyan, V., Vicini, S., and Faden, A.I. (2000). Selective mGluR5 antagonists MPEP and SIB-1893 decrease NMDA or glutamate-mediated neuronal toxicity through actions that reflect NMDA receptor antagonism. Br J Pharmacol *131*, 1429-1437.

O'Malley, K.L., Jong, Y.J., Gonchar, Y., Burkhalter, A., and Romano, C. (2003). Activation of metabotropic glutamate receptor mGlu5 on nuclear membranes mediates intranuclear Ca2+ changes in heterologous cell types and neurons. J Biol Chem *278*, 28210-28219.

Ogawa, S., Kwon, C.H., Zhou, J., Koovakkattu, D., Parada, L.F., and Sinton, C.M. (2007). A seizure-prone phenotype is associated with altered free-running rhythm in Pten mutant mice. Brain Res *1168*, 112-123.

Oldham, W.M., and Hamm, H.E. (2008). Heterotrimeric G protein activation by G-protein-coupled receptors. Nat Rev Mol Cell Biol *9*, 60-71.

Olmos-Serrano, J.L., Paluszkiewicz, S.M., Martin, B.S., Kaufmann, W.E., Corbin, J.G., and Huntsman, M.M. (2010). Defective GABAergic neurotransmission and pharmacological rescue of neuronal hyperexcitability in the amygdala in a mouse model of fragile X syndrome. J Neurosci *30*, 9929-9938.

Orlando, L.R., Ayala, R., Kett, L.R., Curley, A.A., Duffner, J., Bragg, D.C., Tsai, L.H., Dunah, A.W., and Young, A.B. (2009). Phosphorylation of the homer-binding domain of group I metabotropic glutamate receptors by cyclin-dependent kinase 5. J Neurochem *110*, 557-569.

Osterweil, E.K., Chuang, S.C., Chubykin, A.A., Sidorov, M., Bianchi, R., Wong, R.K., and Bear, M.F. (2013). Lovastatin corrects excess protein synthesis and prevents epileptogenesis in a mouse model of fragile X syndrome. Neuron *77*, 243-250.

Osterweil, E.K., Krueger, D.D., Reinhold, K., and Bear, M.F. (2010a). Hypersensitivity to mGluR5 and ERK1/2 Leads to Excessive Protein Synthesis in the Hippocampus of a Mouse Model of Fragile X Syndrome. The Journal of Neuroscience *30*, 15616-15627.

Osterweil, E.K., Krueger, D.D., Reinhold, K., and Bear, M.F. (2010b). Hypersensitivity to mGluR5 and ERK1/2 Leads to Excessive Protein Synthesis in the Hippocampus of a Mouse Model of Fragile X Syndrome. J Neurosci *30*, 15616-15627.

Paradee, W., Melikian, H.E., Rasmussen, D.L., Kenneson, A., Conn, P.J., and Warren, S.T. (1999). Fragile X mouse: strain effects of knockout phenotype and evidence suggesting deficient amygdala function. Neuroscience *94*, 185-192.

Park, J.M., Hu, J.H., Milshteyn, A., Zhang, P.W., Moore, C.G., Park, S., Datko, M.C., Domingo, R.D., Reyes, C.M., Wang, X.J., *et al.* (2013). A prolyl-isomerase mediates dopamine-dependent plasticity and cocaine motor sensitization. Cell *154*, 637-650.

Park, S., Park, J.M., Kim, S., Kim, J.A., Shepherd, J.D., Smith-Hicks, C.L., Chowdhury, S., Kaufmann, W., Kuhl, D., Ryazanov, A.G., *et al.* (2008). Elongation factor 2 and fragile X mental retardation protein control the dynamic translation of Arc/Arg3.1 essential for mGluR-LTD. Neuron *59*, 70-83.

Pause, A., Belsham, G.J., Gingras, A.C., Donze, O., Lin, T.A., Lawrence, J.C., Jr., and Sonenberg, N. (1994). Insulin-dependent stimulation of protein synthesis by phosphorylation of a regulator of 5'-cap function. Nature *371*, 762-767.

Payakachat, N., Tilford, J.M., Kovacs, E., and Kuhlthau, K. (2012). Autism spectrum disorders: a review of measures for clinical, health services and cost-effectiveness applications. Expert Rev Pharmacoecon Outcomes Res *12*, 485-503.

Paylor, R., Nguyen, M., Crawley, J.N., Patrick, J., Beaudet, A., and Orr-Urtreger, A. (1998). Alpha7 nicotinic receptor subunits are not necessary for hippocampal-dependent learning or sensorimotor gating: a behavioral characterization of Acra7-deficient mice. Learn Mem *5*, 302-316.

Peier, A.M., McIlwain, K.L., Kenneson, A., Warren, S.T., Paylor, R., and Nelson, D.L. (2000). (Over)correction of FMR1 deficiency with YAC transgenics: behavioral and physical features. Hum Mol Genet *9*, 1145-1159.

Pende, M., Um, S.H., Mieulet, V., Sticker, M., Goss, V.L., Mestan, J., Mueller, M., Fumagalli, S., Kozma, S.C., and Thomas, G. (2004). S6K1(-/-)/S6K2(-/-) mice exhibit perinatal lethality and rapamycin-sensitive 5'-terminal oligopyrimidine mRNA translation and reveal a mitogen-activated protein kinase-dependent S6 kinase pathway. Mol Cell Biol *24*, 3112-3124.

Peterfi, Z., Urban, G.M., Papp, O.I., Nemeth, B., Monyer, H., Szabo, G., Erdelyi, F., Mackie, K., Freund, T.F., Hajos, N., *et al.* (2012). Endocannabinoid-mediated long-term depression of afferent excitatory synapses in hippocampal pyramidal cells and GABAergic interneurons. J Neurosci *32*, 14448-14463.

Pfeiffer, B.E., and Huber, K.M. (2007). Fragile X mental retardation protein induces synapse loss through acute postsynaptic translational regulation. J Neurosci *27*, 3120-3130.

Pieretti, M., Zhang, F.P., Fu, Y.H., Warren, S.T., Oostra, B.A., Caskey, C.T., and Nelson, D.L. (1991). Absence of expression of the FMR-1 gene in fragile X syndrome. Cell *66*, 817-822.

Pietropaolo, S., Guilleminot, A., Martin, B., D'Amato, F.R., and Crusio, W.E. (2011). Genetic-background modulation of core and variable autistic-like symptoms in Fmr1 knock-out mice. PLoS One *6*, e17073.

Potschka, H., Krupp, E., Ebert, U., Gumbel, C., Leichtlein, C., Lorch, B., Pickert, A., Kramps, S., Young, K., Grune, U., *et al.* (2002). Kindling-induced overexpression of Homer 1A and its functional implications for epileptogenesis. Eur J Neurosci *16*, 2157-2165.

Potter, W.B., Basu, T., O'Riordan, K.J., Kirchner, A., Rutecki, P., Burger, C., and Roopra, A. (2013). Reduced juvenile long-term depression in tuberous sclerosis complex is mitigated in adults by compensatory recruitment of mGluR5 and Erk signaling. PLoS Biol *11*, e1001627.

Proud, C.G. (1994). Peptide-chain elongation in eukaryotes. Mol Biol Rep *19*, 161-170.

Proud, C.G. (2007). Signalling to translation: how signal transduction pathways control the protein synthetic machinery. Biochem J *403*, 217-234.

Raftopoulou, M., Etienne-Manneville, S., Self, A., Nicholls, S., and Hall, A. (2004). Regulation of cell migration by the C2 domain of the tumor suppressor PTEN. Science *303*, 1179-1181.

Ravindran, M.S., Patel, Z.M., Adhia, R.A., D'Souza A, K., and Babu, S. (2005). Validity of analysis of FMRP expression in blood smears as a screening test for Fragile X Syndrome in the Indian population. J Clin Lab Anal *19*, 120-123.

Reddy, K.S. (2005). Cytogenetic abnormalities and fragile-X syndrome in Autism Spectrum Disorder. BMC Med Genet *6*, 3.

Roche, K.W., Tu, J.C., Petralia, R.S., Xiao, B., Wenthold, R.J., and Worley, P.F. (1999). Homer 1b Regulates the Trafficking of Group I Metabotropic Glutamate Receptors. Journal of Biological Chemistry *274*, 25953-25957.

Romano, C., Sesma, M.A., McDonald, C.T., O'Malley, K., Van den Pol, A.N., and Olney, J.W. (1995). Distribution of metabotropic glutamate receptor mGluR5 immunoreactivity in rat brain. J Comp Neurol *355*, 455-469.

Ronesi, J.A., Collins, K.A., Hays, S.A., Tsai, N.P., Guo, W., Birnbaum, S.G., Hu, J.H., Worley, P.F., Gibson, J.R., and Huber, K.M. (2012a). Disrupted Homer scaffolds

mediate abnormal mGluR5 function in a mouse model of fragile X syndrome. Nat Neurosci.

Ronesi, J.A., Collins, K.A., Hays, S.A., Tsai, N.P., Guo, W., Birnbaum, S.G., Hu, J.H., Worley, P.F., Gibson, J.R., and Huber, K.M. (2012b). Disrupted Homer scaffolds mediate abnormal mGluR5 function in a mouse model of fragile X syndrome. Nat Neurosci *15*, 431-440, S431.

Ronesi, J.A., Collins, K.A., Hays, S.A., Tsai, N.P., Guo, W., Hua, J.Y., Worley, P., Gibson, J.R., and Huber, K.M. (2011). Disrupted Group 1 mGluR-Homer interactions mediate altered mGluR signaling, circuit function and behavior in a mouse model of Fragile X Syndrome Nature Neuroscience, accepted, pending editorial revisions.

Ronesi, J.A., and Huber, K.M. (2008a). Homer interactions are necessary for metabotropic glutamate receptor-induced long-term depression and translational activation. J Neurosci *28*, 543-547.

Ronesi, J.A., and Huber, K.M. (2008b). Metabotropic glutamate receptors and fragile x mental retardation protein: partners in translational regulation at the synapse. Sci Signal *1*, pe6.

Rong, R., Ahn, J.Y., Huang, H., Nagata, E., Kalman, D., Kapp, J.A., Tu, J., Worley, P.F., Snyder, S.H., and Ye, K. (2003). PI3 kinase enhancer-Homer complex couples mGluRI to PI3 kinase, preventing neuronal apoptosis. Nat Neurosci *6*, 1153-1161.

Rosen, N., and She, Q.B. (2006). AKT and cancer--is it all mTOR? Cancer Cell *10*, 254-256.

Roux, P.P., Shahbazian, D., Vu, H., Holz, M.K., Cohen, M.S., Taunton, J., Sonenberg, N., and Blenis, J. (2007). RAS/ERK signaling promotes site-specific ribosomal protein S6 phosphorylation via RSK and stimulates cap-dependent translation. J Biol Chem *282*, 14056-14064.

Rozen, F., Edery, I., Meerovitch, K., Dever, T.E., Merrick, W.C., and Sonenberg, N. (1990). Bidirectional RNA helicase activity of eucaryotic translation initiation factors 4A and 4F. Mol Cell Biol *10*, 1134-1144.

Rubenstein, J.L., and Merzenich, M.M. (2003). Model of autism: increased ratio of excitation/inhibition in key neural systems. Genes Brain Behav *2*, 255-267.

Sala, C., Futai, K., Yamamoto, K., Worley, P.F., Hayashi, Y., and Sheng, M. (2003). Inhibition of dendritic spine morphogenesis and synaptic transmission by activity-inducible protein Homer1a. J Neurosci *23*, 6327-6337.

Sala, C., Piech, V., Wilson, N.R., Passafaro, M., Liu, G., and Sheng, M. (2001). Regulation of dendritic spine morphology and synaptic function by Shank and Homer. Neuron *31*, 115-130.

Sanchez-Vives, M.V., and McCormick, D.A. (2000). Cellular and network mechanisms of rhythmic recurrent activity in neocortex. Nat Neurosci *3*, 1027-1034.

Santini, E., Huynh, T.N., MacAskill, A.F., Carter, A.G., Pierre, P., Ruggero, D., Kaphzan, H., and Klann, E. (2013). Exaggerated translation causes synaptic and behavioural aberrations associated with autism. Nature *493*, 411-415.

Scheetz, A.J., Nairn, A.C., and Constantine-Paton, M. (2000). NMDA receptor-mediated control of protein synthesis at developing synapses. Nat Neurosci *3*, 211-216.

Schrader, L.A., Birnbaum, S.G., Nadin, B.M., Ren, Y., Bui, D., Anderson, A.E., and Sweatt, J.D. (2006). ERK/MAPK regulates the Kv4.2 potassium channel by direct phosphorylation of the pore-forming subunit. Am J Physiol Cell Physiol *290*, C852-861.

Serge, A., Fourgeaud, L., Hemar, A., and Choquet, D. (2002). Receptor activation and homer differentially control the lateral mobility of metabotropic glutamate receptor 5 in the neuronal membrane. J Neurosci *22*, 3910-3920.

Shahbazian, D., Roux, P.P., Mieulet, V., Cohen, M.S., Raught, B., Taunton, J., Hershey, J.W., Blenis, J., Pende, M., and Sonenberg, N. (2006). The mTOR/PI3K and MAPK pathways converge on eIF4B to control its phosphorylation and activity. EMBO J *25*, 2781-2791.

Sharma, A., Hoeffer, C.A., Takayasu, Y., Miyawaki, T., McBride, S.M., Klann, E., and Zukin, R.S. (2010). Dysregulation of mTOR signaling in fragile X syndrome. J Neurosci *30*, 694-702.

Shaul, Y.D., and Seger, R. (2007). The MEK/ERK cascade: from signaling specificity to diverse functions. Biochim Biophys Acta *1773*, 1213-1226.

She, Q.B., Halilovic, E., Ye, Q., Zhen, W., Shirasawa, S., Sasazuki, T., Solit, D.B., and Rosen, N. (2010). 4E-BP1 is a key effector of the oncogenic activation of the AKT and ERK signaling pathways that integrates their function in tumors. Cancer Cell *18*, 39-51.

She, W.C., Quairiaux, C., Albright, M.J., Wang, Y.C., Sanchez, D.E., Chang, P.S., Welker, E., and Lu, H.C. (2009). Roles of mGluR5 in synaptic function and plasticity of the mouse thalamocortical pathway. Eur J Neurosci *29*, 1379-1396.

Shigemoto, R., Nomura, S., Ohishi, H., Sugihara, H., Nakanishi, S., and Mizuno, N. (1993). Immunohistochemical localization of a metabotropic glutamate receptor, mGluR5, in the rat brain. Neurosci Lett *163*, 53-57.

Shiraishi-Yamaguchi, Y., and Furuichi, T. (2007). The Homer family proteins. Genome Biol *8*, 206.

Shiraishi, Y., Mizutani, A., Yuasa, S., Mikoshiba, K., and Furuichi, T. (2004). Differential expression of Homer family proteins in the developing mouse brain. J Comp Neurol *473*, 582-599.

Silverman, J.L., Tolu, S.S., Barkan, C.L., and Crawley, J.N. (2010). Repetitive self-grooming behavior in the BTBR mouse model of autism is blocked by the mGluR5 antagonist MPEP. Neuropsychopharmacology *35*, 976-989.

Siomi, H., Choi, M., Siomi, M.C., Nussbaum, R.L., and Dreyfuss, G. (1994). Essential role for KH domains in RNA binding: impaired RNA binding by a mutation in the KH domain of FMR1 that causes fragile X syndrome. Cell *77*, 33-39.

Song, M.S., Salmena, L., and Pandolfi, P.P. (2012). The functions and regulation of the PTEN tumour suppressor. Nat Rev Mol Cell Biol *13*, 283-296.

Spencer, C.M., Alekseyenko, O., Hamilton, S.M., Thomas, A.M., Serysheva, E., Yuva-Paylor, L.A., and Paylor, R. (2011). Modifying behavioral phenotypes in Fmr1KO mice: genetic background differences reveal autistic-like responses. Autism Res *4*, 40-56.

Spencer, C.M., Alekseyenko, O., Serysheva, E., Yuva-Paylor, L.A., and Paylor, R. (2005). Altered anxiety-related and social behaviors in the Fmr1 knockout mouse model of fragile X syndrome. Genes Brain Behav *4*, 420-430.

Stefani, G., Fraser, C.E., Darnell, J.C., and Darnell, R.B. (2004). Fragile X mental retardation protein is associated with translating polyribosomes in neuronal cells. J Neurosci *24*, 7272-7276.

Steriade, M., Nunez, A., and Amzica, F. (1993). A novel slow (< 1 Hz) oscillation of neocortical neurons in vivo: depolarizing and hyperpolarizing components. J Neurosci *13*, 3252-3265.

Sun, J., Tadokoro, S., Imanaka, T., Murakami, S.D., Nakamura, M., Kashiwada, K., Ko, J., Nishida, W., and Sobue, K. (1998). Isolation of PSD-Zip45, a novel Homer/vesl family protein containing leucine zipper motifs, from rat brain. FEBS Lett *437*, 304-308.

Sutcliffe, J.S., Nelson, D.L., Zhang, F., Pieretti, M., Caskey, C.T., Saxe, D., and Warren, S.T. (1992). DNA methylation represses FMR-1 transcription in fragile X syndrome. Hum Mol Genet *1*, 397-400.

Suzuki, A., de la Pompa, J.L., Stambolic, V., Elia, A.J., Sasaki, T., del Barco Barrantes, I., Ho, A., Wakeham, A., Itie, A., Khoo, W., *et al.* (1998). High cancer susceptibility and embryonic lethality associated with mutation of the PTEN tumor suppressor gene in mice. Curr Biol *8*, 1169-1178.

Tadokoro, S., Tachibana, T., Imanaka, T., Nishida, W., and Sobue, K. (1999). Involvement of unique leucine-zipper motif of PSD-Zip45 (Homer 1c/vesl-1L) in group 1 metabotropic glutamate receptor clustering. Proc Natl Acad Sci U S A *96*, 13801-13806.

Takeuchi, K., Gertner, M.J., Zhou, J., Parada, L.F., Bennett, M.V., and Zukin, R.S. (2013). Dysregulation of synaptic plasticity precedes appearance of morphological defects in a Pten conditional knockout mouse model of autism. Proc Natl Acad Sci U S A *110*, 4738-4743.

Tanimura, A., Yamazaki, M., Hashimotodani, Y., Uchigashima, M., Kawata, S., Abe, M., Kita, Y., Hashimoto, K., Shimizu, T., Watanabe, M., *et al.* (2010). The endocannabinoid 2-arachidonoylglycerol produced by diacylglycerol lipase alpha mediates retrograde suppression of synaptic transmission. Neuron *65*, 320-327.

Testa-Silva, G., Loebel, A., Giugliano, M., de Kock, C.P., Mansvelder, H.D., and Meredith, R.M. (2012). Hyperconnectivity and slow synapses during early development of medial prefrontal cortex in a mouse model for mental retardation and autism. Cereb Cortex *22*, 1333-1342.

Thandi, S., Blank, J.L., and Challiss, R.A. (2002). Group-I metabotropic glutamate receptors, mGlu1a and mGlu5a, couple to extracellular signal-regulated kinase (ERK) activation via distinct, but overlapping, signalling pathways. J Neurochem *83*, 1139-1153.

The Dutch-Belgian Fragile, X.C., Bakker, C.E., Verheij, C., Willemsen, R., van der Helm, R., Oerlemans, F., Vermey, M., Bygrave, A., Hoogeveen, A., Oostra, B.A., *et al.* (1994). Fmr1 knockout mice: A model to study fragile X mental retardation. Cell *78*, 23-33.

Thomas, A.M., Bui, N., Graham, D., Perkins, J.R., Yuva-Paylor, L.A., and Paylor, R. (2011a). Genetic reduction of group 1 metabotropic glutamate receptors alters select behaviors in a mouse model for fragile X syndrome. Behav Brain Res *223*, 310-321.

Thomas, A.M., Bui, N., Perkins, J.R., Yuva-Paylor, L.A., and Paylor, R. (2011b). Group I metabotropic glutamate receptor antagonists alter select behaviors in a mouse model for fragile X syndrome. Psychopharmacology (Berl).

Thomas, A.M., Bui, N., Perkins, J.R., Yuva-Paylor, L.A., and Paylor, R. (2012). Group I metabotropic glutamate receptor antagonists alter select behaviors in a mouse model for fragile X syndrome. Psychopharmacology (Berl) *219*, 47-58.

Till, S.M., Wijetunge, L.S., Seidel, V.G., Harlow, E., Wright, A.K., Bagni, C., Contractor, A., Gillingwater, T.H., and Kind, P.C. (2012). Altered maturation of the primary somatosensory cortex in a mouse model of fragile X syndrome. Hum Mol Genet *21*, 2143-2156.

Todd, P.K., Mack, K.J., and Malter, J.S. (2003). The fragile X mental retardation protein is required for type-I metabotropic glutamate receptor-dependent translation of PSD-95. Proc Natl Acad Sci U S A *100*, 14374-14378.

Tu, J.C., Xiao, B., Naisbitt, S., Yuan, J.P., Petralia, R.S., Brakeman, P., Doan, A., Aakalu, V.K., Lanahan, A.A., Sheng, M., *et al.* (1999). Coupling of mGluR/Homer and PSD-95 complexes by the Shank family of postsynaptic density proteins. Neuron *23*, 583-592.

Tu, J.C., Xiao, B., Yuan, J.P., Lanahan, A.A., Leoffert, K., Li, M., Linden, D.J., and Worley, P.F. (1998). Homer binds a novel proline-rich motif and links group 1 metabotropic glutamate receptors with IP3 receptors. Neuron *21*, 717-726.

Turu, G., and Hunyady, L. (2010). Signal transduction of the CB1 cannabinoid receptor. J Mol Endocrinol *44*, 75-85.

Uhlhaas, P.J., and Singer, W. (2006). Neural synchrony in brain disorders: relevance for cognitive dysfunctions and pathophysiology. Neuron *52*, 155-168.

van Woerden, G.M., Harris, K.D., Hojjati, M.R., Gustin, R.M., Qiu, S., de Avila Freire, R., Jiang, Y.H., Elgersma, Y., and Weeber, E.J. (2007). Rescue of neurological deficits in a mouse model for Angelman syndrome by reduction of alphaCaMKII inhibitory phosphorylation. Nat Neurosci *10*, 280-282.

Vanhaesebroeck, B., and Waterfield, M.D. (1999). Signaling by distinct classes of phosphoinositide 3-kinases. Exp Cell Res *253*, 239-254.

Varga, E.A., Pastore, M., Prior, T., Herman, G.E., and McBride, K.L. (2009). The prevalence of PTEN mutations in a clinical pediatric cohort with autism spectrum disorders, developmental delay, and macrocephaly. Genet Med *11*, 111-117.

Vazdarjanova, A., McNaughton, B.L., Barnes, C.A., Worley, P.F., and Guzowski, J.F. (2002). Experience-dependent coincident expression of the effector immediate-early genes arc and Homer 1a in hippocampal and neocortical neuronal networks. J Neurosci *22*, 10067-10071.

Volk, L.J., Daly, C.A., and Huber, K.M. (2006). Differential roles for group 1 mGluR subtypes in induction and expression of chemically induced hippocampal long-term depression. J Neurophysiol *95*, 2427-2438.

Wang, X., Li, W., Williams, M., Terada, N., Alessi, D.R., and Proud, C.G. (2001). Regulation of elongation factor 2 kinase by p90(RSK1) and p70 S6 kinase. EMBO J *20*, 4370-4379.

Wang, X., Snape, M., Klann, E., Stone, J.G., Singh, A., Petersen, R.B., Castellani, R.J., Casadesus, G., Smith, M.A., and Zhu, X. (2012). Activation of the extracellular signal-regulated kinase pathway contributes to the behavioral deficit of fragile x-syndrome. J Neurochem *121*, 672-679.

Waung, M.W., and Huber, K.M. (2009). Protein translation in synaptic plasticity: mGluR-LTD, Fragile X. Curr Opin Neurobiol *19*, 319-326.

Waung, M.W., Pfeiffer, B.E., Nosyreva, E.D., Ronesi, J.A., and Huber, K.M. (2008). Rapid translation of Arc/Arg3.1 selectively mediates mGluR-dependent LTD through persistent increases in AMPAR endocytosis rate. Neuron *59*, 84-97.

Weeber, E.J., Jiang, Y.H., Elgersma, Y., Varga, A.W., Carrasquillo, Y., Brown, S.E., Christian, J.M., Mirnikjoo, B., Silva, A., Beaudet, A.L., *et al.* (2003). Derangements of hippocampal calcium/calmodulin-dependent protein kinase II in a mouse model for Angelman mental retardation syndrome. J Neurosci *23*, 2634-2644.

Wegner, C., and Nau, H. (1991). Diurnal variation of folate concentrations in mouse embryo and plasma: the protective effect of folinic acid on valproic-acid-induced teratogenicity is time dependent. Reprod Toxicol *5*, 465-471.

Weiler, I.J., Irwin, S.A., Klintsova, A.Y., Spencer, C.M., Brazelton, A.D., Miyashiro, K., Comery, T.A., Patel, B., Eberwine, J., and Greenough, W.T. (1997). Fragile X mental retardation protein is translated near synapses in response to neurotransmitter activation. Proc Natl Acad Sci U S A *94*, 5395-5400.

Westmark, C.J., Westmark, P.R., O'Riordan, K.J., Ray, B.C., Hervey, C.M., Salamat, M.S., Abozeid, S.H., Stein, K.M., Stodola, L.A., Tranfaglia, M., *et al.* (2011). Reversal of fragile X phenotypes by manipulation of AbetaPP/Abeta levels in Fmr1KO mice. PLoS One *6*, e26549.

Wijetunge, L.S., Till, S.M., Gillingwater, T.H., Ingham, C.A., and Kind, P.C. (2008). mGluR5 regulates glutamate-dependent development of the mouse somatosensory cortex. J Neurosci *28*, 13028-13037.

Wing, L., and Potter, D. (2002). The epidemiology of autistic spectrum disorders: is the prevalence rising? Ment Retard Dev Disabil Res Rev *8*, 151-161.

Worley, P.F., Zeng, W., Huang, G., Kim, J.Y., Shin, D.M., Kim, M.S., Yuan, J.P., Kiselyov, K., and Muallem, S. (2007). Homer proteins in Ca2+ signaling by excitable and non-excitable cells. Cell Calcium *42*, 363-371.

Xiao, B., Tu, J.C., Petralia, R.S., Yuan, J.P., Doan, A., Breder, C.D., Ruggiero, A., Lanahan, A.A., Wenthold, R.J., and Worley, P.F. (1998). Homer regulates the association of group 1 metabotropic glutamate receptors with multivalent complexes of homer-related, synaptic proteins. Neuron *21*, 707-716.

Yan, Q.J., Asafo-Adjei, P.K., Arnold, H.M., Brown, R.E., and Bauchwitz, R.P. (2004). A phenotypic and molecular characterization of the fmr1-tm1Cgr fragile X mouse. Genes Brain Behav *3*, 337-359.

Yan, Q.J., Rammal, M., Tranfaglia, M., and Bauchwitz, R.P. (2005). Suppression of two major Fragile X Syndrome mouse model phenotypes by the mGluR5 antagonist MPEP. Neuropharmacology *49*, 1053-1066.

Ye, K., Hurt, K.J., Wu, F.Y., Fang, M., Luo, H.R., Hong, J.J., Blackshaw, S., Ferris, C.D., and Snyder, S.H. (2000). Pike. A nuclear gtpase that enhances PI3kinase activity and is regulated by protein 4.1N. Cell *103*, 919-930.

Yuan, J.P., Kiselyov, K., Shin, D.M., Chen, J., Shcheynikov, N., Kang, S.H., Dehoff, M.H., Schwarz, M.K., Seeburg, P.H., Muallem, S., *et al.* (2003). Homer binds TRPC family channels and is required for gating of TRPC1 by IP3 receptors. Cell *114*, 777-789.

Zalfa, F., Giorgi, M., Primerano, B., Moro, A., Di Penta, A., Reis, S., Oostra, B., and Bagni, C. (2003). The fragile X syndrome protein FMRP associates with BC1 RNA and regulates the translation of specific mRNAs at synapses. Cell *112*, 317-327.

Zhang, L., and Alger, B.E. (2010). Enhanced endocannabinoid signaling elevates neuronal excitability in fragile X syndrome. J Neurosci *30*, 5724-5729.